UCLouvain

epl

École polytechnique de Louvain

Augmented feedback for the lower-limb amputees - Can a rhythmic stimulation desynchronise the gait of healthy subjects?

Author: **Guillaume DUPREZ**
Supervisor: **Renaud RONSSE**
Readers: **Aleksandar JANKOVSKI, Benoit DELHAYE**
Academic year 2019–2020
Master [120] in Biomedical Engineering

Abstract

Part of the research on augmented feedback for lower limb amputees, this thesis proposed a new gait perturbation experiment, attempting to desynchronise the gait of healthy subjects using a rhythmic stimulation. The hypothesis is the following: if such stimulation can desynchronise the gait of healthy subjects, it could be used to re-synchronise the gait of lower limb amputees. Indeed, lower limb amputees are experiencing an asymmetrical gait, which can lead to complications such as an increased falling rate, or pathologies like osteoarthritis. Hence, improving their gait symmetry is key to enhance their quality of life. Five healthy subjects participated to the three 6-minute treadmill walking experiments, while rhythmic auditory cues were sent alternately in the left and right ears. Subjects were asked to synchronise their feet to the ipsilateral stimuli. The different experimental conditions consisted in a control experiment, with isochronous stimuli delivery, and two perturbation experiments, where different phase shifts were progressively applied to the stimuli delivery. To assess the effects of the stimulation, the time between two subsequent steps was measured. The results show that the delays induced had no significant effects on gait symmetry. Interestingly though, retention effects have been found after the exposition to the stimulation: gait symmetry is increasing.

Remerciements

Je voudrais remercier toutes les personnes qui m'ont apporté leur aide et qui m'ont permis de mener à bien la rédaction de ce mémoire, et ce malgré la crise sanitaire que nous vivons actuellement.

Merci à mon promoteur Monsieur Renaud RONSSE, pour sa disponibilité hebdomadaire, ainsi que ses conseils et son expertise precieuse tout au long de l'année.

Merci à Virginie OTLET, pour sa disponibilité, ses nombreux retours et suggestions, sans qui ce mémoire n'aurait pas été le même.

Merci au Docteur Jean-Marie VANMARSENILLE, pour avoir accepté de me rencontrer et de répondre à mes questions.

Merci à Monsieur Thierry DARAS, pour sa disponibilité et pour son expertise au niveau du matériel expérimental.

Merci à Madame Yan LIU, pour avoir pris le temps de m'initier à LabView, et ce compte tenu des circonstances difficiles.

Merci à Messieurs Aleksandar JANKOVSKI et Benoit DELHAYE, pour avoir accepté d'être lecteurs de ce mémoire.

Enfin, Merci à mes proches, pour leur soutien, pour avoir accepté de lire plusieurs fois mon mémoire et pour avoir permis la réalisation des expériences en confinement. En particulier, j'aimerais remercier mes parents, ma soeur, Alice, Carmelo et mon ami Luis Felipe.

Contents

List of Abbreviations

LLA	Lower limb amputee
IC	Initial contact
LR	Loading response
MST	Midstance
TST	Terminal stance
PSW	Preswing
ISW	Initial swing
MSW	Midswing
TSW	Terminal swing
CNS	Central nervous system
AP	Action potential
SA	Slowly-adaptive
RA	Rapidly-adaptive
SA1	Slowly-adaptive type 1
SA2	Slowly-adaptive type 2
RA1	Rapidly-adaptive type 1
RA2	Rapidly-adaptive type 2
LF	Low frequency
HF	High frequency
SACH	Solid ankle cushion heel
TSR	Targeted sensory reinnervation
PNS	Peripheral nervous system
VAS	Visual analog scale
COP	Center of pressure
FSR	Force sensing resistor

AMS	Apparent moving sensation
ETD	Electrotactile display
AMS	Apparent moving sensation
HyVE	Hybrid vibrotactile and electrotactile
fMRI	Functional magnetic resonance imaging
LEAFS	Lower extremity ambulatory feedback system
ST	Stance time
SR	Symmetry ratio
RAS	Rhythmic auditory stimulation
RTVF	Real-time visual feedback
%ST	Percent stance time
SI	Symmetry index
POF	Push off force
PCA	Principal component analysis
IMU	Inertial measurements unit
IST	Inter-steps time
IQR	Inter-quartile range
S1	Subject one
S2	Subject two
S3	Subject three
S4	Subject four
S5	Subject five

List of Figures

List of Tables

Introduction

The loss of a limb is a disabling condition that affects the health and consequently, the quality of life of an amputee. It is a process through which not only the motor system is affected but also the sensory system. Patients take time to recover from it, whether on the physical or psychological level. This is especially the case for lower limb amputees (LLAs) who are facing important physical disabilities, pain and increased energy consumption compared to upper limb amputees [1]. These conditions deprive them of getting a physical driven job, which decreases their chances of working and exposes them to unemployment issues (since non-physical jobs usually require higher qualifications) [2].

In England, 42 294 major lower limb amputations[1] were performed from 2003 to 2013 on people older than 50 years, of which 53% were transfemoral amputations[2] and the 47% remaining were transtibial amputations[3] [3]. In Germany, 55 595 people with lower limb amputation were reported in 2015 [4]. In France, 9508 lower limb amputations were performed in 2003. Among these people, less than 1500 patients were under 60 years old, highlighting ageing as a risk factor for lower limb amputation [5]. This trend is confirmed in other countries like Netherlands where 80% of the amputees are aged over 65 years [6]. In Belgium, the number of LLAs is estimated at 7315, with around 1710 new lower limb amputations each year [6], corresponding to three lower limb amputation procedures for 20 000 Belgians yearly. To compare, there were 14 of these procedures for 20 000 Germans in 2015.

The main causes of amputations are vascular diseases including diabetes. These are responsible for more than 82% of the lower limb amputations. Over the last 30 years, the worldwide number of adults with diabetes nearly quadrupled. In 2014, more than 422 millions adults were diagnosed with this disease, while they were 108 million in 1980 as it can be seen in Figure 1. The remaining causes are traumas (16%), cancer (1%) and congenital diseases (1%) [6].

[1] Performed above the ankle
[2] Above knee amputation
[3] Below knee amputation

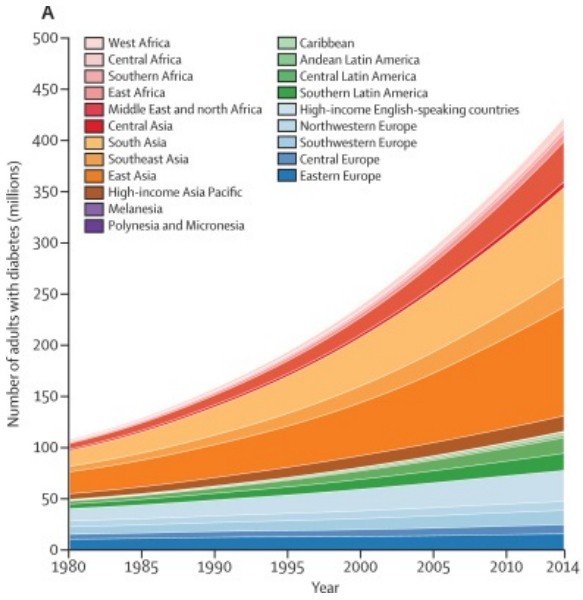

Figure 1: Worldwide diabetes trend over the last 30 years (1980-2014), given in millions of adults [7]

Prostheses for LLAs have evolved throughout the years: starting from a simple piece of wood, they now include hydraulic joints, energy return feet or even processing units which allow live adaptation to the environment. It is safe to say that prostheses now represent good mechanical solutions. Still, they do not allow patients to recover a proper walking experience. Patients walking with prostheses experience gait problems such as an asymmetric walking, which is due to the over-use of the healthy leg [8]. As a consequence, patients tend to consume more energy since the gait mechanics are not efficient [9]. Moreover they often face complications such as back pain and musculoskeletal pathologies like osteoarthritis for the healthy leg, or osteoporosis for the amputated leg [10]. These issues lead to longer rehabilitation periods, hindering the ability of the patient to recover both psychologically and physically [9].

Hence, it becomes obvious that improving the gait characteristics of LLAs, like symmetry, will enhance their quality of life. The lack of sensory feedback provided by current prostheses is believed to be the root cause of these issues, as it will be explained in the first part of Chapter 1. Indeed, feedback augmentation remains insufficiently explored as current prostheses still lack the ability to transmit sensory information, which plays an important role in the way human walk. Therefore, an augmented feedback system embedded into a prosthesis could be key to correct these issues. Consequently, it requires knowledge about the behaviour of sensory feedback in the human gait, which will be presented in the second part of Chapter 1.

This thesis is part of the augmented feedback research for the LLAs. In particular, this thesis will investigate the following hypothesis: is it possible to desynchronise the gait of healthy subjects using a rhythmic stimulation? Hence, if it is possible to disturb the gait of healthy subjects with such stimulation, this could be used to improve the gait of LLAs. More specifically, a prosthesis embedding a system based on such rhythmic stimulation could be designed to improve gait characteristics of LLAs, such as the gait symmetry.

Chapter 1

The sensory feedback in locomotion

This chapter aims at describing the importance of sensory feedback in locomotion. After reviewing (i) the challenges faced by the LLAs (ii) and portraying the current standard prosthesis, the focus of this work will be presented. Then, the chapter will explain how the gait cycle is defined and how it is controlled through the integration of sensory feedback. Finally, an overview of the relevant body sensory receptors will be made: how does the sensory feedback work naturally? What are the key sensory receptors involved in movement? What are their respective role?

1.1 Challenges for lower limb amputees: Problem statement

Understanding the different challenges which LLAs are facing in the daily use of their prosthesis is key to design an efficient sensory feedback system. Hence, Dr. J.M. Vanmarsenille (UCLouvain-Belgium), a specialist in neuro-locomotor rehabilitation, was met on November 26th (2019) at St-Luc hospital.

Throughout the interview, he highlighted that lots of complications occur after the amputation such as healing problems, neuropathic pain, neuroma, phantom pain, etc. It is obvious that these complications have an impact on the LLAs quality of life. He also insisted on the fact that current prostheses are heavy, which makes them difficult to use for some people. Although lightweight prostheses exist, they are not affordable for most people. Finally, he pointed out that LLAs have difficulties to control their prosthetic knee and that a system preventing them from falling would help.

To complement this information, a brief literature review has been done. The following issues have been extracted:

- Increase in falling rate [9, 11];

- Phantom limb sensation (including pain) [12];
- Sub-optimal locomotion, including balance problem or asymmetric gait [9].

Falling seems to be a recurrent problem for LLAs. This issue can be related to the temporal and loading asymmetries in the gait of LLAs [13]. Therefore, improving gait symmetry would prevent falls and enhance the locomotion of LLAs.

1.1.1 Current prostheses

Current lower limb prosthesis can provide good mechanical solutions. The typical prostheses for the major lower limb amputations can be seen in Figure 1.1. The transtibial prosthesis is composed of three parts: the socket, the pylon and the foot. A prosthetic knee is added to the transfemoral prosthesis. All these parts are presented hereunder. More details can be found in Appendix A.

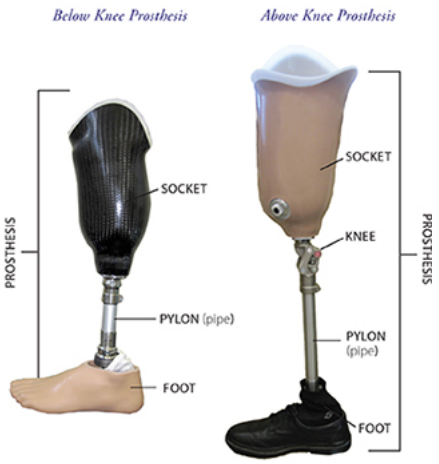

Figure 1.1: Typical lower limb prostheses[14]: transtibial prosthesis (left) and transfemoral prosthesis (right)

1. **The socket**: it is where the stump will be inserted, acting as the interface between the prosthesis and the body. It is composed of two parts. The first one is a rigid material called the hard socket, which is realised by casting of the stump. The second part is the soft socket, also called the liner. It is placed between the hard socket and the skin of the residual limb to reduce the stress applied on the stump [6].
2. **The pylon**: it allows the tuning of the prosthesis parameters such as varus and valgus[1] [6].
3. **The foot**: it ends the prosthetic limb. Several types of prosthetic foot exist, ranging from the basic non-articulated foot (SACH foot), to the more complex ones including energy return or processing units (Figure 1.2) [15].

[1]Varus and valgus refer respectively to orthopedic deformation associated to a bending towards and outwards the body axis

(a) SACH prosthetic foot

(b) Energy return foot (carbon fibers)

Figure 1.2: Prosthetic foot
[15]

4. **The prosthetic knee joint**: it provides stability and mobility. Polycentric knee joints are an example of a passive solution (Figure 1.3).

Figure 1.3: Polycentric prosthetic knee joint (ReMotion Knee)
[16]

As it can be seen, current prosthesis represent good mechanical solutions. However, they do not provide sensory feedback to the user, which is believed to be the root cause of the different issues faced by LLAs. It has been shown that providing sensory feedback helps to improve gait characteristics or reduce phantom pain [17, 18]. As LLAs are suffering from total sensory function impairment[1], sensory replacement is needed, either by using the same sensing modality (i.e. a pressure sensation for a pressure sensation) or using sensory substitution [17].

Therefore, this thesis will focus on sensory feedback techniques which could help to improve symmetry in the gait of LLAs. Knowledge about how the sensory feedback is handled in the human gait becomes a prerequisite.

[1]Complete loss of a sensory function due to the limb amputation

1.2 Gait cycle

The human gait can be described as a periodic sequence of discrete events as illustrated in Figure 1.4. Its period is defined as the time between the initial contact of one foot with the ground and the subsequent initial contact of the same foot. The sequence of events is thus expressed regarding one leg.

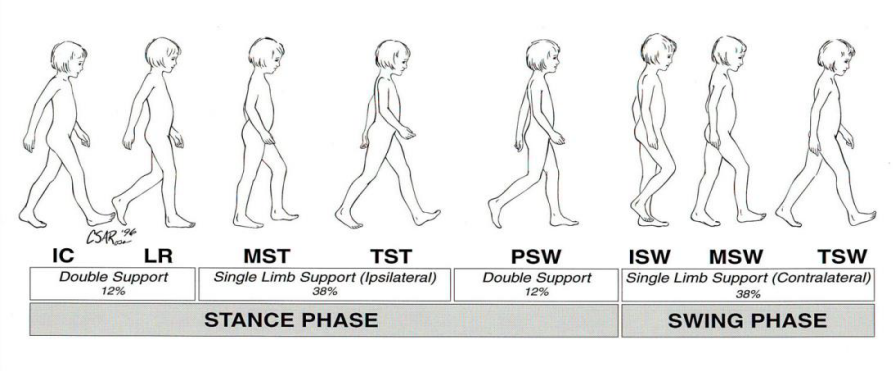

Figure 1.4: Gait cycle and its different events
[19]

The cycle consists of two major phases which are (i) the stance and (ii) the swing phase [19]:

(i) **The stance phase** designates the time period where the foot is in contact with the ground, which corresponds approximately to 62% of the total cycle time. It is composed of five events:

   (a) **Initial Contact (IC)**: it is the beginning of the stance phase with a first contact between the foot and the ground. This contact is done at the heel, that it is also called the *heel strike (HS)*.

   (b) **Loading Response (LR)**: it defines the period of double limb support, starting at heel strike and ending when the controlateral foot leaves the ground. The limb acts as a shock absorber during this time, resulting in knee flexion, associated with body load acceptance and deceleration.

   (c) **Midstance (MST)**: following the LR, it is covering the first half of the single limb support period. It marks the initiation of the opposite limb swing phase and ends with the passage over the stance limb forefoot.

   (d) **Terminal stance (TST)**: it covers the second half of the single limb support. It begins with heel rise and ends with the IC of the controlateral foot.

   (e) **Preswing (PSW)**: last event of the stance phase, it begins at the IC of the controlateral foot and ends with terminal contact of the ipsilateral foot. It is also called the *toe off*.

(ii) **The swing phase** is defined as the time period where the foot loses ground contact, inducing movement of the limb towards the subsequent foot contact. It represents the remaining 38% of the cycle time and begins right after the PSW. It is composed of three phases:

   (a) **Initial Swing (ISW)**: it is initiated at toe off and ends when the ipsilateral leg is aligned with the controlateral one.

   (b) **Midswing (MSW)**: starts at the end of the ISW and lasts until the swinging leg passes in front of the stance limb.

   (c) **Terminal Swing (TSW)**: starts at the end of the MSW, when the ipsilateral tibia is perpendicular to the ground and lasts until the next IC.

1.3 Motor control

Every movement can be divided into three stages: the integration stage, the motor stage and the sensory stage. When an action is about to be taken, the integration stage prepares the neuromuscular system to perform the movement associated with this task. This stage regroups two parts [20]:

(i) **Movement encoding by motor centres for future use**: movements are stored whithin the central nervous system (CNS) as motor programs containing movement sequences and their associated goal. These programs are not related to specific muscle sequences. An example is writing: a sequence of movement is stored for a certain word, which can then be written by many means (with our hands, or even by holding a pen between our lips).

(ii) **Identification of movement errors**: when a movement is selected, an efferent command is sent to the spinal motor centres to trigger muscle activity, while an efferent copy of this command is sent to a forward model. This copy will compute a prediction of the sensory feedback that will be provided. The goal is to check if there is a match between the prediction and the actual sensory output. If they do not match, a reorganisation of the motor command will be done to correct the movement; while if they do, it means that the task has been fulfilled. This is represented in Figure 1.5.

Then, the motor stage is entered when the efferent commands reach the spinal motor centres, activating muscles in order to perform the desired task. This requires complex synchronisation of different muscle groups in order to fulfill the task: antagonist muscles have to decrease their tension while agonist muscles increase theirs. Several synchronisation patterns exist for a single movement. This variability seems to be essential in healthy subjects [20].

Finally, the sensory stage collects information during the movement, which will be used in the comparator model as explained previously. A graphical illustration of the motor control can be found in Figure 1.5.

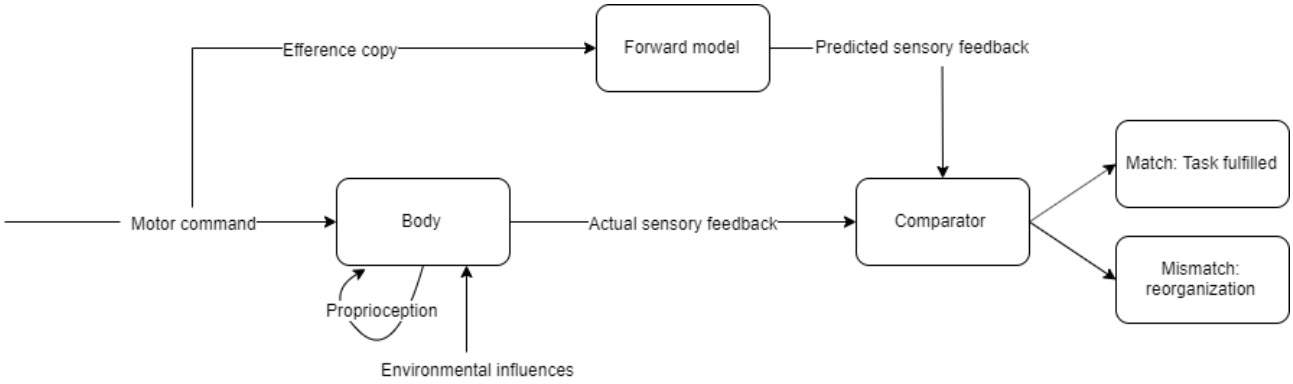

Figure 1.5: Motor control, adapted from [21]

The information collected by the sensory stage is related to the interaction with the environment (exteroceptive nature) and to internal physical events, known as proprioception. The latter includes [22]:

- The detection of movements and perception of their direction, velocity,...;
- The perception of the relative position of body parts to one another;
- The perception of forces generated via the muscles;
- The clues about strength of the muscle contraction compared to its total strength.

This information is provided by several sensory systems such as the visual system, the vestibular system or the somatosensory system. These systems use specialised cells called sensory receptors to transmit information to the brain. This process is covered in Appendix B.

For LLAs, the somatosensory system is affected by the amputation procedure. When walking, this system conveys information about ground pressure on the foot, joints angle, velocity of the joints, etc. Loss of proprioception may lead to inaccurate movements and increases the risk of injury. Moreover, proprioception is essential for motor learning, which is crucial during the rehabilitation period [20]. Indeed, it has been demonstrated that sensory feedback is critical in the control of human gait as it helps correcting on-going movements and avoiding falls [23].

Given the major role of this sensory feedback, the understanding of the somatosensory system becomes of high importance.

1.4 The somatosensory system

The main actors of the somatosensory system are the skin, the muscles and the joints [22], in which sensory receptors are located. These receptors are called the mechanoreceptors. They

detect physical deformations induced by mechanical stimuli, like touch. When a mechanoreceptor is deformed, its permeability is modified, letting ions flow into the cell, modifying its membrane potential (see Appendix B) [24].

1.4.1 Skin sensory afferents

Part of the somatosensory system, the skin is the largest sensory organ. Its receptors are responsible for the tactile sensation: they are able to detect light touch to deep pressure. Moreover, skin receptors can give information about joint position. Some sensory receptors sensible to skin stretch can fire with change of joint angle, giving thus information about movement and position [22]. Distinction between glabrous and hairy skin has to be made since there are morphological and neuro-physiological discrepancies leading to different sensory functions.

Glabrous skin (see Figure 1.6) is covering our hands and feet. It is specialised in discriminative touch, textures and shape determination, providing thus feedback able to influence locomotion [25]. It is composed of four types of mechanoreceptors, all associated with fast conduction velocity. Two groups can be distinguished : slowly-adaptive (SA) or rapidly-adaptive (RA). When a stimulus is applied and sustained, the first group will fire continuously with a firing rate progressively decreasing over time, while the second group will only fire at the onset and offset of the stimulus. SA and RA receptors have two types of ending, defining the SA type 1 (SA1) and SA type 2 (SA2) and reciprocally RA1 and RA2:

- SA1 receptors have Merkel cells as endings. These are sensible to the static nature of the stimulus such as the object's texture, curvature and shape [25];
- SA2 receptors end with Ruffini corpuscles which are sensible to skin stretch [25];
- RA1 receptors terminate in Meissner's corpuscles. These are sensible to low frequency (LF) vibration in the range of 40 Hz, which can be associated to movements across the skin like the slip of an object [25];
- RA2 receptors end with Pacinian corpuscles. These detect high frequency (HF) vibrations (200 Hz), which are associated with vibrations of held objects. [25].

Hairy skin (see Figure 1.6) is associated with affective touch[1] [25]. Although it is composed of the same type of mechanoreceptors as the glabrous skin, the difference is that they form a complex with hair follicles allowing deeper perception of touch. For example, SA1 receptors form a complex called "touch dome" which detects skin indentation. Another difference is that endings of slow-conductivity mechanoreceptors are localised in hairy skin, allowing the perception of pleasurable touch sensation. A summary of the mechanoreceptors located in the skin can be found in Table 1.1.

[1] Touch which produces an emotional response like caressing

Table 1.1: Skin mechanoreceptors

Response type	Nerve fibers	Nerve endings	Location	Modality
SA	II: Myelenated: 6 - 12 µm(Aβ) [26]	Merkel cell	Basal epidermis [25]	Static stimuli [25]
SA	II: Myelenated: 6 - 12 µm(Aβ) [26]	Ruffini corpuscles	Dermis [25]	Skin stretch [25]
RA	II: Myelenated: 6 - 12 µm(Aβ) [26]	Meissner's corpuscles	Dermal papillae [25]	LF vibration (40 Hz) [25]
RA	II: Myelenated: 6 - 12 µm(Aβ) [26]	Pacinian corpuscles	Dermis [25]	HF vibration (200 Hz) [25]

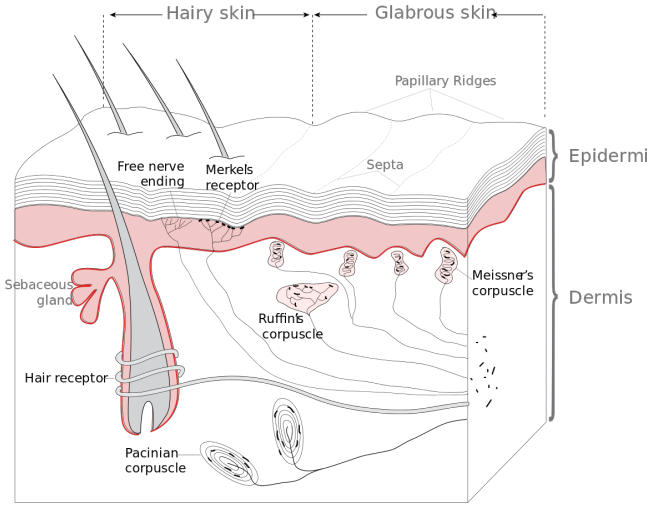

Figure 1.6: Skin sensory receptors
[27]

The two remaining actors of the somatosensory systems are the muscles and joints. These are presented hereunder.

1.4.2 Muscle and joint sensory afferents

A muscle can be seen as a non linear spring that develops a tension force depending on its mechanical state. They are connected to bones by tendons. Its sensory receptors are the muscle spindles and the Golgi tendon organs (see Figure 1.7).

Muscle spindles are elongated sensory organs lying parallel to muscle fibers. They are innervated by two kinds of nerve fibers: the primary muscle spindle afferent (known as Ia) and the secondary muscle spindle afferent (known as II). Both types fire with muscle lengthening, but Ia fibers also detect movement speed. Muscles on both sides of a joint are needed to give information about the movement and position of the limb [22, 28].

The Golgi tendon organs are situated in the musculotendinous junction. They consist of strands of collagen attached to the tendon at one end, and to muscle fibers at the other end. They are also innervated by high velocity nerve fibers (known as Ib) and are sensitive to the tension generated into the attached muscle [22, 28].

Concerning the joint afferents, sensory endings can be localised in the joint capsule and ligaments (see Figure 1.7). When stretched, the joint capsule activates Ruffini endings (SA2). These are mostly activated at the end of the joint motion range, giving information about limb position. Golgi tendon organ-like receptors responding to stretch are found in the ligaments [22]. An overview of these muscle and joint afferents can be found in Table 1.2.

Table 1.2: Muscle and joints mechanoreceptors

Nerve fibers	**Nerve endings**	**Location**	**Modality**
Ia: Myelenated: 13 - 20 µm(Aα) [26]	Muscle spindles	Intrafusal muscle fibers [22, 28]	Muscle lengthening and movement speed [22, 28]
II: Myelenated: 6 - 12 µm(Aβ) [26]	Muscle spindles	Intrafusal muscle fibers [22, 28]	Muscle lengthening [22, 28]
Ib: Myelenated: 13 - 20 µm(Aα) [26]	Golgi tendon organs	Musculotendinous junction and ligament [22, 28]	Muscle tension [22, 28]
II: Myelenated: 6 - 12 µm(Aβ) [26]	Ruffini corpuscles	Joint capsule [22, 28]	Joint stretch [22, 28]

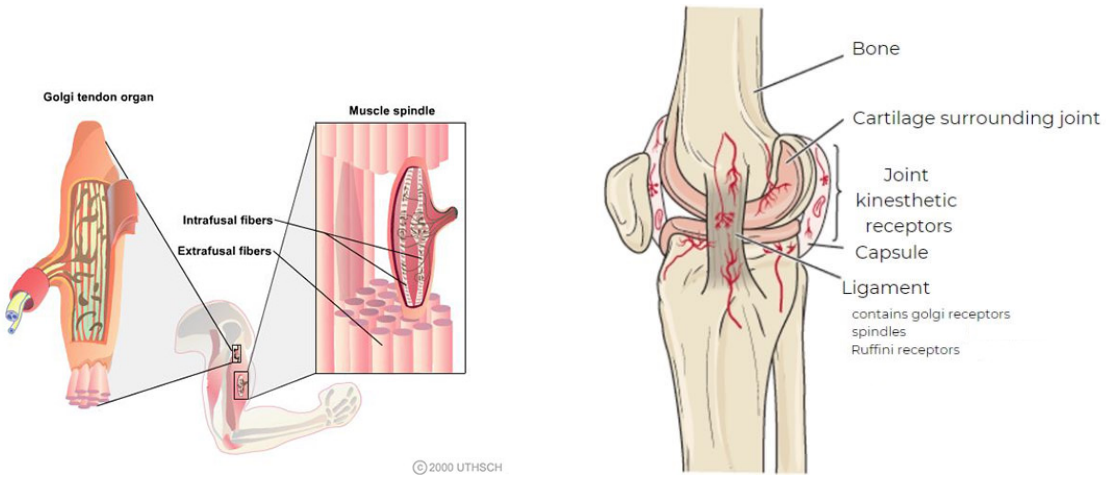

(a) Muscle sensory receptors, from [29] (b) Joint sensory receptors, adpated from [30]

Figure 1.7: Muscle and joint sensory receptors

As it has been observed, sensory feedback has an essential role in lower-limb movements. Nevertheless, current prostheses do not provide any to the user. The next chapter will be devoted to a review of the literature regarding the different techniques available to provide sensory feedback.

Chapter 2

How to provide sensory feedback to lower limb amputees?

This chapter aims to study the different ways to provide artificial sensory feedback for LLAs. The final goal of this chapter is to select a technique to be used in the experimental part of this work.

First, the chapter will start with an overview of the different techniques tested so far. Secondly, it will focus on non-invasive techniques. A section will be dedicated to each one of these, i.e. mechanotactile, vibrotactile, electrotactile, hybrid, auditory and visual based techniques. In each section, a review of articles, covering experimental concepts, applications and results, will be done in order to better understand each technique. Each section will end with a brief discussion on the suitability of the given technique regarding its application in LLAs. Finally, this chapter will conclude by selecting among these techniques the one which will be used in the experimental part of this work.

2.1 Sensory feedback techniques

Two types of method exist to transmit information to the human body: the invasive and non-invasive ones [31]. These can be found in Figure 2.1.

1. **Invasive methods**: these methods are associated with a surgical procedure that may cause nerve damage and post operation complications such as infections or rejections. Here are the different methods:
   (a) **Targeted sensory reinnervation (TSR)**: consists of transferring the nerves that innervated the amputated limb to a conserved site.
   (b) **Peripheral nervous system (PNS) stimulation**: electrodes are implanted in

afferent nerves in the residual limb, allowing perception through nerve stimulation. Depending on the type of electrode used, the risk of nerve damage can be reduced.

(c) **CNS stimulation**: implantation of electrodes directly into the brain.

2. **Non-invasive methods**: the feedback is provided on the skin, i.e. on the residual limb or elsewhere on the body, but also through the ears or eyes. It requires to learn what a stimulus in a given location represents. That is why it is preferable to choose a body location with low cognitive load such as the chest, shoulders or lower back [32]. The different methods are:

   (a) **Mechanotactile feedback**: described as an object pushing normally to the skin. It can be seen as a modality-matched feedback in the case of a force feedback.

   (b) **Vibrotactile feedback**: the feedback is provided by a vibrotactile actuator placed on the skin. It is a miss-matched modality feedback in the case of a force feedback.

   (c) **Electrotactile feedback**: small electric current is delivered through the skin, activating the underlying nerves allowing pressure and slipping perception.

   (d) **Hybrid stimulation**: multiple modalities are combined. For example, the combination of electrotactile and vibrotactile modalities allows to take advantage of both techniques.

   (e) **Substitution**: uses another sense, like hearing or vision, as a sensory substitution. For example, Lundborg et al. [33] used small microphones to allow the perception of different structures during active touch thanks to different sounds.

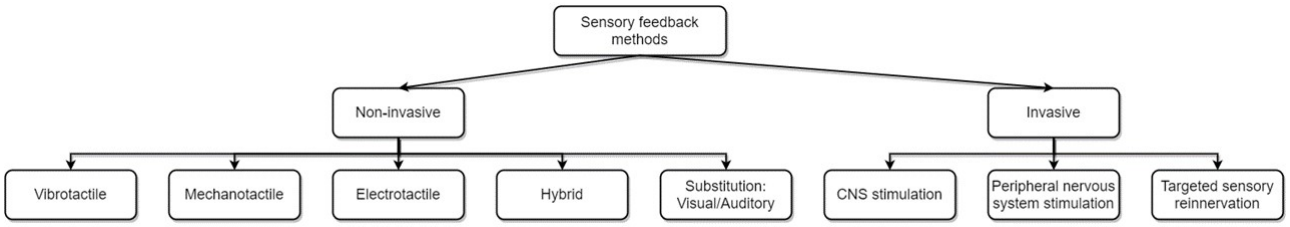

Figure 2.1: Methods of sensory feedback

The respective pros and cons of each modality are described in Table 2.1.

Table 2.1: Summary of types of sensory feedback

Type	Pros	Cons
Mechanotactile	Modality-match (lower cognitive load), "real" touch sensation [31]	Bulky, power consumption [31]
Vibrotactile	Cheap, small, low consumption [31]	Annoying (if continuous), sensible to adaptation [31, 9]
Electrotactile	Accuracy, small, low consumption [9, 34]	Electrodes sensible to skin state [9]
Hybrid	Additional information provided to mimick intact limb [31]	Overload of sensation [31]
Substitution	Good results obtained, can reduce the cognitive load if combined, easy [31, 35]	Not suitable for everyday life as it can be noisy [31, 35].
TSR	No implants, natural sensation [36]	Recovery time [31]
PNS	Somatotopically matched [31]	Invasive, risk of nerve damage, biocompatibility [31]
CNS	Somatotopically matched [31]	Highly invasive, biocompatibility [31]

As non-invasive techniques do not require any surgical procedure, these techniques are more likely to be accepted by most of the patients. Moreover, it will be easier to experiment with these in the framework of this work. Therefore, this thesis will focus on non-invasive techniques to provide sensory feedback.

2.2 Literature review

A literature review of the different sensory feedback modalities can be find in this section. For each of them, review of articles has been made in a chronological fashion, while highlighting the results obtained. Complement articles for the vibrotactile and electrotactile modalities can be find in Appendix C. Finally, the review of each modality will be concluded with a brief discussion about the use of the given modality for LLAs.

2.2.1 Mechanotactile Stimulation

Examples of mechanotactile stimulation used as a sensory feedback are common in upper-limb prosthesis. Antfolk and colleagues [37] developed in 2012 a system providing tactile stimulation through a non-invasive pneumatic system on the arm stump. Their system used the phantom hand sensation map: by putting pressure on specific locations on the stump, it is possible to evoke sensations from specific fingers of the missing hand. In other words, when a prosthetic finger touches something, a corresponding pressure sensation is transferred to the stump location evoking the appropriate phantom sensation. They showed that amputees are able to correctly identify the location of a finger corresponding to a stimulus.

However, few examples exist regarding LLAs. In a 2008 study [9], Fan et al. developed a haptic feedback prototype for transfemoral LLAs relaying information from the prosthetic feet to the remaining limb. The device featured four piezoresistive force sensors placed against the prosthetic foot on locations where static weight forces are the greatest: the hallux, central heel, first and second metatarsal heads. These points are critical in the relay of ground contact information. It was also equipped with a pneumatic control system with four silicone-based balloon actuators placed around the thigh. Depending on the force pattern detected by the piezoresistive sensors, the balloons will deform the skin's surface in a certain way allowing proportional perception of pressure by the mechanoreceptors in the residual limb's skin.
They showed that the relationship between input pressure and balloon deflection is monotonic, implying deterministic and controllable output deflection. Most importantly, subjects are able to detect the inflation pattern, the direction of the pressure stimuli and the different force levels as well as to discriminate gait movements with high level of accuracy.

Conclusion about Mechanotactile Stimulation:

Mechanotactile based feedback systems present the advantage to be modality matched, i.e. a pressure is transmitted through a pressure sensation [9, 37]. This makes the feedback more intuitive. In particular, subjects are able to identify, with precision, different pressure patterns, which can be matched to gait movements [9]. However, as they require actuation, such systems might be relatively bulky. In a field where space matters, this is problematic. Nevertheless, more studies about mechanotactile feedback for LLAs could correct this point.

2.2.2 Vibrotactile Stimulation

In early 2002, Verschueren et al. [38] studied the influence of a vibrotactile stimulation in the spatio-temporal control of humain gait. They asked healthy subjects to walk blindfolded on a treadmill while disturbing proprioceptive information by means of tendon vibration on several joints, including (i) ankle joint, (ii) hip joint and (iii) knee joint. Produced by cylindrical vibrators, tendon vibrations were applied transversely to the targeted tendon or on the muscle belly, as close as possible to the selected tendon. In the case of knee joint, the targeted tendon was the patellar tendon. First, they studied the influence of tendon vibration on spatial

characteristics of the joint displacements, hypothesising that vibration would cause lengthening illusion of the vibrated muscle, leading to a decrease in joint displacement. Secondly, they investigated how tendon vibration affected temporal relationship between different joints and limbs, expecting interlimb coordination to be affected rather than intralimb coordination.
They showed that tendon vibration leads to local changes (shortening) in joint displacement, suggesting that muscle spindles input is used in the online scaling of joint angles during gait. Their results are in concordance with lengthening illusion induced by muscle spindles stimulation. Moreover, they showed that vibration does not affect interlimb coordination as the non perturbed leg experiences no effect. Similarly, intralimb coordination is not affected suggesting that coordination between joints might be controlled by a central pattern generator, unaffected by proprioception disturbance of a joint.

In 2011, the team of Wentink and colleagues [39] studied the suitability of vibrotactile stimulation as a sensory feedback modality for transfemoral amputees using vibrators consisting of eight *Pagers* motors. They investigated (i) the effects of vibration location and frequency on perception, (ii) the effects of different stimulation methods, and finally (iii) the habituation to these stimulations.
For the first experiment, eight vibrators were placed in four pairs at different location on the upper leg of subjects respectively on the lateral, medial, posterior and anterior side, covering the whole area of the upper leg. Different frequencies in the range of 30-80Hz (activating Meissner's and Pacinian's corpuscles) were applied randomly to each vibrator. Subjects were asked to rate the stimulus intensity felt on a visual analog scale (VAS)[1].
To answer the second point, they conducted an experiment where the vibrators were placed 2cm spaced in a row, making an array. Subjects received random 60Hz vibration pattern under sequential and simultaneous stimulations. They were asked to select vibrators they thought were active. They did the experiment both on the posterior and anterior side of the upper leg.
To determine habituation to vibrotactile feedback, they continuously activated a vibrator on the anterior side of the upper leg for 15min at 80Hz. Subjects had to report their perceived sensation each 40s.
The authors showed that when frequency increases, perception increases. Moreover, this increase depends on the location of the stimulus with greater increase at posterior and medial side as it can be seen in Figure 2.2. Furthermore, they showed that sequentially applied stimuli are better perceived than simultaneous ones. Finally, they showed that it takes about 5min of continuous stimulation to lower by half the perceived sensation.

[1]VAS consists in a 10cm horizontal line with increasing intensity from left to right (no sensation to strong sensation)

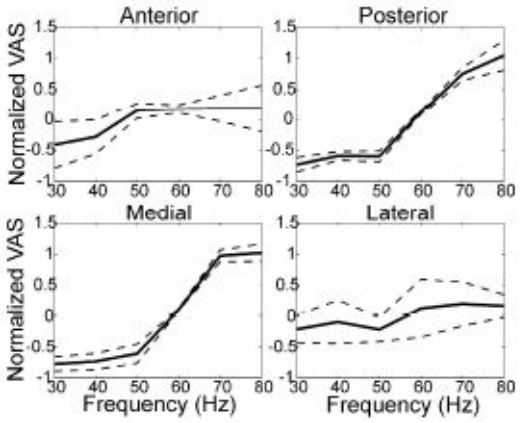

Figure 2.2: Effect of vibration frequency at different location of the upper leg [39]

In 2014, Sharma and colleagues [40] investigated voluntary reaction times and accuracy following vibratory stimulus on the lower limb. In particular, the effects of stimuli frequency and location on reaction time were assessed. They placed three vibrotactile motors at three different locations on the thigh, while measuring the reaction times of subjects.
They showed that higher frequency stimuli are better perceived than low frequency ones. Moreover, reaction times can be modulated depending on the location of the stimulus: they obtained faster reaction times ($\geq 0.6s$) when vibrotactile motor were placed on the anterior region of the leg. If they could be acceptable for postural control, these reaction times are consequent when giving sensory feedback in dynamic conditions such as gait. One way to tackle these delays could be to adopt a feedforward strategy, whereby information from previous gait cycles are used to predict appropriate corrective actions in a subsequent cycle.

In 2015, Crea et al. [41] introduced a feedback system conveying information from a prosthetic foot sole to the user. The system provided discrete feedback, synchronously with specific gait-phase transitions. Pressure sensitive insoles were used to detect these phase transitions. Each insole was made of an array of pressure sensitive elements, connected to an electronic board computing the center of pressure (COP) location as well as the vertical ground reaction force value in order to sequence the gait phases. Three vibrotactile units were placed along the thigh and each one was assigned to a phase transition, namely the PSW, the IC and the MST. They were activated during 100ms when their respective gait phase transition occurred. During the trials, they introduced random catch trials consisting of (i) missing stimulation, (ii) 200/500ms delayed stimulation, (iii) activation of another vibrotactile unit.
They showed that subjects can learn spacial and temporal relationship between the vibrotactile feedback and gait phase transitions and that subjects are able to tell when an expected stimulation was missing.

Aiming to improve dynamic gait in transfemoral amputees, Plauché et al. elaborated in 2016 [8] a prototype conveying information about ground contact based on the measurement of the COP under the prosthetic foot. As COP location on healthy subjects can be mapped to each phase of the gait cycle, the goal was to geographically map the COP position to vibrotactile

feedback around the residual thigh. The device was composed of force sensing resistors (FSRs) measuring ground pressure. They were placed under the prosthetic foot at major pressure points. The signal from the FSRs was processed by a microcontroller which computed the COP and the most relevant feedback. Finally, the feedback was provided by linear resonant actuator motors equally spaced along the circumference of the thigh. They proposed two feedback strategies. The first one consisted of a continuous feedback about the live location of the COP of the prosthetic foot, while the second consisted of a discrete stimulation triggered when the COP deviated from its nominal path.
They observed improved position control of the prosthetic leg and torso with better results with the discrete feedback condition.

Later in 2017, Lauretti and colleagues [42] investigated the effects of vibrotactile feedback on balance control and if such feedback could restore knee-joint proprioception in LLA. They used FSRs placed on the prosthetic foot in order to assess balance loss through COP knowledge. When imbalance conditions are met, vibrotactile feedback is sent. They also used two accelerometers placed on the user's thigh and leg to compute the knee joint angle. The angle feedback was based on a phenomenon called "Apparent Moving Sensation" (AMS), where the user feels a moving dot on the skin through the action of two vibrotactile actuators activated simultaneously. By modulating the intensity of the stimulus of each actuators, it is possible to make this apparent dot move in the space between the actuators. The point perceived will be equidistant to the two actuators if their intensity is equal or it will be shifted towards the more intense actuator stimulus. They used continuous feedback (with two tactors) and discrete feedback (requiring at least three tactors) as it can be seen in Figure 2.3. Two experiments were conducted: (i) assessing the subjects ability to control their posture on a moving platform under several feedback conditions and (ii) evaluating the subjects ability to relate vibrotactile feedback to the knee-joint angle under several feedback conditions (location of the vibratory units, continuous and discrete feedback). To do so, subjects were asked to reach several angular position with their knee.
They showed that patients have better postural control as well as an increase in precision under feedback condition. However, they did not see any significant discrepancies between continuous/discrete nor between the different tactor positioning.

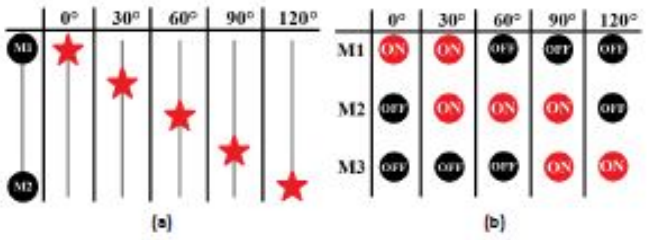

Figure 2.3: Feedback system based on AMS: a) continuous feedback through the activation of actuators M1 and M2; the star, representing the point felt, can be shifted between the actuators depending on the relative intensity of M1 and M2; b) discrete feedback through the activation of one or two adjacent actuators M1, M2 and M3 at maximum intensity
[42]

Conclusion about Vibrotactile Stimulation:

Being widely studied, vibrotactile systems are an efficient way to provide feedback. For example, association between gait phase transitions and vibrations can be learned [41], while position control can be improved [8, 42]. Moreover, vibrotactile units are compact, cheap and have low consumption [31, 39]. In addition, such devices are reliable, as they are not influenced by external inputs, like the skin state. They only suffer from habituation, which can be easily reduced using higher frequency stimulations and discrete stimulation patterns [39]. Moreover, discrete stimulation patterns seem to lead to greater performances compared to continuous ones. The most interesting property about vibrotactile feedback is that kinesthetic illusions can be elicited [38]. This paves the way towards a body integrated type of feedback, which will be more intuitive and modular. Still, vibratory stimulations take time to be processed by the brain, which prevents real-time feedback applications [40]. Would training shorten this reaction time?

2.2.3 Electrotactile Stimulation

In a 2007 study [43], Buma et al. investigated the application of an electrotactile display (ETD) for feedback about the prosthetic knee angle. More precisely, they studied the effects of stimulus amplitude and discrete stimulation on habituation. The ETD featured several electrodes, each of them corresponding to a certain part of the knee angle range. In the first experiment, they measured sensation decay under continuous stimulation, with stimulation levels in the range between sensation and pain thresholds. In the second experiment, they applied burst stimulation while varying their duration as well as the duration of the interburst intervals.
They showed that applying discrete and more intense stimulation can reduce the habituation effect. Indeed, when applying continuous stimulation at the highest acceptable stimulation intensity (i.e. 80% in the range between sensation and pain thresholds), they observed that the perceived sensation decreased to almost zero in 15min, reaching a 50% decrease in perception in 185s. However, when applying discrete stimulus at the same intensity and by fine tuning of the (i) duration of the stimulus and the (ii) inter-stimulus interval, they managed to reach a decrease of 50% in perception in 473s, showing that habituation is drastically reduced when using intermittent stimulation.

In 2010, Pfeifer et al. [44] investigated the use of ETDs to encode the COP location through AMS. It can be elicited by using two pairs of electrodes spaced by a small distance (4cm) while varying their relative intensities. They used a voltage-based electrotactile stimulator providing biphasic square pulses at 4 kHz on the two pairs of electrodes. The electrodes were self-adhesive squares of 25 cm^2 and were placed on the lower back of subjects. The region defined between the two pairs of electrodes was discretised in five subregions were the AMS will move. These subregions were mapping foot regions. The experiment was devided into two parts. The first one was a static localisation task: subjects had to identify the correct active region by identifying it on a virtual foot sole placed in front of them. The second part consisted in a dynamic localisation task were moving patterns, inspired from locomotor activities, were produced.

They showed that subjects are able to recognise static as well as dynamic patterns even without training period.

Still on AMS, the team of Arieta et al. [45] studied in 2011 the recognition rate of AMS elicited with electrotactile stimulation. They used a stimulation frequency of 2kHz and round electrodes. These were placed by pairs in the lower back similarly as [32]. After first defining the sensory threshold, subjects were asked to identify the direction of the AMS while being exposed to 20 different stimulation patterns.
Through their results, they managed to produce a perceptible AMS with a recognition rate of 74.56%. However two out of the 16 participants had a recognition rate below 50%, which might be related to individual differences such as higher skin impedance or body fat distribution.

Earlier this year, Seps and colleagues [32] studied the influence of the electrical stimulation frequency and electrode size. They used three different stimulation frequencies, 2, 4, 6kHz, and three different electrode sizes, 4.9, 8 and 25cm^2. Electrodes were placed on different spots in the lower back of subjects. This region was chosen due to its low cognitive load. The experiment was divided into several parts and repeated for each frequency and size. The first part consisted of evaluating the stimulation range that can be applied, i.e. defining the sensory threshold, comfort threshold and pain threshold. The second part aimed to assess the threshold sensation awareness for each electrode pair respectively. They also measured the evolution of skin impedance, inflowing current as well as power consumption of the electrodes.
They showed that a higher mean stimulation range can be obtained when using smaller electrode sizes. Frequency also increases the mean stimulation range. Moreover, big sized electrodes seem to reduce the inter individual differences. They also showed that skin impedance decreases when electrode size increases, resulting in higher inflowing current. Finally, they showed that smaller electrodes have higher consumption to reach their comfortable threshold compared to big sized electrodes. These results seem to give the edge to larger sized electrodes over small ones.

In 2012, Webb et al. [46] studied the sensory threshold related to an electrotactile stimulation on the thigh of subjects. Moreover, they aimed to determine if different movement patterns can enhance or diminish the perception ability. To do so, they used an array of eight equidistant spaced annular electrodes (33mm diameter) delivering asymmetrical biphasic pulses. This electrode ring was placed around the thigh of healthy subjects. In the first session, subjects were asked to adopt different postures such as laying supine, static knee flexion whilst standing and static knee extension whilst seated. In the second session, subjects were asked to walk on a treadmill at a self-selected comfortable speed. In these two sessions, they assessed the sensation, the discomfort threshold levels and the ability to discriminate the location (in case of stationary stimulus), the speed and direction of a stimulus.
They showed that subjects are able to identify correctly the stimulus characteristics. Most importantly, they showed that the mean comfort sensation level increases a bit when walking: it raised from 30.5mA to 37.8mA at 40Hz. Moreover, a separation between comfort and discomfort levels remains in static and in walking conditions. This separation is key in biofeedback device as it allows to provide a stimulation while avoiding the pain threshold.

Conclusion about Electrotactile Stimulation:

Electrotactile stimulation presents some advantages. Electrodes are relatively small, cheap and low consumption [34]. Moreover, they can be used to provide, with success, several types of sensations including vibration, tingling, pressure, itching or AMS [44, 45], which can be elicited without pain [46]. However, there are some limitations such as habituation but, just as for vibrotactile stimulations, this can be prevented using higher frequency or discrete stimulations [43]. Bigger electrodes perform better than small ones [32], introducing a trade off between a compact system and an efficient one. Electrodes are sensitive to the ever-changing condition of the skin, altering the amount of current passing through. Furthermore, inter-individual differences exist such as body fat location, that can increase the impedance [45]. This makes electrotactile feedback based systems difficult to design as (i) their performances are not constant and (ii) they need to be patient tailored.

2.2.4 Hybrid Stimulation

In 2014, D'Alonzo and colleagues [47] proposed a hybrid vibrotactile and electrotactile (HyVE) stimulation to produce sensory feedback for upper-limb prosthesis. Based on the fact that these feedback modalities activate different skin receptors, they hypothesised that they can be used to provide two simultaneous afferent information streams, which will be perceived independently by the user, even though they are delivered at the same location. It could, thus, enable to deliver two types of information about a given external stimulus with one single device, whereas it would require two single modality devices to do the same. The HyVE physical interface consisted of a vibratory unit placed on top of a self-adhesive electrode delivering current pulses. The first experiment they did consisted of assessing if subjects were able to discriminate the two modalities under HyVE stimulation. They managed to show its feasibility. Then, they tested if HyVE allowed to transmit more information than a single modality stimulation. While receiving stimulation, subjects were asked to recognise a set of discrete information that were communicated.
They demonstrated that HyVE interface increases the number of successfully recognised sets of information, improving the information transmission.

Later that year, they published another paper assessing the ability of healthy subjects to recognise multi-channel stimuli from HyVE [34]. They focused on five channel interfaces, as it would be the case for hand sensory feedback applications.
When comparing performances with five channel single modality interfaces, they showed that multi-channel sensory information is transferred better using HyVE. Indeed, HyVE stimulation pattern recognition rate is higher and more consistent than single modality interfaces.

Conclusion about Hybrid Stimulation:

Not much has to be said about HyVE: it is a combination of electrotactile and vibrotactile feedback, which takes advantages of both techniques [34, 47]. Where HyVE is standing out is that it allows to transmit two types of information simultaneously with only one device. This is interesting as more characteristics about an external stimulus can be transmitted. Consequently, it is less bulky than a vibrotactile or electrotactile based system providing the same amount of information. This allows to save space on the stump.

2.2.5 Auditory Stimulation

In 1999, Lundborg et al. [33] investigated the possibility of using hearing as substitution for hand tactile sensation. They proposed a sensor glove with five small electric condenser microphones (one for each finger of the hand) to detect friction sounds due to active touch. In order to be able to differentiate the origin of the sounds, these were sent to the ears with different intensities. Experiences were made on several subjects including those with median nerve injuries, those with fresh replantation of amputated forearms, as well as two patients with cosmetic prosthesis. Two types of experiments were conducted with 10 trials each. In the first one, patients were asked to identify, without looking at the hand, which fingers were randomly touched. In the second experiment, subjects were asked to differentiate between textures (glass tube, aluminium tube, paper roll and tree trunk) while moving their hand, or prosthetic hand, onto the surface. For both experiments, a training period of less than 10 minutes was done.
They showed that auditory feedback could be used as a sensory substitution mean. Indeed, subjects were able to better identify the touched fingers and textures under auditory feedback condition with respect to the no feedback condition.

In a subsequent study, Lundborg et al. [48] investigated the role of training in audiotactile interaction. To do so, they gathered six subjects to whom they equipped the terminal phalanx of the right index finger with a miniature microphone picking up the friction sound as described above. This sound was then transposed to an earphone in the right ear. The experiments consisted of presenting the subject with a tactile stimuli, i.e. brushing the index finger at 1Hz with and without auditory feedback. Finally, subjects were also presented with auditory stimulations alone, matching those obtained with finger stimulation. Prior to the experiment, three subjects were untrained while the others had a daily 15-minute training session with the device during a week before the experiment. During the experiments, functional magnetic resonance imaging (fMRI)[1] was used.
Thanks to fMRI, they showed that in trained subjects, auditory stimulations alone are processed in the somatosensory cortex, which is not the case for untrained subjects. This shows that substitution of sensibility with hearing is possible after training.

In 2012, Yang et al. [49] proposed a lower extremity ambulatory feedback system (LEAFS) providing real-time gait feedback. The system was based on auditory information in order to

[1] fMRI measures brain activity by detecting blood flow variation: when a brain area is used, blood flow increases in that area

reduce gait asymmetry in lower-limb amputees. The LEAFS was made of an insole containing several force sensing resistors through which ground-reaction forces are measured. The IC time and PSW time were extracted from the sensor data, allowing computation of the stance time (ST) (see Equation 2.1). Then the symmetry ratio (SR) was computed as in Equation 2.2. If this SR was below a certain threshold, the LEAFS emitted a beep, indicating strong asymmetry. Three transtibial amputees participated to the experiments. They performed a pre-test (control), a training session with the LEAFS, and finally a post-test. During the experiments, trunk sway was also measured.

$$ST = t_{IC} - t_{PSW}; \tag{2.1}$$

$$SR = \frac{ST_{Affected\,Leg}}{ST_{Intact\,Leg}} * 100\%; \tag{2.2}$$

They showed improvement of SR by comparing pre- and post-tests with an overall increase of 9.9±14.5%. They also observed a reduction of trunk sway. This suggests that auditory feedback can be used to improve gait symmetry in LLAs.

The coordination of rhythmic movement with an external rhythm is called sensorimotor synchronisation, and it has been widely studied over the last years. Auditory pacing has shown its benefits for patients with walking deficits [50].

In a 2007 study, Hausdorff et al. [51] investigated the effects of rhythmic auditory stimulation (RAS) on the stride-to-stride variability in patients with Parkinson's disease. 26 patients having the disease participated to the study, along with 26 age and sex matched healthy subjects. The RAS was provided by a metronome set to a desired rate, to which subjects were asked to match their ICs over a 100m distance. To extract gait parameters, a force-sensitive system was used. It was composed of a pair of shoes containing eight pressure sensitive sensors measuring the vertical forces under the foot. This allowed computation of gait parameters including the average stride time (and cadence), average swing time (as percentage of gait cycle), stride time variability and swing time variability. The variability measures were quantified using the coefficient of variation defined as the ratio between the standard deviation of a parameter and the mean of that parameter. Comparison of the performance between the two groups, i.e. subjects with Parkinson's disease and healthy subjects, was made over six walking experiments, with a 2-minute break between each. These were performed in the following order: (i) walking without RAS at usual pace (baseline), (ii) walking with RAS matched to the baseline cadence, (iii) walking at comfortable pace without RAS, (iv) walking with RAS at 110% of the baseline cadence, (v) walking at comfortable pace without RAS and, after 15-min rest, (vi) walking at comfortable pace without RAS. The comfortable pace experiments were designed to assess immediate and delayed retention effects.
They showed that RAS reduces the stride-to-stride variability in subjects with Parkinson's disease. Moreover, carry over effects were observed both immediately and 15min after walking with RAS. Still, the effects may be rate dependent, as significant effects were only observed with RAS at 110% of the baseline cadence. In contrast, RAS induces an increased variability in healthy subjects and fewer carry over effects were observed for them.

The same year, Roerdink et al. [52] assessed the effects of acoustically paced treadmill walking on gait coordination in people after stroke. 10 people who had a stroke, along with nine

healthy subjects, participated to the study. Small diodes were mounted on the subjects shoes, which allowed movements recording through a three dimensional active-marker motion analysis system. The rhythmic acoustic pacing stimuli were produced by a computer and alternately sent to the left and right ear through an earphone. After defining each subject's comfortable walking speed, three experimental speed conditions were designed: (i) slower than comfortable speed, (ii) comfortable speed and (iii) faster than comfortable speed. For each speed condition, subjects were asked to walk naturally on a treadmill for 90s. Then, it was followed by a three-minute walk at comfortable speed, where the auditory stimuli were activated. Subjects were asked to synchronise their ICs with the ipsilateral stimuli. During the walk, the frequency of the auditory cues were increased from 90% (for ±60s) via 100% (for 60s) to 110% (for ±60s) of the preferred stride frequency observed in the comfortable speed condition.
They observed that the stride frequency increased significantly with increasing acoustic pacing frequency, which illustrates that patient are able to adapt their gait to the rhythmic stimulation. Moreover, they showed that the RAS improved the temporal and spatial symmetry in after-stroke subjects.

Last year, Forner-Cordero et al. [53] studied the adaptation of gait pattern to imperceptible variations of rhythmic auditory cues, i.e. beep sounds, generated by a metronome. Infrared cameras were used to monitor reflexive markers placed to the right and left heels and on the back of the dominant hand. Patients were asked to walk on a treadmill at 1.11 m/s for five minutes while synchronising their gate to the auditory cue period. They used a ±1ms variation as subliminal change in the auditory cue. Three experimental conditions were performed. In the first one, subjects were asked to walk at the sound of an isochronous[1] metronome with period of 566ms for 231 steps. In the second experiment, subjects walked 59 steps under isochronous metronome (566ms), followed by a ramp increase of the period until reaching a period value of 596ms. Then subjects experienced a plateau phase at 596ms for 30 steps and finally a ramp decrease back to 566ms, followed by an isochronous period at 566ms for 26 steps. The third condition followed the same template as the second one, except that the first 59 steps are now followed by a ramp decrease to 536ms then back to 566ms. An illustration of these three experimental conditions can be found Figure 2.4.
First of all, they observed that subjects synchronise rapidly to the auditory cues. Moreover, they showed that subjects are able to synchronise with subliminal auditory cue changes, even though these are not consciously detected. This suggests that supraspinal inputs at least strongly influence the central pattern generators.

[1]With regular time intervals

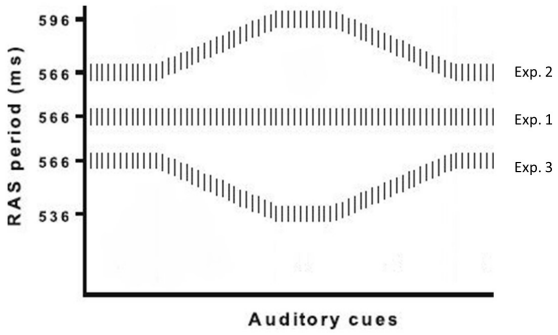

Figure 2.4: Rythmic Auditory Stimulation (RAS) period evolution over the three experimental conditions, adapted from [53]

Conclusion about Auditory Stimulation:

Interesting results have been shown using auditory stimulation, including improvement in gait symmetry, trunk sway reduction and even allowing discrimination between textures [33, 49]. Still, this technique requires training in order to be fully effective [48]. Nevertheless, the most interesting aspect relies on the sensorimotor synchronisation, which describes the property of rhythmic movements, such as walking, to be driven by an external rhythm. More specifically, subjects are able to synchronise and follow, even subconsciously, the variations of a RAS, which can help reduce gait variability and tune gait parameters such as stride frequency [51, 52, 53]. Hence, auditory stimulation is a suitable tool for gait rehabilitation. However, it is not adequate for a daily use as it requires the constant wearing of earphones. Moreover, it can be very annoying to hear recurrent beeps, which could be corrected by decreasing the beep's occurrence as in [49].

2.2.6 Visual Stimulation

In 1996, Dingwell and colleagues [54] evaluated the effectiveness of Real-Time Visual Feedback (RTVF) to improve gait symmetry in LLA. To do so, they used a treadmill/force plate device allowing collection and comparison of gait parameters of both legs in real time. A screen was placed in front of the treadmill, providing the RTVF. Three different feedback conditions were used. The first one consisted of displaying the path of the COP for each feet, allowing to see differences between the two such as difference in stride length. The second one consisted in displaying the Percent Stance Time (%ST) computed as in Equation 2.3. Alongside was also displayed its typical value (60%). Finally, a feedback of a Symmetry Index (SI) based on the Push Off Force (POF) was displayed. POF represents the maximum force recorded on the rear force plate for each foot. SI was computed as in Equation 2.4, ranging from -100% to +100%. Perfect symmetry was obtained when SI = 0%. Subjects (six healthy and six transtibial amputees) were asked to walk on a the treadmill first without feedback then with feedback (in the case of amputees). To assess asymmetry between both limbs, they computed, when

feedback was off and on, $SI_{COP}, SI_{\%ST}, SI_{POF}$ and $SI_{SingleStanceTime(SST)}$. This last one was used to assess the effects of the feedback on a variable not directly linked with the displayed feedback.

$$\%ST = \frac{ToeOff - PreviousHellStrike}{HeelStrike - PreviousHeelStrike}; \tag{2.3}$$

$$SI = \frac{POF_{right} - POFleft}{POFright + POF_{left}} * 100\%; \tag{2.4}$$

The authors showed that asymmetries for amputees are on average 4.6 times greater than for normal subjects. Moreover, they showed that subjects are able to modulate their gate pattern according to the RTVF. Indeed, RTVF can induce significant decrease in the degree of asymmetry for the displayed variables. However, the effects of RTVF on SI_{SST}, which was not displayed, are not obvious. Some feedback conditions seem to increase its asymmetry while others seem to decrease it. This may suggest that subjects alter their gate pattern to decrease one form of asymmetry while increasing others.

Five years later, Davis et al. [55] investigated the effects of RTVF on energy consumption. 11 amputees participated to this study. They were required to walk, at self-preferred speed, on a treadmill under five test conditions. The first and fifth tests were conducted without visual feedback. The second, third and fourth included visual feedback displayed on a screen. The first two consisted of the %ST ratio and POF feedbacks as in the study of Dingwell. The third feedback condition consisted of a butterfly plot displaying real time shear and vertical force information. Subjects were asked to make the displayed images as symmetric as possible. During the trial, a cardiopulmonary stress test system (VmaxST, SensorMedic) was used to measure gas exchange parameters.
Besides confirming the observations made by [54], they showed that RTVF can be used to reduce energy consumption. They observed an improvement of 22% in tidal volume[1] as well as a 6% and 3% improvements in VO_2 [2] and heart rate.

Last year, the team of Day et al [56] proposed a Principal Component Analysis (PCA) based RTVF for re-training walking on a treadmill. This system allowed to give visual feedback about multiple gait characteristics condensed into one-dimensional summary. Ten healthy and ten chronic stroke patients participated to the study. Subjects were asked to match a goal pattern based on the evolution of four parameters: the bilateral hip and knee joint angles. Healthy subjects had to match a stroke gait pattern while stroke patients had to match an healthy gait pattern. Visual feedback displayed a white goal zone, centered on a white target line alongside a red trace showing the subject's deviation from the goal pattern. Subjects were asked to adapt their gait pattern in order to maintain the red trace in the goal zone. Two experimental conditions were conducted. In the first one, subjects had no verbal explanations of which gait parameters they had to change in order to stay in the goal zone. In the second one, they were explicitly informed about which gait parameters were influencing the red trace.
They showed that, using PCA-based RTVF, subjects were able to improve their performance (i.e. stay in the goal zone). Moreover, non-stroke subjects are able to improve further when

[1] Air volume inhaled during normal breath
[2] Oxygen volume consumption per time unit during exercise

instructions are provided. This PCA-RTVF goes beyond the device proposed by [54, 55], enabling multi-dimensional feedback in a nice fashion.

Conclusion about Visual Stimulation:

RTVF seems to be promising in the framework of rehabilitation. It has proven to improve several gait parameters in an intuitive fashion, including gait symmetry [54]. However, RTVF is bulky, which makes it is not suitable for daily use as it relies on a screen; and to date, the long term effects it may have on the gait pattern of subjects are not fully understood [54, 55, 56]. Will LLAs be able to integrate a new gait pattern and be able to reproduce it without the RTVF? If so, RTVF could change rehabilitation. Moreover, gait improvements will be obtained without the need of wearing extra devices to provide feedback.

2.3 Selection of a technique for this thesis

Each of the techniques portrayed previously present advantages. Nevertheless, only the vibrotactile and the electrotactile modalities (and so the HyVE) seem to be more suitable for a daily life application as they are relatively small and more easy to accommodate to different body areas. However, due to the fact that the performance of electrotactile feedback is hard to control due to its high sensitivity regarding skin state and the presence of inter-individual variations, vibrotactile modality will be the selected technique to provide sensory feedback. This modality seems more reliable, more easy to control and offers a broad range of ways to provide feedback.

In the following chapter, the experimental part of this work, based on vibrotactile units, will be presented.

Chapter 3

Materials and methods

This chapter aims to describe the experimental part of this thesis. First, the goal of the experiments will be explained: what are we trying to observe? How are we planning to do it? Next, the materials used will be presented, followed by an explanation of the experiments that were conducted. Afterwards, the data acquisition and processing will be explained. Adaptations made due to the Covid-19 situation will be presented. Finally, this chapter will be concluded by mentioning what are the objectives and hypotheses regarding the experimental results, and explaining how will the data be analysed.

3.1 The experimental concept and research questions

As said previously, LLAs experiment sub-optimal locomotion leading to an asymmetric gait pattern. This asymmetric pattern can lead to complications such as musculoskeletal pathologies due to the extra stress placed on the intact leg. Therefore, a system that could improve gait symmetry would improve the LLAs quality of life.

Since LLAs subjects were not available for this study, we propose to work differently. Here, we will attempt to induce asymmetry in the gait pattern of healthy subjects using vibrotactile actuators. While subjects will be walking on a treadmill, these actuators will provide bilateral rhythmic stimulation to which a unilateral phase shift will be induced over time. The subjects ability to synchronise to this rhythmic stimulation will be observed. More specifically, is it possible to disturb/desynchronise the gait of healthy subjects without them noticing?

Moreover, the experiment will be repeated on different stimulated areas. The goal is to see whether, for a same perturbation, different synchronisation profiles can be observed by stimulating on different tendons. More precisely, is it possible to influence the knee flexion profile through tendon rhythmic vibratory stimulation?

3.2 Stimulated Area

Vibrotactile stimulations will be provided on several spots as it can be seen in Figure 3.1 below.

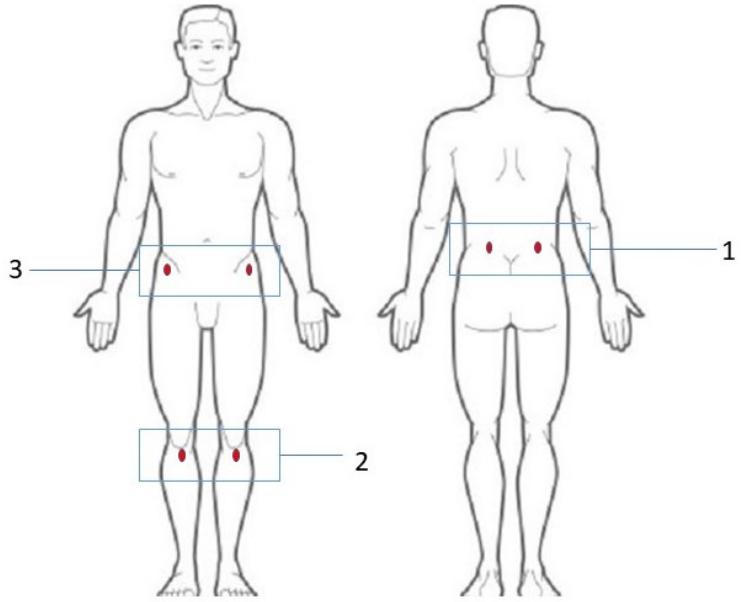

Figure 3.1: Vibrotactile units body placement; three different regions will be tested; the red dots represent vibrotactile units, adapted from [57]

The first region will be the lower back. This region is often chosen to provide feedback because it has low cognitive load [32]. Moreover, as it has no proprioceptive relevant influence on the gait mechanics, it will work as control situation for the rhythmic situation.
The two following regions are tendons: the patellar tendon (see region 2 in Figure 3.1) at the knee and the rectus femoris proximal tendon (see region 3 in Figure 3.1). These two tendons can be seen on the Figure 3.2 below. They were chosen because of their accessibility and due to their influence on the knee. Indeed, when stimulating these two tendons, Verschueren and colleagues [38] (see Section 2.2.2) observed effects on the knee displacement during gait. Moreover, these tendons are kept after both transtibial or transfemoral amputation, making them suitable spots for LLA stimulation.

The anatomy of interest is represented in Figure 3.2. The rectus femoris is a muscle belonging to the quadriceps muscle group. It is attached to the patella by the quadriceps tendon, and to the hip through the proximal tendon. It allows extension of the leg at the knee joint while allowing thigh flexion at the hip joint [58].

The patellar tendon is an extension of the quadriceps tendon from the patella, which connects the latter to the tibia. As it connects two bones, it is rather a ligament than a tendon. Its functions are the following. First, it assists during leg flexion, enabling proper leg extension.

Secondly, it helps maintaining the patella in its proper position [59].

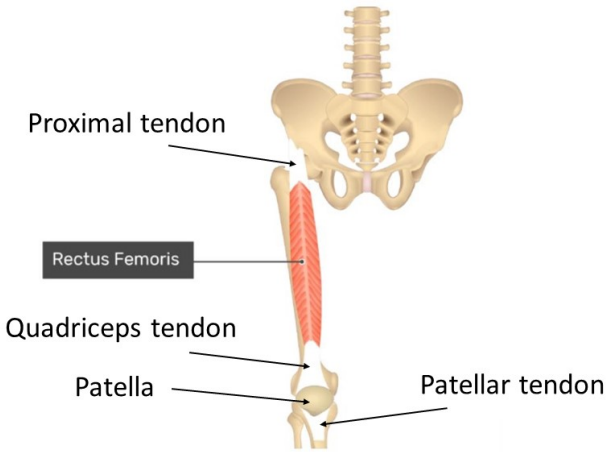

Figure 3.2: Anatomy of interest, adapted from [60]

3.3 Materials

Two *Haptuator Planar* vibratory units from *Tactile Labs* (Montreal, Canada) are used (Figure 3.3). These are 12x12x12mm^3 vibratory units designed for direct skin stimulation, having a bandwidth of 50-500Hz. They act like speakers and are connected to a computer through the jack entry. The vibratory units are be placed on the given body location using adhesive paper and cohesive bandages.

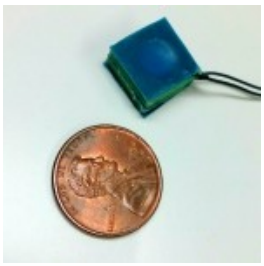

Figure 3.3: *Haptuator Plannar* from *Tactile Labs*, compared to a coin [61]

Four inertial measurements units (IMUs), the *NGIMU* from *x-io Technologies* (Bristol, UK) (see Figure 3.4), are used to measure the evolution of the knee joint angle across gait cycles. These incorporate several triple-axis sensors but only the gyroscopic signal is used, with sampling

frequency f_s of 100Hz. The IMUs are placed around the thigh and shank of both legs as seen in Figure 3.4. They allow to monitor the knee joint angle of each leg during the experiments thanks to the embedded gyroscope.

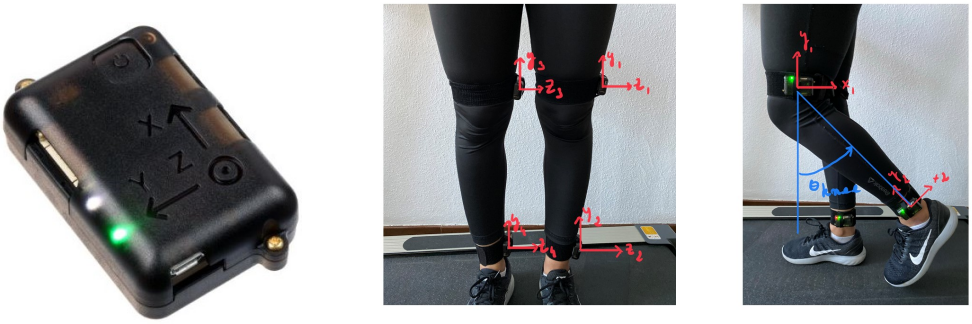

(a) IMU from *x-io Technologies*

(b) IMUs placement around the thigh and shank, and knee joint angle definition (θ_{knee})

Figure 3.4: IMUs

Finally, experiments take place in the gait laboratory of UCLouvain (Woluwé), using the available treadmill.

3.4 Methods

This section covers the experimental protocol and the data processing. All the proposed experiments and data treatment, to extract relevant information, will be explained throughout this section. Unfortunately, this part had to be adapted because of the Covid-19. Nevertheless, the first part of this section will explain how the experiments should have been carried out and how the data should have been processed. Finally, the adaptations made due to the Covid-19 will be addressed.

3.4.1 Experimental protocol

A 70Hz vibration of 100ms duration is used as vibratory stimulus. The stimulus delivery is timed according to the phase value of a sine wave of 1.3s period. Two walking experiments are conducted: a no delay situation and a unilateral induced delay. Each experiment is repeated among the different body regions presented in Figure 3.1.

1. **No delay**: in this experiment, subjects are asked to walk on the treadmill at 3,6km/h. After 30s of walking, the vibratory units are activated. The stimuli are isochronous and delivered between the right and left units with 0.65s interval as seen in Figure 3.5. Subjects are asked to make a step with their left/right foot when the left/right unit vibrations are

perceived. The stimulation lasts for 6min. The no delay experiment made on the first region is defined as control situation, for the reasons mentioned previously (see Section 3.2).

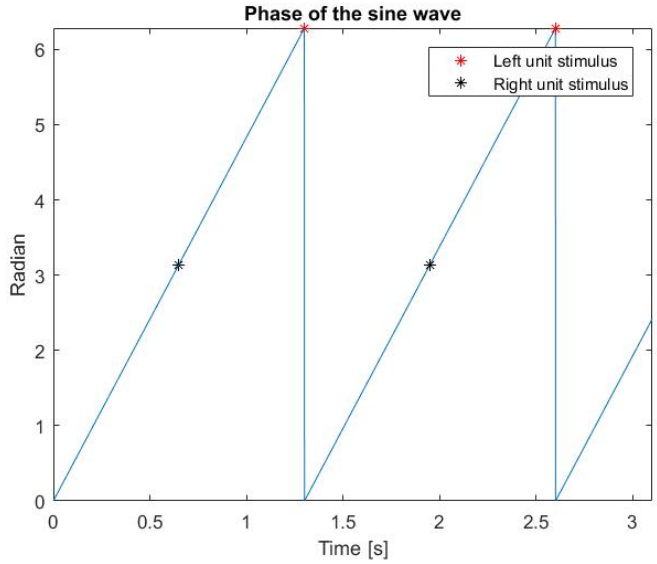

Figure 3.5: Stimuli delivery (no delay)

2. **Unilateral delay**: This experiment follows the same layout as the control experiment. Subjects start walking on the treadmill at 3,6km/h while the stimulation starts after 30s walk. Here, the right unit stimulus is no longer isochronous. After 60s of stimulation, a 1ms delay in the delivery of the vibrations is induced. Such 1ms delay is not consciously perceived (see Section 2.2.5). The evolution of the delay is represented in Figure 3.6. It follows a ramp increase of +1ms every two right stimulus, until a total delay of +30ms is reached. Then, it is followed by a 60s plateau phase at the new stimulus configuration. Finally, a ramp decrease of -1ms every two right stimulus is induced until the delay is fixed. The stimulation lasts again 6min.

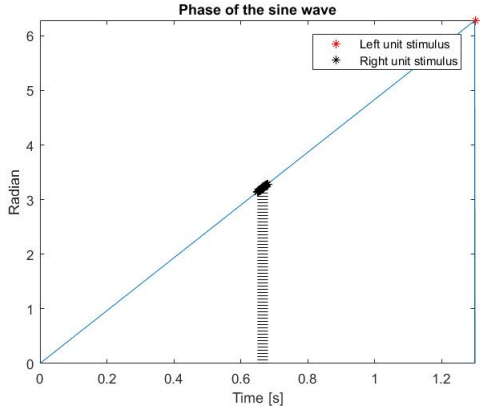

(a) Delay induced on the right unit stimulus delivery; the shaded region covers 30 ms

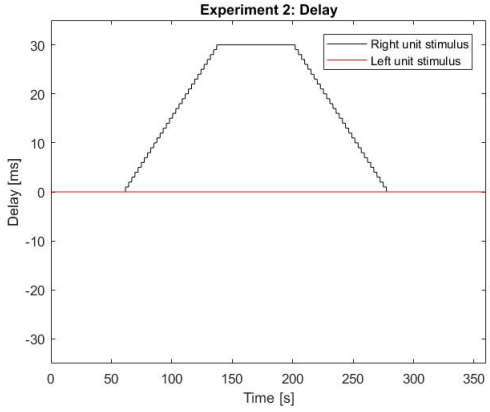

(b) Evolution of the delay throughout the stimulation

Figure 3.6: Experiment 2: unilateral delay

3.4.2 Data acquisition and processing

The signals of interest are given by the gyroscopes embedded in the IMUs. These gyroscopic signals give the angular velocities of the shank and thigh in [°/s]. The goal is to extract first the knee angle profile and then the timing of the ICs as seen in Figure 3.7. The knee angle profile is supposed to be used in data analysis to assess the effects of the different stimulation locations on the knee movement. The occurrence of the ICs will be used to assess the effects of the delays induced in the stimulus delivery.

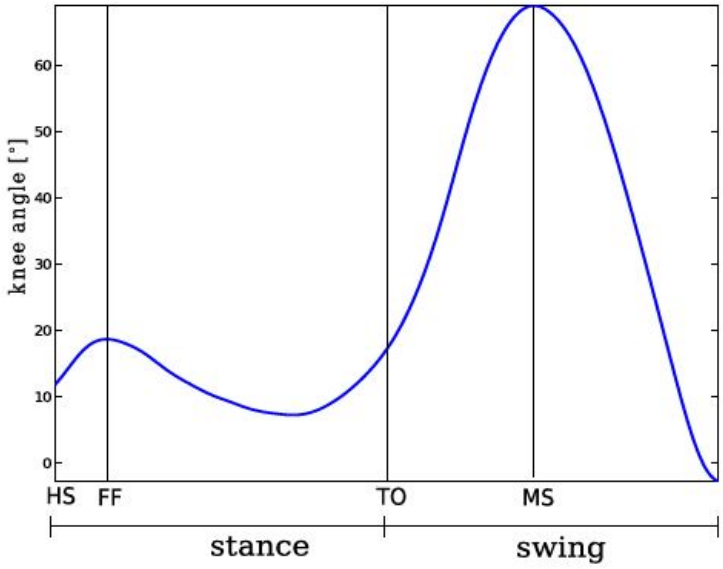

Figure 3.7: Knee angle profile and IC (HS in the Figure) detection; MS, TO and FF correspond to other gait events
[62]

First, the offset due to the IMUs placement is corrected. This is done by subtracting to the gyroscopic signals their respective mean value when the subjects are standing still.
Second, in order to extract the knee flexion angle as defined in Figure 3.7, the knee angular velocity must be obtained. This is done by subtracting the thigh angular velocity to the shank angular velocity. The resulting signal can be seen in Figure 3.8. Afterwards, this signal is filtered using a zero phase lag 2nd order butterworth filter with normalised cut off frequency $f_c = 0.1$[1]. The *Matlab* "butter" function is used for the design of the filter, giving the transfer function found in Equation 3.1. The spectrum of the filter, as well as the one of the original signal, can be seen in Figure 3.8. The *Matlab* function "filtfilt" is used to filter the signal. The result can be seen in Figure 3.8.

$$H(z) = \frac{0.0201 + 0.0402z + 0.0201z^2}{1 - 1.561z + 0.6414z^2} \tag{3.1}$$

[1]The normalised frequency is defined as $f_N = \frac{2\pi * f}{f_s}$

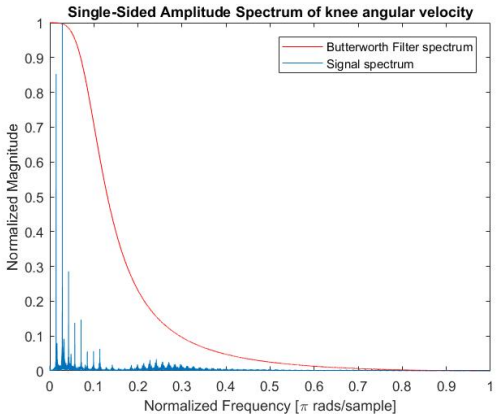

(a) Spectra of the knee angular velocity and the filter

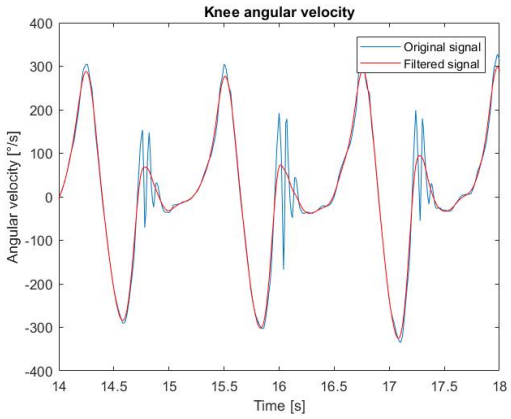

(b) Original and filtered knee angular velocity

Figure 3.8: Filtering

The fourth step consists of integrating the filtered signal to obtain the knee flexion angle. However, the accumulation of the signal noise during the integration process induces a drift in the resulting signal: the resulting values deviate from their true value [63]. To correct this deviation, interpolation of the signal with a polynomial of degree 20 has been made. In order to avoid negative values of the knee angle, the resulting signal is corrected by subtracting the mean negative peak value. The resulting knee angle profile can be seen in Figure 3.9.

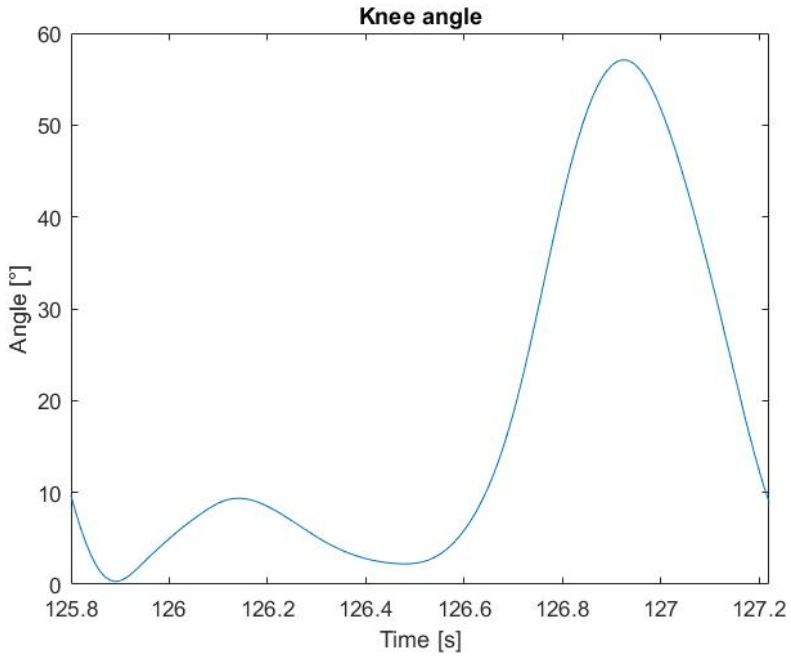

Figure 3.9: Knee angle profile

The fifth and final step consists of extracting the IC events. The variation in the occurrence

of ICs will be used to assess the effects of the delays in the rhythmic stimulation. To do so, the shank angular velocity is used. Indeed, it is possible to extract the IC event using the shank's angular velocity around the z-axis defined in Figure 3.4(b). The IC is corresponding to the first negative peak appearing after the local angular velocity maximum [64] as seen in Figure 3.10. This maximum corresponds to the MSW.

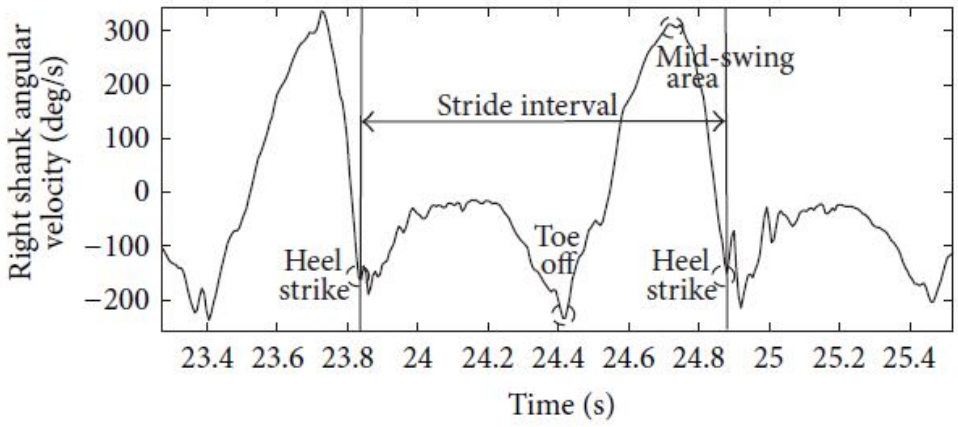

Figure 3.10: Gait events and shank angular velocity profile [64]

The extraction is done as follows. First, a zero phase lag 2nd order butterworth filter with normalised cut off frequency $f_c = 0.1$ is applied to the signal using the *Matlab* 'butter' and 'filtfilt' functions. Second, three thresholds, th_1, th_2 and th_3 are defined according to [65], with some adaptations. Their definitions can be find in Equations 3.2, 3.4 and 3.4.

$$th_1 = 0.6 * max(\omega), \tag{3.2}$$

$$th_2 = 0.8 * \frac{1}{N} * \sum_{i=1}^{N} (\omega_i > \overline{\omega}) \tag{3.3}$$

$$th_3 = 5 * |\frac{1}{N} * \sum_{i=1}^{N} (\omega_i < \overline{\omega})| \tag{3.4}$$

Where ω represents the shank angular velocity, $\overline{\omega}$ represents the mean shank angular velocity and N represents the number of samples. Using these thresholds, the MSW can be find as the local maximum ω_j satisfying the following conditions:

$$\omega_j > th_2; \tag{3.5}$$

$$\omega_j - th_1 \geq min_{j-1} \tag{3.6}$$

Where min_{j-1} represents the local minimum happening right before the given local maximum ω_j. Finally, an IC is found whenever a local minimum ω_j meets the following conditions:

$$\omega_j < \overline{\omega} \tag{3.7}$$

$$\omega_j + th_3 \leq max_{j-1} \tag{3.8}$$

If met, max_{j-1} represents the local maximum happening or the MSW before the local minimum ω_j. The results of this procedure can be found in Figure 3.11(a) and (b).

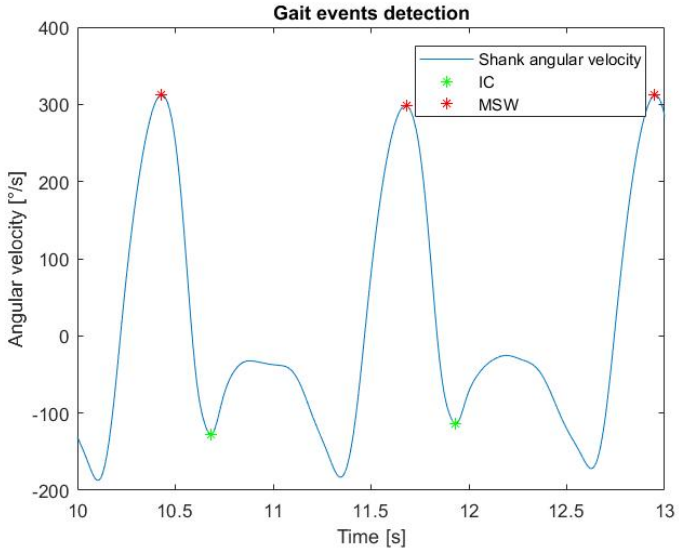

(a) Detection of the MSWs and ICs based on shank angular velocity

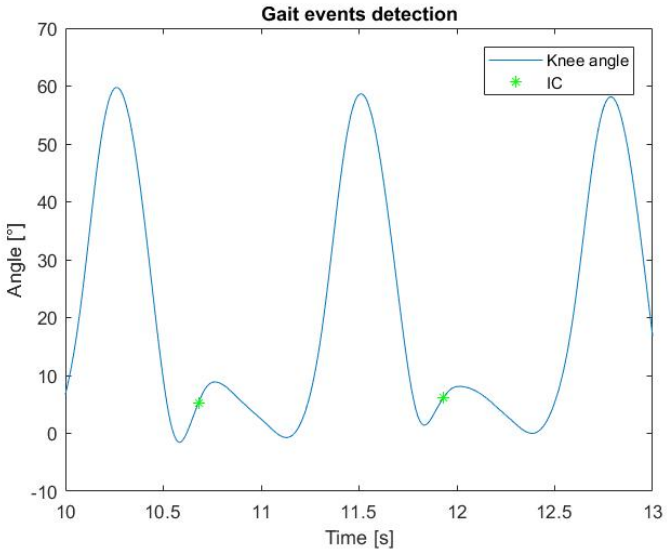

(b) Knee angle profile and detection of the ICs

Figure 3.11: ICs detection

3.4.3 Adapted experimental protocol due to Covid-19

Due to the global pandemic we are still facing at the time of writing, several adaptations to the proposed work were made. The first one concerns the location were experiments were

supposed to take place. They were set to be done in the gait laboratory of UCLouvain (Woluwe). However, the lab closed due to the measures taken by the government. Experiments will be done using my home treadmill, the *Powerpeak fTM8317P* treadmill (see Figure 3.12). This is a motorised treadmill enabling to set speed from 0 to 16 km/h as well as ground level. In the framework of this thesis, a flat level was used.

Figure 3.12: *Powerpeak* treadmill
[61]

The second one is regarding the stimulation modality. Indeed, one vibratory unit broke a little before the start of the lockdown on March 18th. It is currently not possible to reach a specialist to repair this unit and hard to get another one. This compromises the experimental set-up which has been planned, as it requires two working vibratory units. To palliate this problem, the experimental set-up has been adapted. Auditory stimulation will be used to replace the vibratory stimulation. A 100ms sinusoidal wave of 1000Hz is used as auditory stimulus and a pair of headphones (*Beats Mixr* from *Beats by Dre*) are used to receive the auditory stimulus provided by a custom made *Matlab* code. The headphones are connected to a computer running the *Matlab* code using a jack cable. In order to keep the bilateral stimulation principle, auditory cues are distributed on both ears: vibratory stimulation which were dedicated to the left/right leg, are replaced by auditory cues on the left/right ear. However, it will not be possible to see the influence of stimulation location with auditory cues. Consequently, the ICs timing are the only relevant data to analyse.

Furthermore, the effects of a new delay profile will be studied (see Figure 3.13). This last experiment is pretty similar to the second one. The difference resides in the left unit stimulus, which is not isochronous anymore. The experiment is conducted the same way as the second one, with the delay applied in a mirror fashion to the left unit stimulus. This creates a total 60ms perturbation. Besides that, the experimental protocol remains identical.

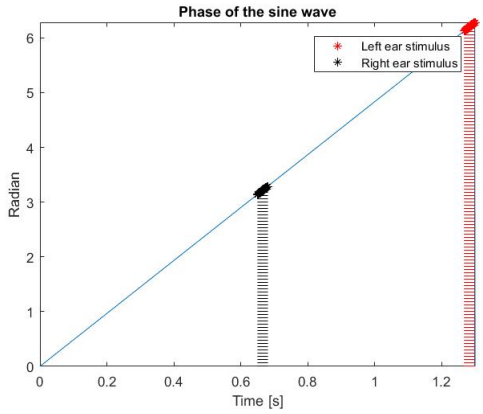

(a) Delays induced on the right and left unit stimuli delivery; the shaded regions cover 30 ms each

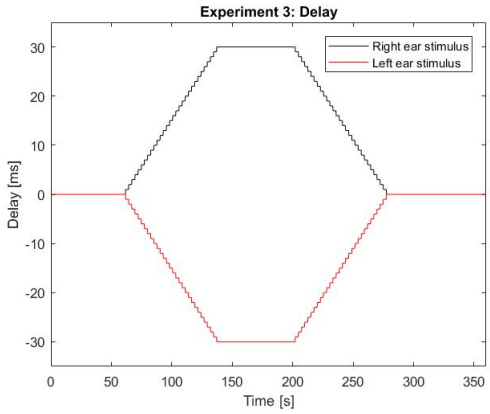

(b) Evolution of the delay from stimulation onset

Figure 3.13: Experiment 3: bilateral delay

Finally, due to the confinement measures, the sample size is limited. Five healthy subjects (four with no particular medical history) participated to the experiments: three females (height 171 ± 2,65cm; weight 68.33 ± 6.51kg; age 32.33 ± 19.35 years; mean ± standard deviation) and two males (height 189 ± 4.24cm; weight 79 ± 8.48kg; age 42 ± 26.16 years). Among these subjects, only one had a medical history: subject two had a surgery procedure in the left femur in the '80s and broke his left ankle in the '90s.

3.5 Objectives, hypotheses and statistical analysis

This section concludes this chapter. It regroups the different objectives and expectations regarding the future results. Moreover, this section will present the different statistical tests that will be used. These were conducted in *R*. The different assumptions made by these tests are discussed in Appendix G.

As mentioned previously, showing the effects of tendon vibration location is no longer part of the objectives of this work. The final objectives are the following:

- Show that subjects managed to synchronise to an external rhythm;
- Show that subjects are keeping in memory a trace of the rhythm;
- Show that the delays induced in the stimuli delivery managed to disturb the gait of subjects.

3.5.1 Rhythm synchronisation

The stimulation profile for the control experiment, along with the expected behavior of the inter-steps times (ISTs) can be seen in Figure 3.14. As it can be seen, several temporal markers and regions are represented. Their signification will be clearer across the following points. In region one, subjects are walking at their own pace at 3.6km/h, with a certain mean IST represented by the black dashed line; the black solid line represents the standard variation of the IST. After 30s of walk, the beeps are turned on (region 2A). This creates a first perturbation to the gait of subjects. It is expected that the onset of the beeps will cause an increase in the variation of the IST. This is illustrated by the spread of the points in region 2A, as well as the deviations of the black solid line. After a certain time, this increased variation will naturally decrease and stabilise around 0.65s IST in region 2B, as seen in Figure 3.14.

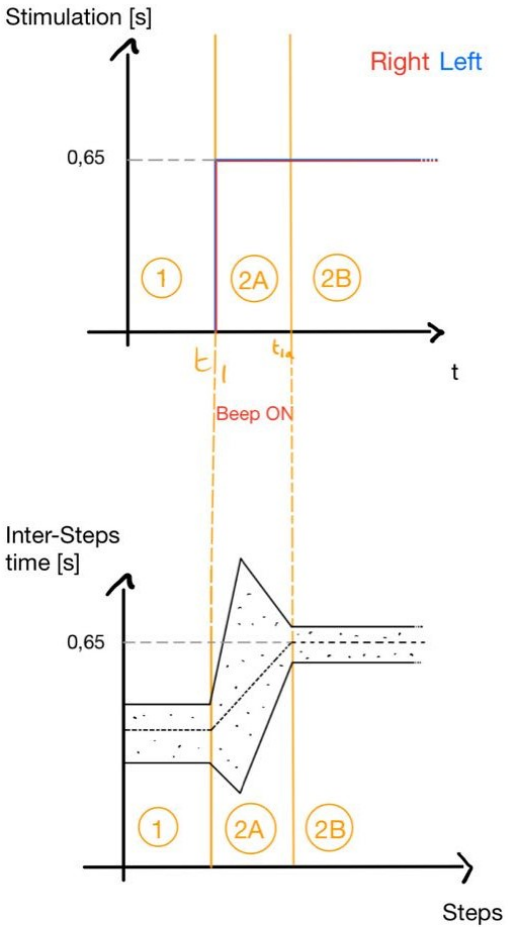

Figure 3.14: Expectations about the rhythm synchronisation

To assess the precision of the synchronisation, a one sample T-Test is proposed. This tool allows to compare the mean of a sample with an expected value. Hence, it will compare, for each subjects, the mean of the IST starting from region 2B (see Figure 3.14) with 0.65, the expected mean. The hypotheses of the T-Test are the following [66]:

$$\begin{cases} H_0 : \mu_i = \mu \\ H_A : \mu_i \neq \mu \end{cases}$$

Where μ_i and μ represent respectively the IST mean of the considered sample, and the expected mean.

3.5.2 Rhythm memory

The expectations regarding memory are represented in Figure 3.15. Since each experiment begins with a free walk in region one, and ends with a walk paced by the beeps, a memory effect is expected to be observed in the first region from one experiment to the other. It is expected that (i) the initial pace will progressively shift towards the imposed rhythm (see green "i" in Figure 3.15). This will show that subjects keep a trace of the rhythm induced in the previous experiment. Second, (ii) a decrease in the stabilisation time, that is a reduction of the duration of region 2A, is expected (see green "ii").

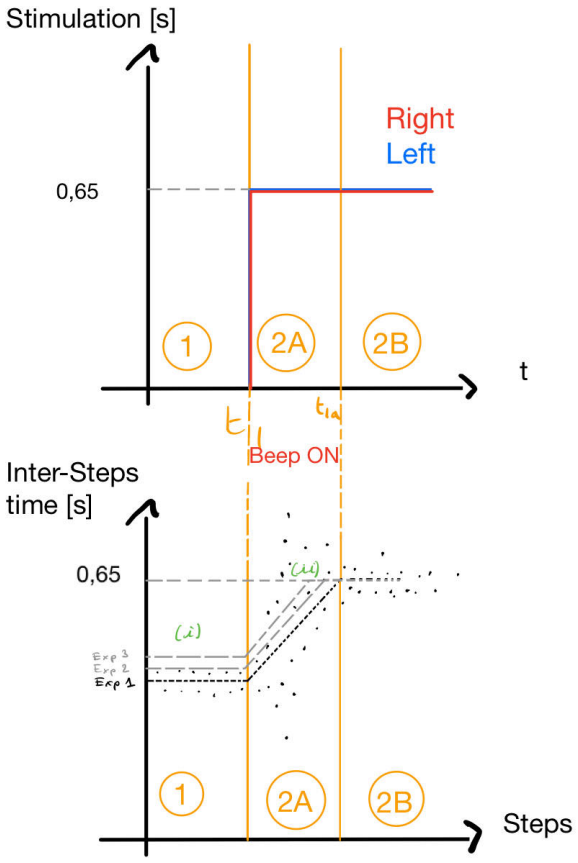

Figure 3.15: Expectations about the memory effects

To check assumption (i), a one-way ANOVA with repeated measures is suggested. This test is used to compare performance (i.e. the mean) of the same group of participants among different experimental conditions. The test will be performed on the first region. Its hypotheses are the following [67]:

$$\begin{cases} H_0 : \mu_{1i} = \mu_{2i} = \mu_{3i} \\ H_A : \mu_{1i} \neq \mu_{2i} \neq \mu_{3i} \end{cases}$$

Where μ_{1i}, μ_{2i} and μ_{3i} represent the mean of the IST for each of the three experimental conditions for subject i.

Thereafter, assumption (ii) will be assessed by fitting a curve to the data from region 2A and analysing the evolution of the time constant of this model. However, the time, or rather the step number n_{t1}, at which the region 2A begins must be defined first. Thanks to a sliding window of size five, the variance in the IST will be computed, for a given sample. After finding the step corresponding to maximum variance (max_{var}) in the early ISTs, n_{t1} will be defined as:

$$n_{t_1} = max_{var} - 2 \tag{3.9}$$

The following model is proposed for the data:

$$IST_{2A}(x) = a + b(1 - e^{-c(x - n_{t1})}) \tag{3.10}$$

With parameters a, b and c. The first two are defined as followed: (i) parameter a represents the offset in the y-axis, i.e. the mean IST of the first region. (ii) Parameter b is the difference between the steady state, i.e. the mean IST from region three to the end region, and parameter a. The third parameter, c, is defining the time constant $\tau = \frac{1}{c}$. This parameter will be defined according to an optimisation of the sum of squared errors. The curve of the model is represented in Figure 3.16.

Before optimisation, outliers must be carefully removed as they might affect the process. Outliers removal is done on each region independently, according to the following rule:

$$\begin{cases} if(IST(x) > q_{0.75} + 1.5IQR) : \\ \quad IST(x) = q_{0.95} \\ if(IST(x) < q_{0.25} - 1.5IQR) : \\ \quad IST(x) = q_{0.05} \end{cases}$$

Where the q_i are representing the quantile for the cumulative probability i and IQR stands for inter-quartile range. Defining τ for each experimental conditions will allow to assess the stabilisation time taken in each experiment. More specifically, a decreasing time constant across experiments will verify assumption (ii).

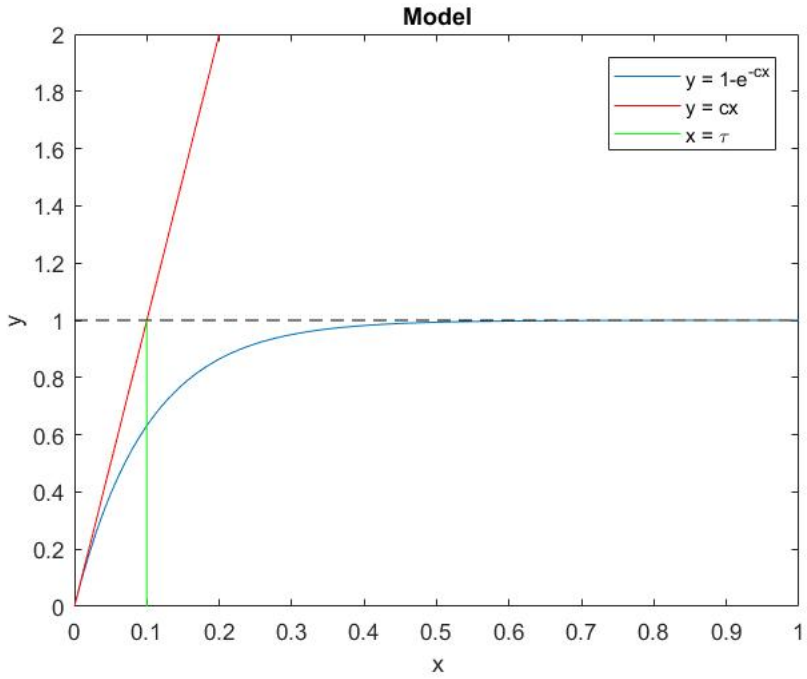

Figure 3.16: The model for $a = 0, b = 1, c = 10, n_{t1} = 0$

3.5.3 Rhythm disturbance

The predicted effects of the delays, along with the stimulation profiles for the different experiments, are illustrated in Figure 3.17. When comparing to the control experiment in region three, the delays, which start in the third region, are expected to induce an increase in the variation of the IST. This is represented by the brown and purple solid lines, which progressively deviate from the black solid line, which represents the variation of IST for the control experiment. When compared to region 2A, the way the variation in the IST settles in will be less sudden. This is due to the subconscious nature of the ramp increase.

The increasing variation is due to the phase shift between right and left stimuli, which will make the IST no longer equal. The right-to-left step ISTs will get shorter and shorter, while the left-to-right ISTs will be longer and longer (see Figures 3.6 and 3.13), until stabilising in region four. For the unilateral delay experiment (brown solid line in Figure 3.17), the left-to-right and right-to-left ISTs are expected to be modified by a value of $+\phi = 30$ms and $-\phi = -30$ms respectively. For the bilateral delay experiment, this value is expected to be doubled (2ϕ). Moreover, unlike in region 2A, no decrease in variation is expected when the plateau is reached in the fourth region. Indeed, right-to-left and left-to-right ISTs are not equal in the delay experiments. Therefore, variations in the IST are expected to oscillate between $0.65 \pm \phi$ms (unilateral delay experiment) and $0.65 \pm 2\phi$ms (bilateral delay experiment) in the fourth region. These variations are expected to decrease with delay suppression in the fifth region. When the sixth region is reached, the amount of variation will be similar to the variation in region 2A.

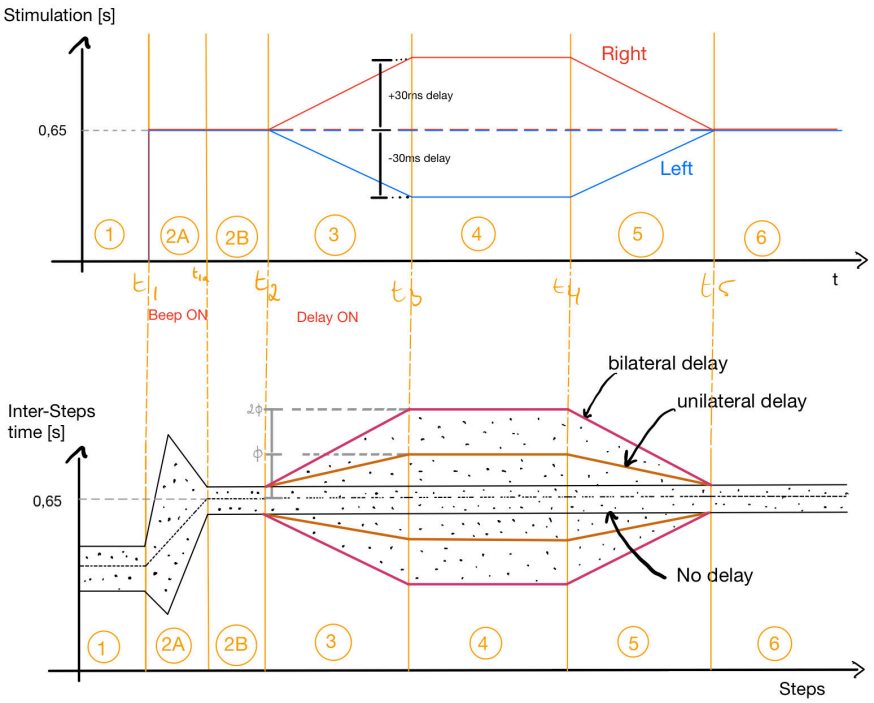

Figure 3.17: Expectations about the delays effects

To verify the delays effects, a Levene's test is proposed. This test is used to assess the variance equality between samples. Variances over region four will be compared between the three experiments. The test's hypotheses are the following [68]:

$$\begin{cases} H_0 : \sigma_1^2 = \sigma_2^2 = \sigma_3^2 \\ H_A : \sigma_1^2 \neq \mu_2^2 \neq \mu_3^2 \end{cases}$$

Where σ_1, σ_2 and σ_3 represent the standard deviation of the ISTs for each experimental condition.

The assumptions of each statistical test are discussed in Appendix A. Before conducting the experiments, the *Matlab* code was executed while the emitted beeps were recorded on a audio track. This procedure was done for each experimental conditions. These tracks were played for the experiments, ensuring that each subject received the exact same set of stimuli. Experiments were conducted according to the protocol presented above. The different ISTs were extracted and analysed. The results are presented in the subsequent chapter.

Chapter 4

Results

This chapter aims to present and analyse the obtained results. It will be divided in three sections, each corresponding to one of the objectives presented in the previous chapter. The results will be first presented graphically and analysed. Finally, statistical tests will be performed, allowing conclusions to be taken regarding the hypotheses which were made in Section 3.5.

4.1 Rhythm synchronisation

In this section, the results about RAS synchronisation (see Section 3.5.1) will be presented. More specifically, did subjects synchronise to the imposed rhythm? Results can be found below and in Appendix D.

First, n_{t_1} was computed according to its definition in Section 3.5.2, enabling the delimitation of the first region for each subject as in Figure 3.15. The results can be seen in Figure 4.1, where the black dotted lines are representing the limit of the first region. This limit corresponds to the activation of the beeps, which clearly disturbed the way subjects were walking (see Figure 4.1). Prior to the beep activation, subjects had respectively a mean IST (rounded up) of 0.6267, 0.6368, 0.6384, 0.6014 and 0.614s (leftward red dotted lines in Figure 4.1). The beep activation induced a disturbance in their gaits. However, the way subjects reacted to it varied. It seems that subject three (S3) and subject four (S4) reacted smoothly to the disturbance, suggesting that the first auditory stimulus, i.e. the right one (see Figure 3.5), happened more or less when the right foot was on the ground. For the other subjects, this was not the case as outliers are present after the beep activation. Subject two (S2) has an outlier reaching nearly 2s (see Appendix D.2), while subject one (S1) and subject five (S5) have theirs around 0.4s (see Figure 4.1(a) and (e)). These are representing two different strategies to synchronise to the auditory cues. On one hand, S2 increased the duration of his ISTs. One foot remained in the air, waiting for the correct stimulus to make the step. The amount of time a given foot may remain in the air is limited by the length of the treadmill. On the other hand, S1 and S5 preferred doing quick steps to synchronise, reducing the ISTs.

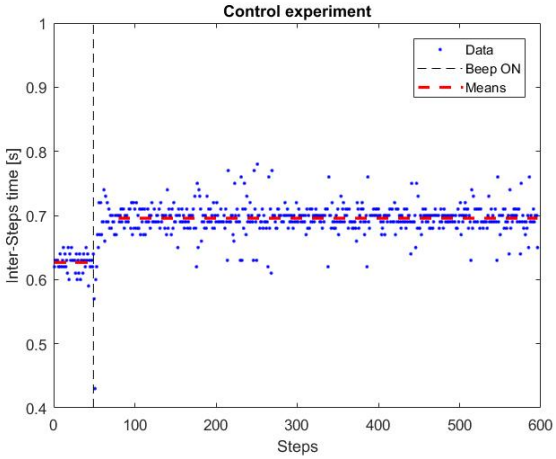

(a) S1

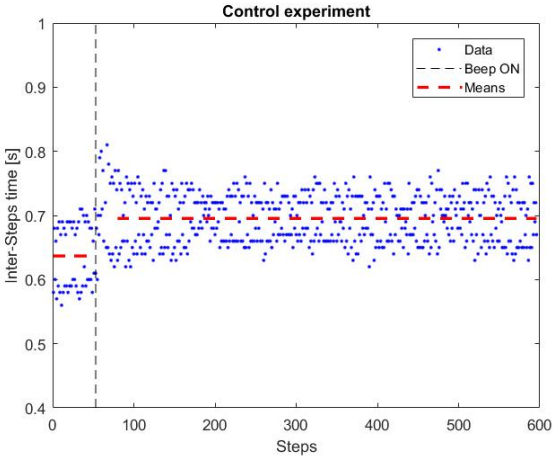

(b) S2 zoomed in: some outliers are not visible

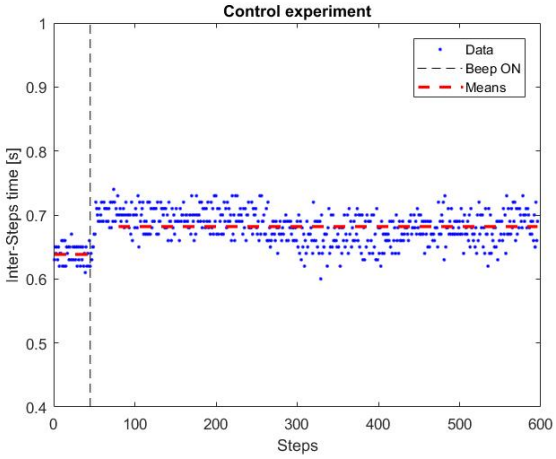

(c) S3

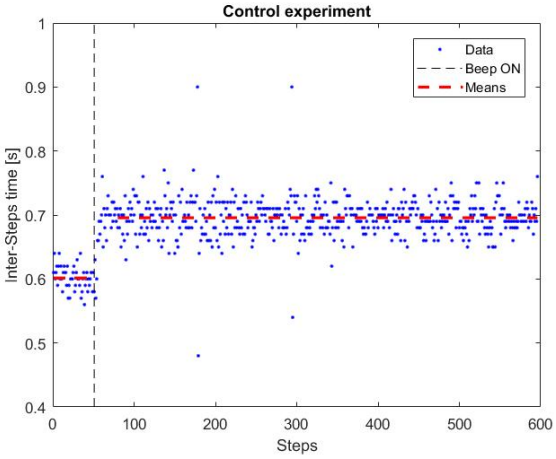

(d) S4

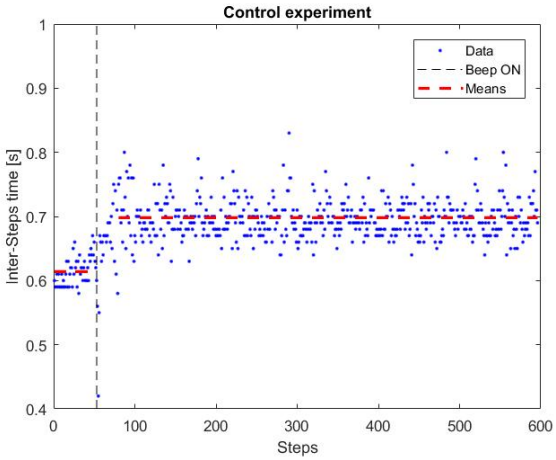

(e) S5 zoomed in: some outliers are not visible

Figure 4.1: Evolution ISTs in the control experiment for each subject; prior beep onset (black dotted line), subjects were walking at their own pace; after beep onset, their ISTs converged to a new value

Second, it can be seen that after some time, subjects were able to adapt: the ISTs stabilised around certain values (rightmost red dotted lines in Figure 4.1). Still, one can see that IST variations remain. These are due to the cognitive load of the task: synchronising to auditory cues during six minutes requires constant focus. Subjects have to maintain attention to detect frequent events (the beeps), which is exhausting. These fluctuations might be due to distractions. Furthermore, the amount of variation in the ISTs after beep onset is greater than prior the onset for four out of five subjects (see Table 4.1), which implies that the RAS increases the variability in the gait of healthy subjects.

Moreover, performances vary across subjects as it can be seen in Figure 4.3. Several red line segment can be seen in Figure 4.3. These are representing the different IST means, which were defined through windows of length n_{t_1}. By computing the variance of these means from the beep onset, one gets the values found in the second column of Table 4.1. These values show that S1, S2, S4 and S5 had the most constant ISTs. In other words, they had the most constant rhythm. This suggests that they were able to quickly notice when they were off rhythm, enabling faster correction, whereas S3 had more trouble doing so.

Still, when looking at Figure 4.3(b), it seems that S2 stands longer on one feet than the other as he is constantly oscillating around a mean value. This intuition is confirmed by Figure 4.2, where it can be seen that S2 stands longer on his left leg than on his right one. For the other subjects, the distributions of the left-to-right and right-to-left ISTs are mixed up (see Appendix D.3).

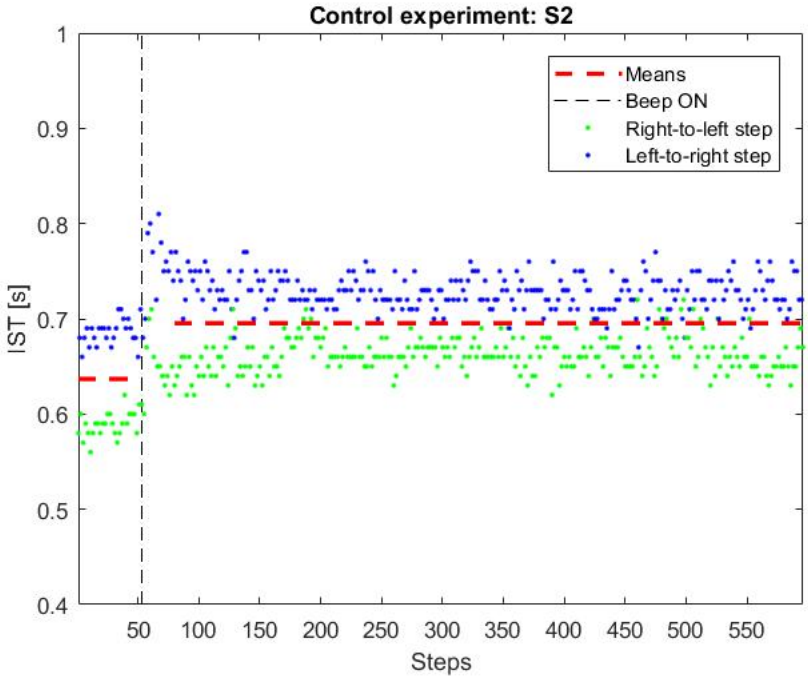

Figure 4.2: S2 oscillating behavior (zoomed in): left-to-right step (blue dots) and right-to-left step transitions (green dots) highlighted

Hence, S2 seems to be far from stable in term of ISTs. This is confirmed by computing

the mean of the variation after beep onset. Doing this analysis, with the same windows, gives the results in the third column of Table 4.1. These values are representing the stability of the ISTs. They show that S1 was the most stable, as he demonstrated less oscillations while S2 is oscillating the most, with a mean variance of 1519.24ms^2, which is far greater than the other values. However, as it can be seen in Figure 4.3(b), S2 had the same oscillating behavior prior beep onset. This suggests that his oscillating behavior is independent of the auditory cues and related to his gait mechanics, which may be impacted because of his medical history (see end of Section 3.4.3). Thus, his oscillating behavior will not be taken into consideration. Nevertheless, it is interesting to notice that S2 is the only subject depicting a decrease in variability after the beep onset (see Table 4.1), which suggests that the RAS improved his gait in term of IST variability.
For the other subjects (i.e. S1, S3, S4, S5), the performance discrepancies, in terms of constancy of the overall rhythm and stability, may be due to external factors like environmental distractions or the initial level of tiredness of the subjects.

Table 4.1: Subjects IST performances regarding the beep onset

Subjects	**Variance prior onset [ms^2]**	**Mean variance post onset [ms^2]**	**Variance of the means post onset[ms^2]**
S1	184.95	442.13	29.38
S2	2533.74	1519.24	75.85
S3	217.98	446.14	12.70
S4	332.08	588.22	36.72
S5	482.08	872.69	76.55

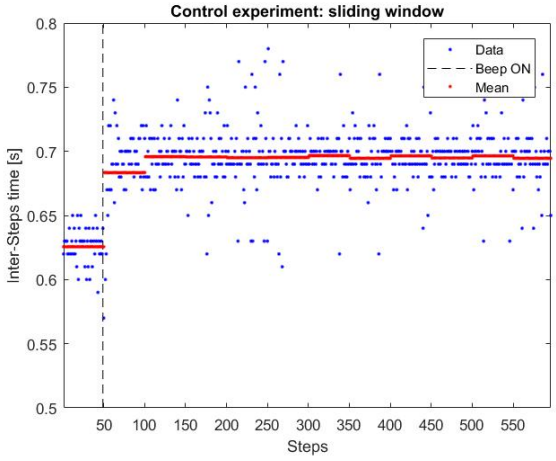

(a) S1

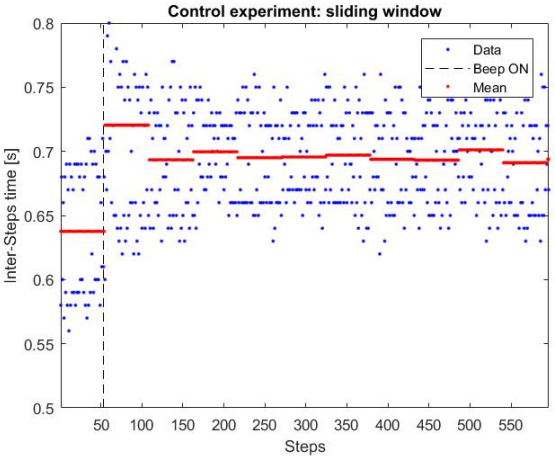

(b) S2

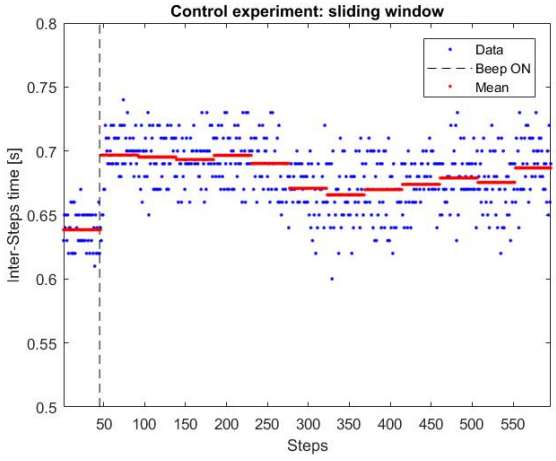

(c) S3

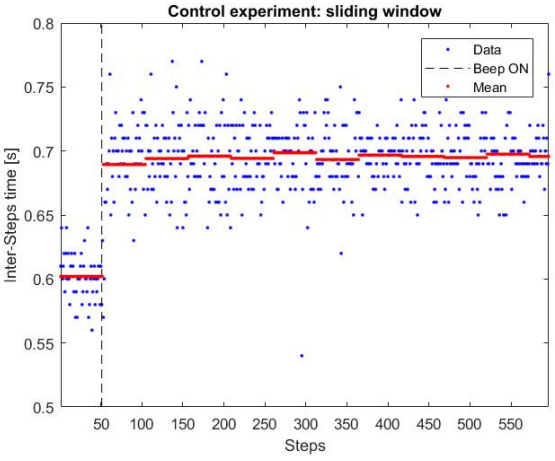

(d) S4

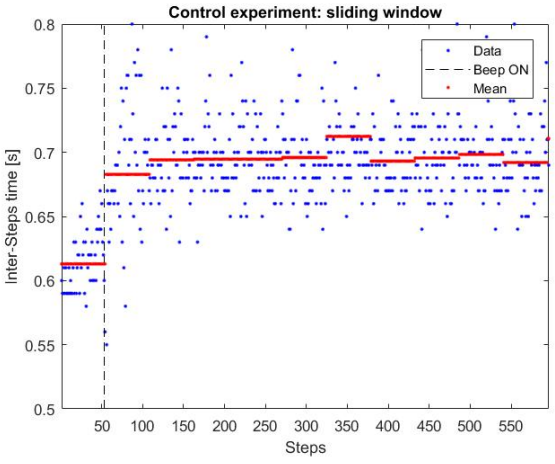

(e) S5

Figure 4.3: Variability of the mean value of the ISTs (window size = n_{t_1}) in the control experiment

Finally, by looking back at Figure 4.1, one could think that the subjects managed to synchronise to the rhythm. Indeed, they seem to have more or less the same IST mean after beep onset. S1 stabilised around a value (rounded up) of 0.6956s while S2, S3 and S5 were around 0.6954, 0.6818, 0.6956 and 0.6980s respectively, which are close values. However, these are deviating from the expected one, which was 0.65s. The results of the different T-Tests, used to compare the measured means to the expected one, are presented in Table 4.2.

Table 4.2: T-Tests: $\hat{\mu} = 0.65s$ ($\alpha = 0.001$)

Subjects	μ [s]	**p-value**	**t statistics**
S1	0.695648	<2.2e-16	49.129
S2	0.695377	<2.2e-16	27.830
S3	0.681818	<2.2e-16	30.629
S4	0.695590	<2.2e-16	35.269
S5*	0.695768	<2.2e-16	39.773

The '*' symbol in Table 4.2 highlights that outliers were removed according to the rule defined in Section 3.5.2. The resulting p-values are below the significance level $\alpha = 0.001$: the null hypothesis H_0 of the T-Tests (see Section 3.5.1) must be rejected. Statistically, it must concluded that subjects were not able to synchronise to the imposed rhythm. A reason that may explain these deviations of the measured means of the ISTs is related to the language used. *Matlab* is not adapted for real-time programming, hence working in the order of 1ms might be complicated. As a consequence, the mean ISTs is expected to vary between different executions of the code. Fortunately, as the experiments were conducted with recorded tracks of given executions, this variability is suppressed. Still, it remains the uncertainty concerning the performance of the recorded executions.

Therefore, an estimation of the delay of *Matlab* has been realised to assess if subjects were able to synchronise. Graphical representations of the time taken for each iteration, which is supposed to be of 1ms per iteration, can be found in Appendix D.4. The effective time taken for doing such iteration was computed, giving a mean time of 1.0656ms per iteration. Given the delay in *Matlab*, each beep should now occur every 0.69264s instead of 0.65s as previously thought. It is worth insisting that this value might slightly differ from the ones in the recorded executions, as execution performance varies between two executions. Nevertheless, it gives a good insight about what to really expect. Performing again the one sample T-Tests with the new expected mean gives the results in Table 4.3.
The resulting p-values for S1, S2, S4 and S5 are above the significance level $\alpha = 0.001$ (red in Table 4.3). It means that the null hypothesis can not be rejected: the measured IST means do not differ from the expected one. In other words, the conclusion is that subjects were able to synchronise to the rhythm.

Table 4.3: T-Tests: $\hat{\mu} = 0.69264s$ ($\alpha = 0.001$)

Subjects	μ [s]	**p-value**	**T statistics**
S1	0.695648	0.0013	3.237
S2	0.695377	0.0938	1.679
S3	0.681818	<2.2e-16	-10.417
S4	0.695590	0.0229	2.282
S5*	0.695768	0.0068	2.718

4.2 Rhythm memorisation

This section will attempt to answer the following questions (see Section 3.5.2): (i) did the initial pace evolve towards the expected mean throughout the experiment? (ii) Did the subjects react faster throughout experiments? To answer these questions, the model presented in equation 3.10 was used to fit the data. The fitting of S1 data can be found in Figure 4.4. To fit the model parameters, outliers were removed according to the rule presented in Section 3.5.2. This is why several dots seem to have the same value in Figure 4.4(c). For the other subjects results, one should refer to the Appendix E.1. A more practical representation can be found in Figure 4.5, allowing performance comparison between experiments.

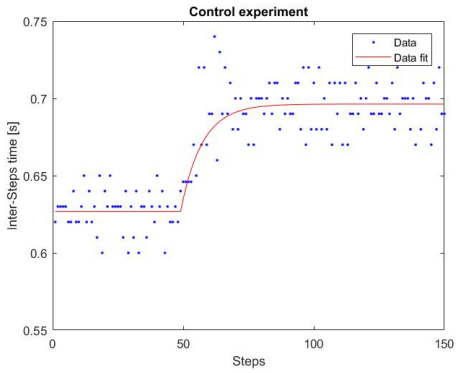

(a) S1: control

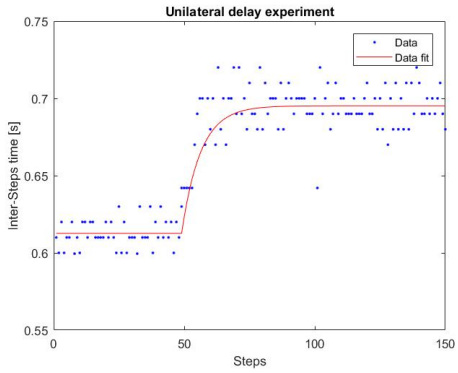

(b) S1: unilateral delay

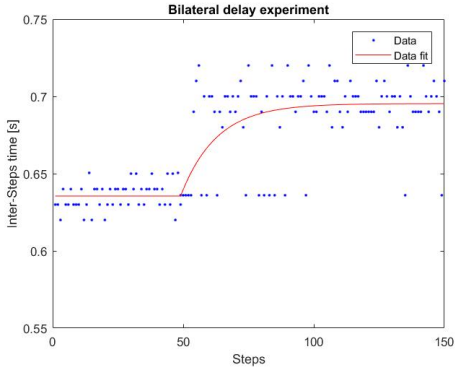

(c) S1: bilateral delay

Figure 4.4: Model parameter fitting to the ISTs for the different experiments: (a) control experiment, (b) unilateral delay experiment, (c) bilateral delay experiment

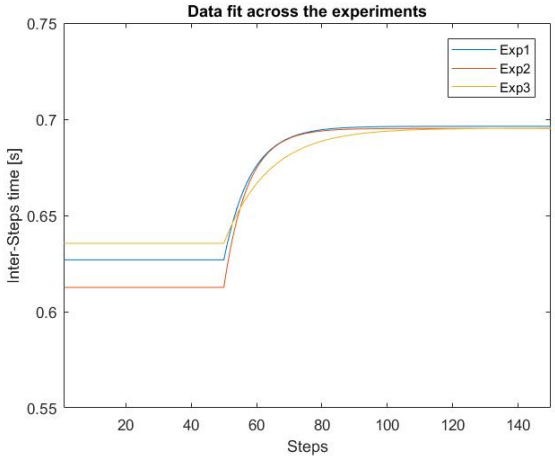

(a) S1

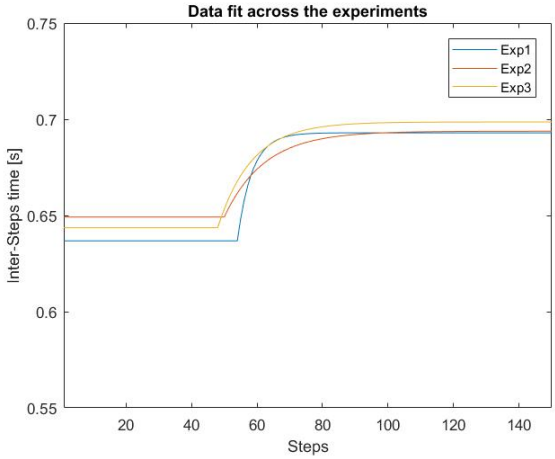

(b) S2

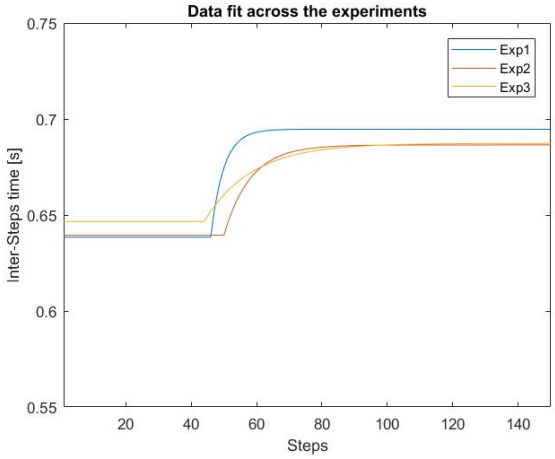

(c) S3

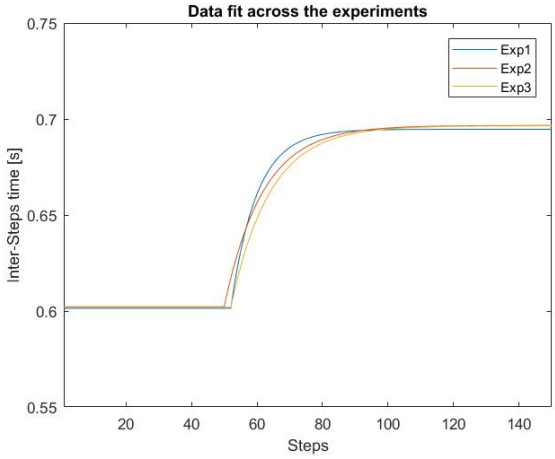

(d) S4

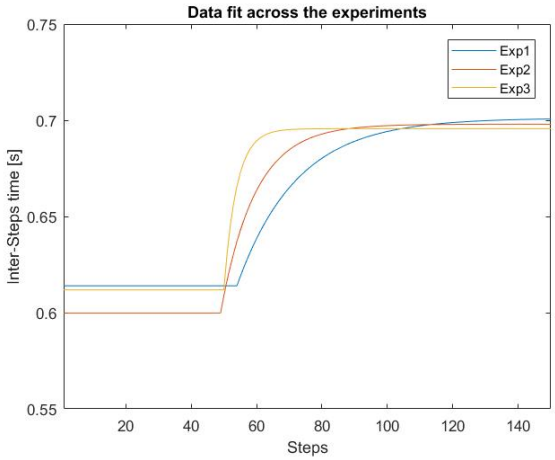

(e) S5

Figure 4.5: Superpositin of the curves fitting the IST data for the control experiment (blue curve), unilateral delay experiment (red curve) and the bilateral delay experiment (yellow curve)

It can be observed graphically that the ISTs means in the first region do not shift towards the desired value of 0.65s throughout the three experiments, but rather that they are randomly ordered from subject to subject, contrary to assumption (i). To verify this intuition, a study of the ISTs means in the first region has been done (see Section 3.5.2). The evolution of the ISTs means can be found in Table 4.4.

Table 4.4: Evolution of the ISTs means μ [s]

Subjects	$\mu_{control}$	$\mu_{unilateral}$	$\mu_{bilateral}$
S1	0.6267	0.6127	0.6359
S2	0.6368	0.6492	0.6436
S3	0.6384	0.6398	0.6472
S4	0.6014	0.6022	0.6020
S5	0.6149	0.6004	0.6118

The one-way repeated measure ANOVA ($\alpha = 0.1$) gave a p-value of 0.2927[GG][1], which is above the significance level α: the null hypothesis (see Section 3.5.2) can not be rejected. Hence, assumption (i) is not verified: no significant differences in the ISTs means were observed throughout the experiments. No memory effects have been found in the initial pace.

In order to test assumption (ii), the time constants (τ) of the models have to be compared. These can be found in Table 4.5. To ease interpretation, a graphical representation of the trend is shown in Figure 4.6.

Table 4.5: Evolution of τ [steps]

Subjects	$\tau_{control}$	$\tau_{unilateral}$	$\tau_{bilateral}$
S1	8.1235	7.2150	13.7174
S2	4.4563	12.3001	10.3627
S3	3.9124	8.1235	14.4509
S4	7.8678	11.7371	12.4688
S5	18.0505	10.5152	3.8805

As it can be seen, only S5 had a clear decreasing trend: it took him about 18 steps to stabilise in the first experiment, 10 for the second, and only three steps for the last experiment. For the other subjects the general trend is an increase in the time constant. Indeed, the time constants of experiment three are always greater than the ones of experiment one. This suggests that four out of five subjects got worse at stabilising throughout the experiment, which is rather unexpected. However, the answer is not as straightforward. Indeed, the only factor influencing the stimuli onset is time: it is not related to any event in the gait cycle. Therefore, in each experiment, the stimuli onset happens at different locations in the gait cycle. For some subjects, the first right beep might happen in synchronisation with a right IC, facilitating the stabilisation. For others, it might happen in complete phase opposition with the right IC, increasing the complexity. Therefore, the performance depicted here might well only be due to chance. In order to compare the evolution of the time constants, the stimuli onset conditions should have

[1]Greenhouse-Geisser Epsilon correction, see Appendix G

been fixed. As a consequence, assessing the retention effects based on the evolution of the time constant is not relevant.

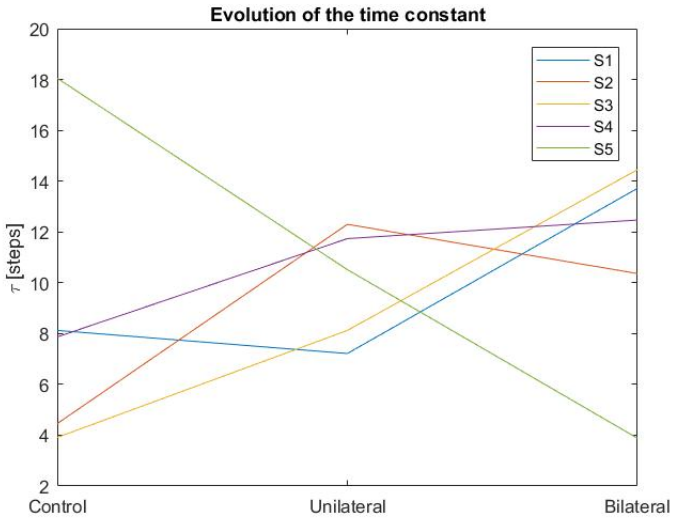

Figure 4.6: Evolution of the time constant from the first experiment (Control), via the second (Unilateral) to the third (Bilateral)

To complement this analysis, an investigation of the RAS memory effects on gait variability has been made. In particular, the variance of the ISTs in region one has been studied. This would allow to assess the performance without any prior RAS exposition (Control), with one prior exposition (Unilateral) and with two prior expositions (Bilateral). The results can be found in Figure 4.7 and in Table 4.6. As it can be seen, all subjects except S1 showed a decrease in ISTs variability after RAS exposition. Moreover, this effect seems to be proportional to the number of expositions. To assess the significance of this decrease in variance, Levene's tests have been performed, whose results can be found in the fifth column of Table 4.6. It turns out only S2 and S5 (red in Table 4.6) had a significant decrease in gait variability. Hence, only two subjects out of five depicted memory effects regarding gait variability.

Table 4.6: Levene's tests on region one IST variances σ^2 [ms^2] ($\alpha = 0.1$)

Subjects	Control	Unilateral	Bilateral	p-value	F-statistics
S1	84.949	119.898	91.326	0.3491	1.0601
S2	2533.745	1120.153	732.285	2.443e-09	22.785
S3	217.980	364.541	220.598	0.3087	1.1858
S4	332.078	301.105	300.078	0.9865	0.0136
S5	482.075	438.121	202.806	0.0143	4.372

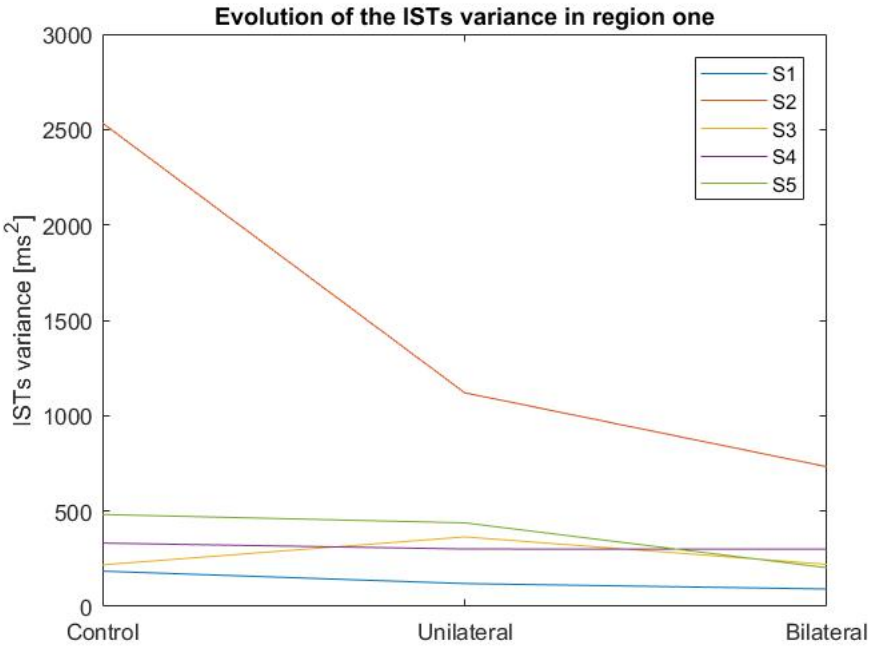

Figure 4.7: Evolution of the ISTs variance of each subject in region one throughout the experiments

To conclude this investigation, an inspection of the effects of the RAS on gait symmetry has been realised in a similar fashion. In particular, an analysis of the evolution of the gait symmetry, regarding left-to-right and right-to-left ISTs, has been made in region one. This analysis attempts to capture retention effects on gait symmetry after several exposition to the RAS. To do so, the following SR is defined, which is inspired by Equation 2.2:

$$SR = \frac{IST_{RL}}{IST_{LR}} * 100[\%] \tag{4.1}$$

Where IST_{RL} and IST_{LR} represent respectively the time taken for a given right-to-left step transition and the next left-to-right step transition. This ratio is expected to be close to 100% when walking normally. A graphical representation of S5's results can be found on Figure 4.8. The remaining representations can be found on Appendix E.2. The results are summarised in Table 4.7, where $SR_{control}$ represents the performance achieved when subjects have not yet been exposed to the RAS, while $SR_{unilateral}$ and $SR_{bilateral}$ represent, respectively, the performance after one and two six-minute RAS sessions. When looking at the values in Table 4.7, it is interesting to notice that none of the median values are above 100%, which could be related to the fact that all the subjects involved in this study were right-handed people. Moreover, the median SR steadily increased throughout the experiments for four out of five subjects (red in Table 4.7).

A one-way repeated measure ANOVA ($\alpha = 0.1$) has been performed on the evolution of the SR. It yielded a p-value of 0.0944[GG], which is below the significance level α. Thus, not only was the gait symmetry significantly improved after several exposures to RAS, but also that this

effect is memorised since it was found in the first region, where RAS is turned off. Hence, it can be concluded that memory effects have been found regarding gait symmetry.

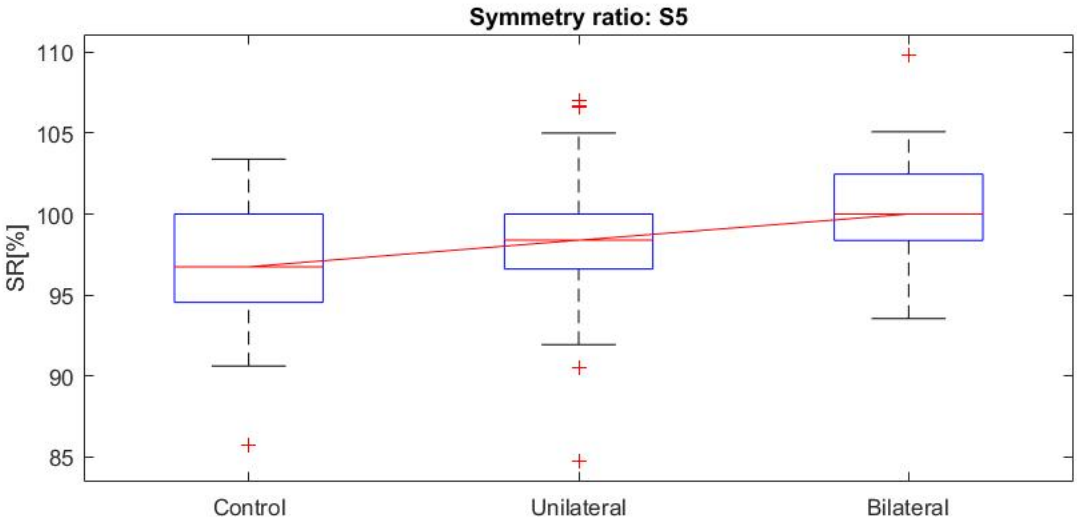

Figure 4.8: Evolution of SR for S5 in region one, from the control experiment (Control), via the unilateral delay experiment (Unilateral) to the bilateral delay experiment (Bilateral)

Table 4.7: Evolution of SR (median) [%] in region one

Subjects	$SR_{control}$	$SR_{unilateral}$	$SR_{bilateral}$
S1	96.92	98.36	98.46
S2	85.61	91.11	92.54
S3	96.87	97.01	97.74
S4	98.29	96.72	98.33
S5	96.75	98.39	100

4.3 Rhythm disturbance

This section will cover the main focus of this work. The research question was: "is it possible to disturb/desynchronise the gait of healthy subjects?" Before answering this question, a preliminary one must been answered: did subjects feel the perturbation in the rhythm? This question has been asked to all subjects after the experiments. Only one subject (S3) noticed something strange in the task but attributed it to tiredness. S1, S2, S4 and S5 did not notice it, confirming that the perturbation was not perceived.

A prerequisite to this analysis of the disturbance is to find region four as defined in Figure 3.17. In the delay experiments, this region is expected to be marked with an increased variance, with respect to the control experiment (see Section 3.5.3). First, a visual inspection of the ISTs can be performed to assess if any significant variation could be seen and used. To do so,

comparison of the performance between experiments was performed for each subject individually. The results can be found in Figure 4.9.

It can be seen that the IST mean of each subject remained around the expected mean (red lines in Figure 4.9). This behavior was expected as the mean of the ISTs was not supposed to evolve. As it was explained in Figure 3.17, the delays are expected to shorten the left-to-right IST and to lengthen the right-to-left IST by the same factor ϕ. Therefore, the mean should not vary, what is confirmed by Figure 4.9. Next, increase in variance was expected to mark region four. However, this is not expressed on any of the graphs. This implies that defining region four through variance increase will not be possible. Moreover, it suggests that no effects can be observed. Still, another approach was attempted. This consisted in looking for the times corresponding to the expected start and end of region four in the stimuli audio track. Once these are obtained, region four can be extracted by looking for the ICs corresponding to these times. After investigation, region four is expected to start after 180s and stop after 245s. The corresponding mean step number are 259 steps before the onset of region four and 352 steps for its end. These regions are represented in Figure 4.10.

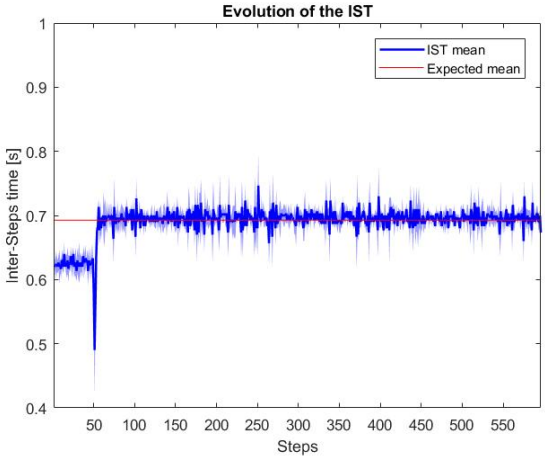

(a) S1

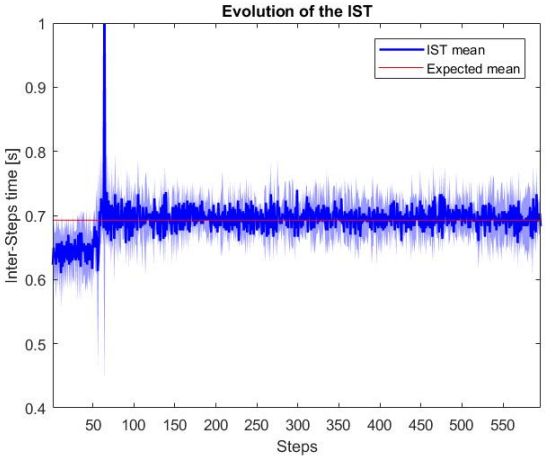

(b) S2

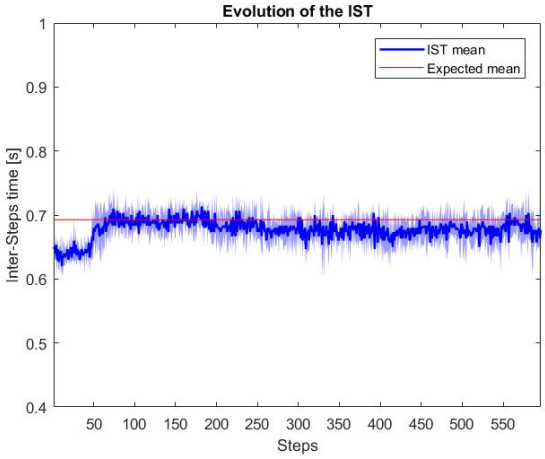

(c) S3

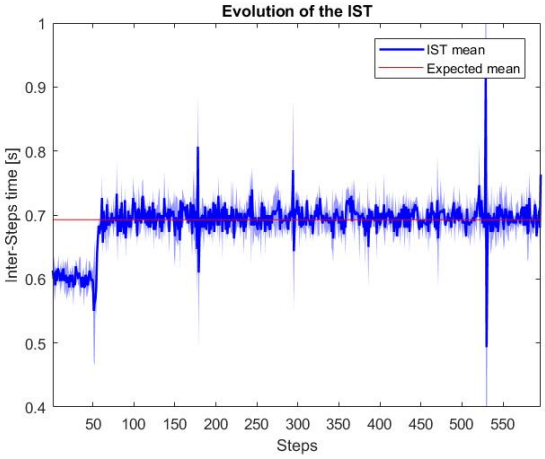

(d) S4

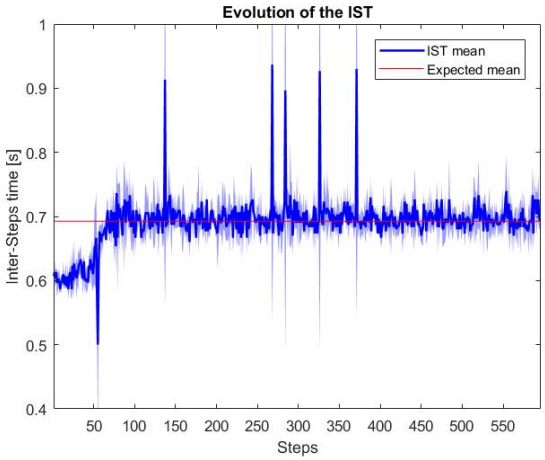

(e) S5

Figure 4.9: Performance comparison between experiments; the dark blue line represents the mean of the IST values, taken from experiment one to experiment three; the red line represents the expected mean (i.e. 0.69264s); the shaded area represents the standard deviation of the IST

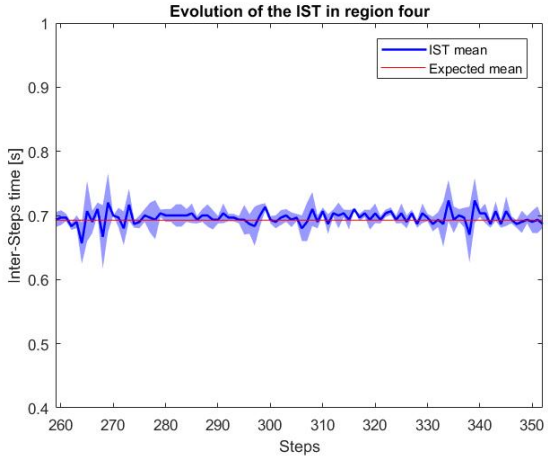

(a) S1

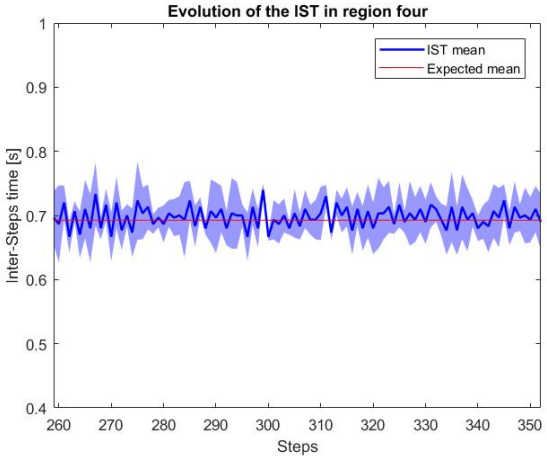

(b) S2

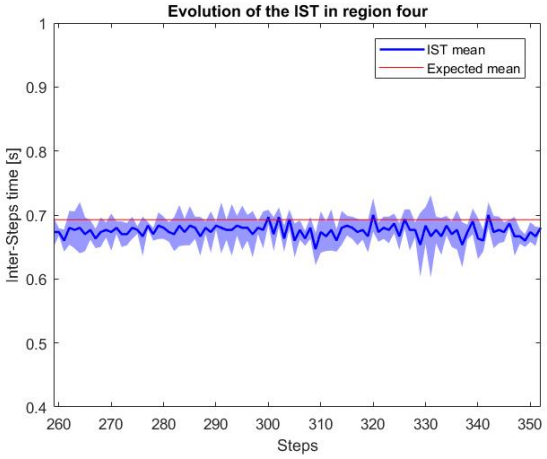

(c) S3

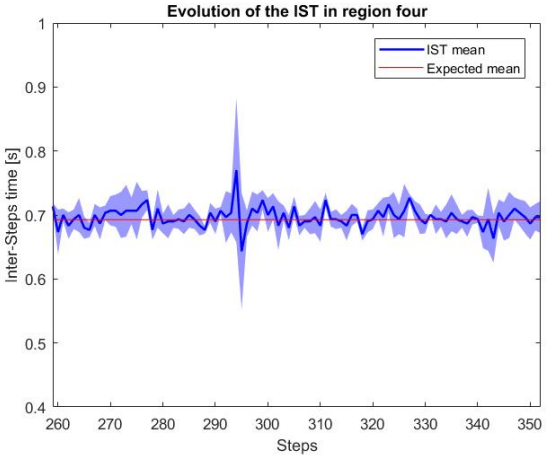

(d) S4

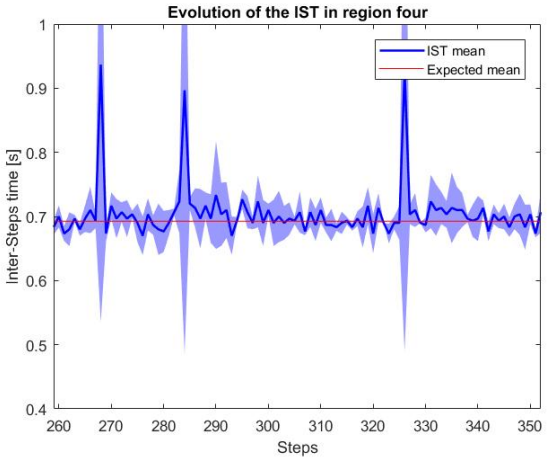

(e) S5

Figure 4.10: Region four comparison between experiments; the dark blue line represents the mean of the IST values, taken from experiment one to experiment three; the red line represents the expected mean (i.e. 0.69264s); the shaded area represents the standard deviation of the IST

Again, no significant variance increase can be seen in Figure 4.10. However, the four rightmost peaks that can be seen on the graph of S5 in Figure 4.9 are all close to the fourth region: three of them are inside, and the rightmost is just after. As it can be seen in Figure 4.11, one is due to the control experiment, one in the unilateral experiment, and two in the bilateral experiment. As the spike in the control experiment might just be due to a distraction, the others might reflect the effect of the disturbance. However, the latter is a strong assumption, as this effect is not represented on any of the other subjects.

Levene's tests were performed to compare the variance σ^2 in region four after outliers removal in each experimental conditions (represented by the '*' symbol). The results can be found in Table 4.8. Every p-value is above the significance level $\alpha = 0.05$. Plus, the F statistics are relatively low. In other words, the variances are homogeneous throughout the experiments. This suggests that the delay induced did not perturb the gait.

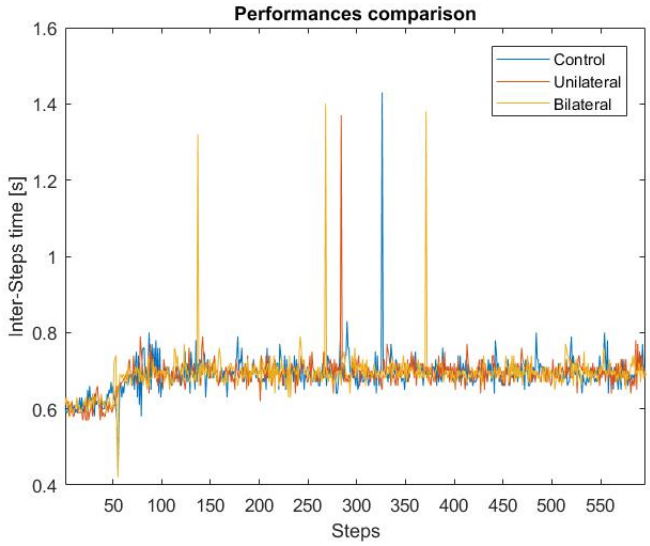

Figure 4.11: S5 IST evolution for the control experiment (blue line), unilateral delay experiment(red line) and for the bilateral delay experiment (yellow line)

Table 4.8: Levene's tests on region four IST variances σ^2[ms^2] ($\alpha = 0.1$)

Subjects	$\sigma^2_{control}$	$\sigma^2_{unilateral}$	$\sigma^2_{bilateral}$	**p-value**	**F statistics**
S1*	144.28	212.67	183.85	0.3393	1.09
S2*	1133.56	1222.01	947.48	0.1483	1.92
S3*	439.50	409.83	458.40	0.6988	0.36
S4*	513.98	423.71	512.06	0.7427	0.30
S5*	844.44	610.66	457.39	0.1131	2.20

To complement this analysis, an inspection of the gait symmetry has been realised. In particular, analysis of the symmetry in the left-to-right and right-to-left ISTs has been made in region four. Since the delays induced are expected to influence differently these transitions (see Section 3.5.3), an analysis of the evolution of the SR in region four is relevant. The SR has

been defined as in Equation 4.1. This ratio is expected to deviate from 100% when the delays are introduced. Hence, the following deviation δ is defined:

$$\delta = |100 - SR|\% \tag{4.2}$$

In particular, δ is expected to increase from the control via the unilateral delay to the bilateral delay experiment (see Section 3.5.3). A graphical representation of the evolution of SR for S1 in region four can be found on Figure 4.12. The remaining graphical representations can be found on Appendix F. The results are summarised in Table 4.7. As it can be seen, only S3 depicted the expected behaviour as δ progressively increases throughout the experiments (see red in Table 4.9). For the other subjects, the evolution of δ is random.

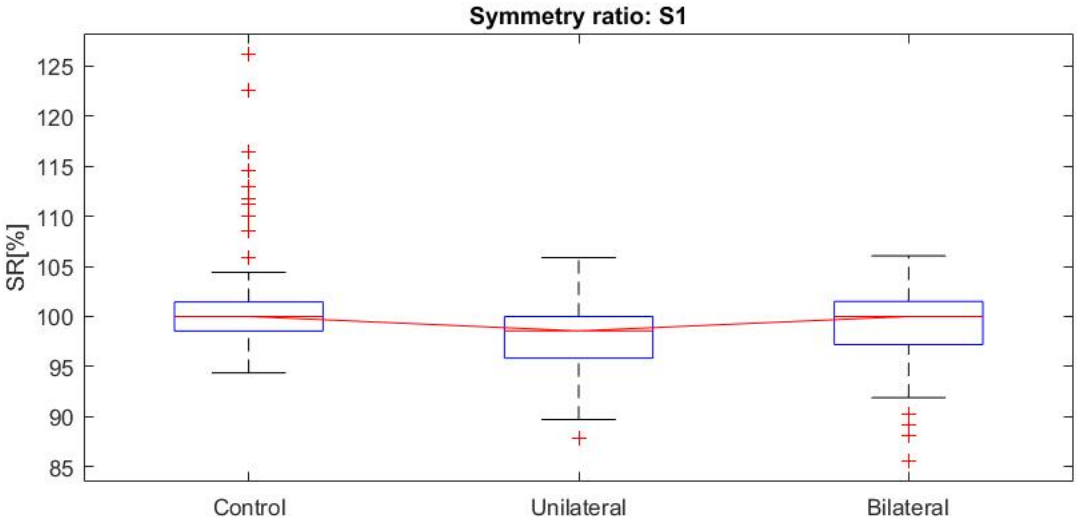

Figure 4.12: Evolution of SR for S1 in region four, from the control experiment (Control), via the unilateral delay experiment (Unilateral) to the bilateral delay experiment (Bilateral)

Table 4.9: Evolution of SR (median) and δ [%] in region four

Subjects	**Control**		**Unilateral**		**Bilateral**	
	SR	δ	SR	δ	SR	δ
S1	100	0	98.56	1.44	100	0
S2	91.78	8.22	93.10	6.90	93.77	6.23
S3	97.01	2.99	95.77	4.23	95.65	4.35
S4	101.43	1.43	98.62	1.38	98.53	1.47
S5	100.69	0.69	101.40	1.40	100.68	0.68

Therefore, three two-sample T-Tests ($\alpha = 0.1$) were performed to assess the significance of the increase of δ, depicted by S3. The test, whose assumptions can be found in Appendix G, was realised for each experimental condition pairs, i.e. the control-unilateral, unilateral-bilateral and control-bilateral pairs. The results are presented on Figure 4.13. Although, the increase in deviation is not significant neither in the control-unilateral pair (p-value = 0.766[BF][1]) nor in

[1]Bonferroni correction

the unilateral-bilateral one (p-value = 0.892[BF]), it becomes significant in the control-bilateral pair (p-value = 0.089[BF]): the bilateral delay experiment managed to disturb the gait of S3. However, since S3 is the only subject portraying this behaviour, it can not be concluded that the delays induced desynchronised the gait of the subjects.

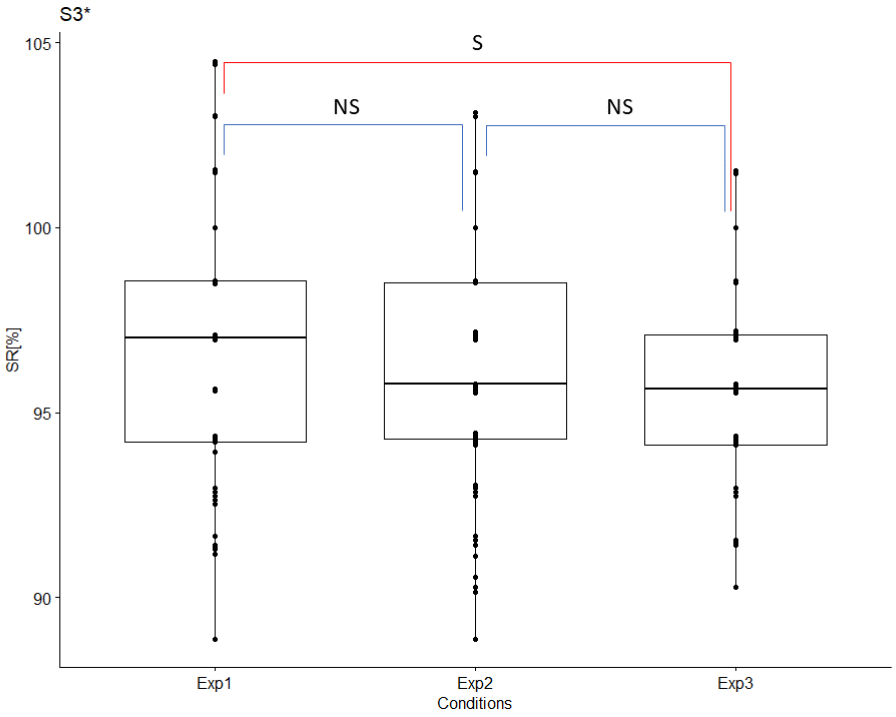

Figure 4.13: Two-sample T-Test of the Evolution of SR for S3 in region four, from the first experiment (Exp1) to the third (Exp3); the "*" symbol highlights that outliers were removed to agree with the test assumptions; the different pairs are joined by the top lines and the tests results, i.e. either non significant (NS) or significant (S), are present on top of these lines

This chapter presented and analysed the results of this work. First, these show that subjects are able to synchronise to auditory cues with ease. Next, the hypothesis that a trace of the previously induced rhythm could be found in the gait of subjects has not been proven. However, retention effects regarding gait variability and gait symmetry have been observed respectively in two and four out of five subjects. Finally, no evidence of gait disturbance due to the phase shifts of the auditory stimuli has been highlighted. In the following chapter, a discussion of the results along with the limitations and possible perspectives of this work will be presented.

Chapter 5

Discussion

This chapter aims at putting the results presented previously into perspective. First, the different results regarding each hypothesis will be discussed. Then, the limitations of this work will be pointed out. Finally, this chapter will be concluded by indicating the perspectives of this study.

5.1 Discussion of the results

This section will discuss the results of this work. More specifically, how do the results compare with the assumptions and the literature?

5.1.1 Rhythm synchronisation

The results presented in Section 4.1 show that subjects are able to synchronise easily with RAS, which has already been shown in the literature [50, 51, 52, 53]. This phenomenon, called sensorimotor synchronisation, is due to the strong connections between auditory and motor areas in the brain. When the auditory cues were presented, subjects synchronised their gait within a few steps ($\tau_{mean} = 9.81[steps]$), which is similar to what Forner-Cordero et al. observed [53]. Moreover, the results show an increase in the ISTs variance after beep onset, which implies that RAS increases the variability in the gait of healthy subjects. This result is in concordance with the results of Hausdorff et al. [51], which observed an increase in stride-to-stride variability under RAS for healthy subjects (see Section 2.2.5).

5.1.2 Rhythm memorisation

None of the two hypotheses regarding rhythm memory has been shown. As explained in the previous chapter, the second assumption was not relevant regarding the way experiments were performed. But why was the first assumption not verified?

A possible explanation is that the time of exposition to the rhythm was too brief to elicit rhythm retention. Indeed, six-minute stimulation may not be sufficient to integrate the rhythm into the gait. However, the team of Hausdorff et al. [51] (see Section 2.2.5) managed to observe retention effects only after a 100m walk at $\pm$1m/s under RAS, which results in a shorter rhythm exposition. Still, these retention effects were observed mainly in patients with Parkinson's disease, while the only retention effect found in healthy subjects was a small but significant increase in stride time variability. Hence, either rhythm retention actually requires longer exposition time to be elicited or the assumption was too strong.
Moreover, Hausdorff et al. also observed that RAS rendered the gait of healthy subjects more "abnormal" by inducing an increase of variability in their gait pattern. A similar result has been obtained here, as an increase in ISTs variability was observed under RAS (see Section 4.1). This might explain why no memory effects were observed: RAS increases variability in the gait of healthy subjects, which is corrected as soon as RAS is turned off. Indeed, the results obtained tend to confirm this correction hypothesis. On one hand, the ISTs variability in region one did not evolve throughout the experiments for most of the subjects. On the other hand, a small portion of the subjects depicted a significant decrease in the variability in region one after RAS exposition, which might be interpreted as an "over correction" of the variability experienced.

The effects of RAS on gait symmetry were assessed in this work, but not by Hausdorff et al.. The results show that RAS improves gait symmetry. Indeed, when comparing the SR in region one (Table 4.7) with those in region four for the control experiment (Table 4.9), it can be seen that the SR is greater in region four than in region one, which suggests that the SR is greater when RAS is turned on. In addition, this effect is memorised.

5.1.3 Rhythm disturbance

Finally, no effect of the delays induced have been highlighted, which is contrasting with the results of Forner-Cordero et al. [53]. However, the works are different. First, they used a single auditory source, pacing both legs, while two were used here. Second, they induced perturbations by changing the period of the auditory cues, where a phase shift in the delivery of a specific source was done here, independently of the other. In other words, in their work, the variation of the stimuli is keeping the gait symmetry, while here asymmetry was expected to be induced with the variation.

Why did the subjects not react to the phase shift induced? One hypothesis could be found in the nature of the motor system. As explained in Section 1.3, tasks are stored as schemes containing information about the movement sequences. Walking is one of them. Once a sequence is learned, it is difficult to modify it: they are robust to change and remain largely unaltered

through life [21]. Still, some parameters of the sequence can vary. For walking, these could be the walking speed or the IST. The latter was the parameter which Forner-Condero et al. altered: they changed the period of the auditory cues, asking subject to adapt their ISTs. A shorter period required shorter ISTs and vice versa.

Here, although the ISTs were analysed, the phase shift induced was supposed to alter the way subjects were walking by breaking gait symmetry. Thus, subjects have been required to "rewrite" the stored sequence to adopt an asymmetrical walk. However, it is rather unlikely, and it could explain why subjects did not react to the induced delays.

5.2 Limitations of this work

Throughout the presentation of the results and their discussion, several limitations have been identified. These are presented below.

- **Location of the experiments**: the first limitation of this work, although independent of the work itself, is related to the place where the experiments were conducted. The place was not as quiet and controlled as a real laboratory. Distractions certainly affected the level of focus of the subjects, which is critical in the task proposed. Indeed, a single distraction may cause a drift from the rhythm. Thus, these perturbations may have impacted the performance of subjects.
- **Real time coding**: as explained in Section 4.1, *Matlab* delay plays an important part in the analysis of the results. Indeed, if not taken into account, it could have skewed the results. Some of the variability induced have been removed, thanks to the use of audio tracks of the different stimulations. This ensured that each subjects received exactly the same stimulation, for each experimental condition. However, the exact delay in the tracks is unknown and can only be estimated. Moreover, the delay in the track corresponding to the control experiment differs from the one of the unilateral and bilateral experiments. The use of a real-time code would have made it possible to correct these uncertainties. For instance, this could have been done by using Labview and its myRIO tool.
- **Stimuli onset**: the stimuli onset occurred after 30s of walk: it was independent of any gait event. Therefore, depending on their pace, each subject received the first auditory stimuli in different conditions. As stated in the previous chapter, for some subjects the onset was favorable to a fast stabilisation, while for others, it induced more complexity in stabilising. Although this is not a problem for the experiment, this aspect introduced a random effect in the transition from region one to region two, which affected the hypothesis stating that subjects would get better at stabilising throughout the experiment. Timing the onset with a gait event, such as the first right IC after 30s walk, would correct this aspect. This could be resolved by using the IMUs data in real-time.
- **Small sample size and subjects**: five healthy subjects participated in the experiments, which is a small sample size. Hence, it is though to draw statistically relevant conclusions

on such a small sample. In addition, only healthy subjects were available, where it could have been interesting to include LLAs.

5.3 Perspectives

This work attempted to desynchronise the gait of healthy subjects using a rhythmic auditory stimulation. The results suggest that it is not possible to do so.

However, it might still be possible to desynchronise gait by eliciting illusory movements. It has been shown that illusory movements can be elicited through tendon vibration: Verschueren et al. [38] managed to modify the knee flexion angle during gait by stimulating different tendons. Hence, illusory movements could be key to desynchronise the gait of healthy subjects. As a consequence, it will be interesting to compare the results which would be obtained using a rhythmic tendon vibratory stimulation.

Nevertheless, the results have shown that gait symmetry is improved under RAS. Moreover, the subject who depicted the strongest asymmetry, i.e. S2, depicted the most impressive symmetry correction (+8%, which is similar to what Yang et al. [49] observed), making the RAS a dedicated tool for gait retraining. In addition, this improvement in symmetry lasts even after RAS removal, which can have interesting applications. In particular, a mobile system integrating RAS could be designed for daily gait retraining. For example, this system could be embedded into a prosthesis for LLAs. If the gait symmetry of the user is measured below a certain threshold, this system would activate a RAS session to correct this asymmetry. By relying on the memory effects, the RAS session could be relatively short. Still, two unknowns remain: the RAS exposition time needed to elicit memory effects, and their duration. If the ratio between the two is small, i.e. small exposition time and long lasting memory effects, the more efficient the system would be, while minimising the duration of the auditory stimulation. Indeed, it can quickly be boring to hear recurrent beeps. This motivates to investigate the effects of rhythmic tendon vibratory stimulation.

If similar results are obtained with a rhythmic tendon vibratory stimulation, this would pave the way towards new means of doing gait rehabilitation. In particular, if gait desynchronisation is shown, it will mean that it is possible to subconsciously tune the gait of people. Hence, the potential of the proposed system regarding gait symmetry correction will be amplified. Such a device will make profit of the advantages of vibratory stimulation over auditory stimulation.

To the knowledge of the author, no other study attempted to desynchronise the gait of healthy subjects, neither using auditory nor vibratory rhythmic stimulation.

Chapter 6

Conclusion

Sensory feedback plays a major role in the way humans walk. Critical information such as limb position or limb velocity are provided by our mechanoreceptors, which allow us to engage in tasks, such as walking, with control. However, due to the loss of a limb and the absence of prostheses providing efficient sensory feedback alternative, LLAs are experiencing poor control, which impacts their gait mechanics. Hence, LLAs demonstrate problems such as an increased falling rate, balance issues or an asymmetrical gait, which are affecting their quality of life.

In the framework of the research on sensory feedback for LLAs, this thesis investigated a new gait sensory perturbation aiming at desynchronising the gait of healthy subjects. If successful, such perturbation could be used to reduce gait asymmetry in LLAs.

The literature review showed that the vibrotactile sensory feedback modality has more potential regarding integration in a prosthesis. In particular, vibrotactile stimulation can elicit illusory movements through tendon vibration, which can have interesting sensory feedback applications.

In this framework, a protocol was presented. The proposed experiments were based on a bilateral rhythmic vibrotactile stimulation, while subjects were asked to synchronise their ICs with the vibrations. Three different stimulation locations were proposed. The first one was the lower back of subjects, acting as a control condition. The two others were tendons: the patellar tendon at the knee, and the proximal tendon at the hip. These tendons were chosen as, when vibrated, they can have an impact on the knee trajectory during gait. Hence, gait desynchronisation, or at least perturbation, could be observed. For each body locations, two experiments were proposed: (i) an experiment with isochronous rhythmic vibration and (ii) a unilateral delay experiment, where a phase shift was progressively induced in one of the vibratory unit. A recording of the gait characteristics with IMUs and an analysis of the occurrence of ICs and knee flexion angle were suggested to test the effects of the perturbation.

Unfortunately, the rhythmic vibratory stimulation were changed to rhythmic auditory cueing due to the Covid-19 situation. Thus, the effects of tendon vibration on the knee trajectory were

not investigated: only the evolution of the time between successive ICs was analysed (ISTs). A third experiment was proposed. It consisted in (iii) a bilateral delay experiment, where the phase shift induced in one unit was mirrored into the other.

Three questions were proposed: did subjects synchronise to the rhythm? Did subjects showed retention (memory) effects after the RAS? Did the delays, induced in the delivery of the auditory cues, had an influence on the gait of subjects? Positive results were shown regarding the two first questions as subjects synchronised with ease to the rhythm, and retention effects, regarding gait symmetry, were observed. However, no significant effects were captured for the last question. To explain it, a hypothesis was stated: the nature of motor control and, more specifically, the way movements are stored in unalterable sequences, could explain why the delays in the auditory cues had no effects on the gait of subjects.

Limitations of the work were mentioned, which include (i) the location where the experiments took place, which was noisy, (ii) the presence of delays due to Matlab coding and finally, (iii) the stimuli onset which was independent of any gait event and (iv) the small sample size.

Finally, perspectives of this work were presented, by proposing two tasks and one possible application. The first task is to reproduce the experiments using a rhythmic tendon vibratory stimulation. The second aims at studying the retention effects. When are they elicited? How much time do they last? If gait synchronisation or long-lasting memory effects are demonstrated, a prosthesis incorporating such rhythmic stimulation could be designed to improve the gait symmetry of LLAs.

Appendices

Appendix A

Current prosthesis

In this Appendix, one will find complementary information about the current standard prostheses, which have been presented in Section 1.1.1.

A.1 Socket

There exist different ways to design the socket, depending on the level of amputation (see Figure A.1). These are presented below.

- Transtibial amputees: The first design was the specific surface bearing (SSB) sockets. From the '50s, the goal of this socket type is to apply loads on regions that are more tolerant to high pressure values, the standard being the patellar tendon bearing (PTB). As its name suggests, this type of socket is characterised by weight bearing at the level of the patellar tendon [69]. But due to the uneven distribution of load, patients wearing these often suffer from ulcers or other skin issues on the bearing surface. In the '80s, total surface bearing (TSB) sockets were designed to solve this. TSB sockets distribute the load on the total stump area, reducing stresses and enhancing comfort [69].
- Transfemoral amputees: SSB sockets characterised by ischial weight bearing were used, called sub-ischial sockets. The most popular ones were the quadrilateral sockets (QUAD) until the late '90s. Lately, ischial containment sockets (ICS) replaced the QUAD design. Several configurations exist for this type of sockets, such as the normal shape-alignment or the Marlo anatomical socket. Most are TSB sockets and improve the alignment of the femur and the prosthesis axes, enhancing stability [69].

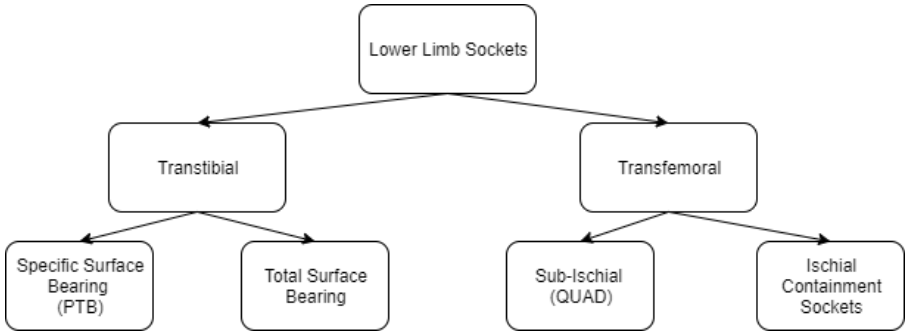

Figure A.1: Socket types, adapted from [69]

A.2 Prosthetic foot

Different types of prosthetic foot exist.The first one is the non-articulated feet, known as Solid Ankle Cushion Heel (SACH) feet. It was the previous standard for prosthetic feet. Nowadays, this model is used for low activity patients due to its limitations as it consists only of a rigid foot with no ankle articulation [6, 15]. The articulated feet is an improvement of this design regarding mobility. It attempts to mimic anatomical movement of the ankle such as plantar and dorsiflexion, increasing stability [15]. In order to reduce the energy consumption of LLAs, feet with energy return have been design. Such foot is based on a spring molded carbon fiber plates to allow energy restitution after the stance phase. It is the most popular one and preferred for patients with good mobility like young people. Moreover, it reduces the impact and stress on the healthy leg [6, 15]. Finally, microprocessor feet, including ankle and foot control by a small computer and sensors, have also been proposed. They allow live adjustment of characteristic of the prosthetic feet such as its range of motion and speed. However, as microprocessor feet are more expensive, most of the amputees will be equipped with one of the previous feet [15].

A.3 Prosthetic knee joint

It is designed according to the mobility of the patient. If the patient is old, the knee will not be articulated in order to prioritise security [6]. However, if the patient is mobile enough such as young patients, a prosthesis allowing knee flexion is preferred [6]. The polycentric prosthetic knee joint, presented in Chapter 1 (see Figure 1.3), attempts to mimic the movement of a normal knee joint during gait. Moreover, it increases stability and provides about 165° knee motion range, allowing movements such as kneeling, squatting or even biking [16]. It is equipped with an oil-filled nylon polymer, which allows self lubrication of the knee with use. More sophisticated knee joints exist, such as pneumatic or hydraulic joints, allowing modulation of the knee flexion according to walking velocity [6]. Finally, there are some electronic knee joints like the model 3E80 from Ottobock [70]. This one combines the advantages of hydraulic knee joints with electronic control to allow live adaptation of the joints characteristics to the users activity. However, they are not often used due to their price (up to 25 000€) [6].

Appendix B

Sensory process

In this Appendix, one will find complementary information about the sensory process, which has been presented in Section 1.3.

Every sensory process is composed of four steps : detection, transduction, transmission and perception. First, a stimulus is detected by a sensory receptor. This receptor can be either a cell like a neuron, or a cell that regulates neurons through neurotransmitters. Both types can be found below in Figure B.1.

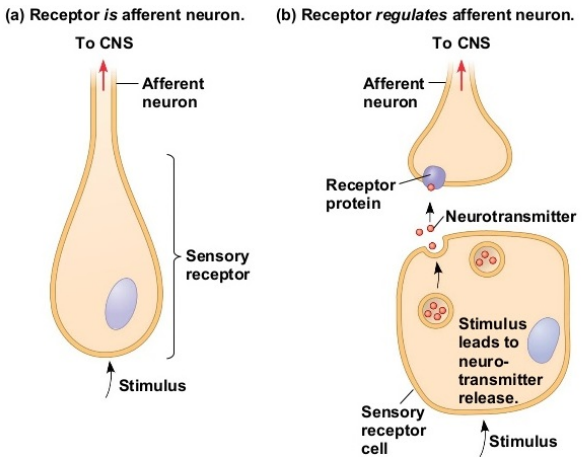

Figure B.1: Types of sensory receptors
[24]

Signal transduction occurs next. It is the conversion of the energy of the stimulus in membrane potential variation of the receptor thanks to the opening or closing of ionic channels due to the stimulus. The transmission of the signal follows when the receptor membrane potential triggers action potentials (APs) in neurons, which are the communication units of the CNS. The intensity of the stimulus influences proportionally the firing rate of the neurons: the more intense the stimulus, the more APs the neuron triggers. Finally, perception occurs when

the APs reach the brain, where neuronal circuits treat the information in order to interpret it [24].

Appendix C

Literature review complements

In this appendix, one will find complement articles to the literature review, which has been performed in Section 2.2.

C.1 Vibrotactile Stimulation

In 2005, Collins and colleagues [71] studied how skin stretch could be integrated to vibratory stimulus in order to create movement illusions. To assess this, they compared the amplitude of illusory movements evoked by these two means when they were activated (i) separately and (ii) simultaneously. They tested on several body areas including the knee joint. For this one, subjects were seated while skin stretch and vibratory stimulus were applied respectively on the anterior thigh and at the patellar tendon. Skin stretch was applied in order to mimic skin strain during small and large joint flexions. It was provided through fine threads, connected to elastic bands, attached to the skin with adhesive tape. Tendon vibration was applied at 100 Hz.
They showed that skin stretch evokes significant illusory movements and that their amplitudes are stronger under strong stretch conditions. Still, the illusions produced are smaller than those obtained with tendon vibration. However, they showed that by coupling tendon vibration with skin stretch, illusory movement amplitudes are above those produced by tendon vibration alone.

The effects of vibratory feedback on static and dynamic balance in unilateral transtibial amputees were investigated in 2012 by Rusaw and colleagues [72]. The feedback system was composed of pressure sensors (Flexiforce transducers) at the prosthetic foot. Their voltage output was sent to a control unit producing current for the vibrating tactors on the thigh. A representation of the system can be seen below in Figure C.1. The tactors provided minimal vibrations when standing in neutral position whereas vibration increased when the pressure sensors were under load. They performed standing balance test (maintaining a posture for 20s under several sensory conditions), limit of stability test (measuring the maximal excursion an individual can cover without stepping or losing balance) and rhythmic weight shift test (measuring synchronization and directional control).

They showed that subjects have faster reaction times when feedback was on in the limit of stability test, as well as an increase in stability in the standing balance test.

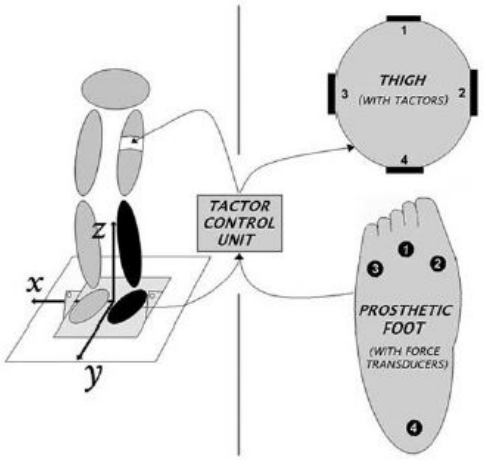

Figure C.1: System based on pressure sensors at the prosthetic foot, providing tactile feedback through vibrating units placed around the user's thigh.
[72]

Last year, Demircan et al. [73] studied the human perception accuracy of different types of vibrotactile feedback during locomotion. They evaluated (i) the effects of the number of actuators activated at once, (ii) the effects of the vibration type, i.e. continuous or discrete and finally (iii) they addressed how well subjects can interpret higher order of simultaneous feedback. They did two experiments consisting of running and walking trials. In the first experiment, subjects were asked to run on a treadmill for several minutes under randomly generated feedback patterns: one to four out of 10 motors (placed on different body locations) were activated with continuous or discrete pulses. They measured the feedback perception accuracy, i.e. the percentage of success of subjects that identified correctly the number of actuators in two different vibration modes. The second experiment consisted of walking trials and two running trials. While moving at constant speed on a treadmill, subjects received vibrations on the same 10 body locations. The vibrations were continuous or staggered: the activated motors vibrated at the same time (up to four motors) for the continuous model, while they vibrated in sequential manner with 0.5s delay between each motor for the staggered mode. The feedback perception accuracy was also measured.
In concordance with the team of Wentinck and colleagues, they showed that sequential vibration perception was significantly higher. However, average perception accuracy for all motor combinations decreased by 9.3% when subjects were running.

C.2 Electrotactile Stimulation

In 2016, Pagel et al. [74] explored if continuous feedback through AMS had an impact on postural control in three transfemoral amputees. They assessed the effects of COP and knee angle feedback on unperturbed standing and treadmill walking as well as perturbed standing. To produce AMS they used two pairs of round electrodes placed in the lower back of subjects, producing charge-balanced biphasic signals at 6 kHz. COP feedback was provided during quiet stance and stance phase in the gait cycle. To map the AMS to COP trajectory, they used a force/moment sensor embedded in between the prosthetic foot and shank tube, measuring two force components and the sagittal plane's bending moment. The signal from the sensor was processed to extract COP data. Knee angle feedback was provided during the swing phase of the gait cycle. To provide knee joint angle data, they used a goniometer-gyroscope sensor system. The first part of the experiment consisted in defining the individual stimulation thresholds. Then, they performed the (i) standing and (ii) walking experiments. In (i), subjects were standing in self-selected comfortable position with each foot placed on a force sensor plate. They were asked to stand as still as possible under several conditions such as eyes open, eyes closed, soft ground and others. Each task was performed with and without feedback. In (ii), subjects were asked to walk as symmetric as possible at self-selected speed on a treadmill. This was also tested with and without feedback.
Their results showed that AMS is not beneficial as it decreases stability and increases the cognitive load as AMS interpretation seems to be difficult without training. Indeed it is preferable to have a feedback modality that requires less attention to be more intuitive or to train subjects.

Appendix D

Rhythm synchronisation

In this Appendix, one will find complementary information about the rhythm synchronisation results, which have been presented in Section 4.1.

D.1 Region one delimitation

In this section are presented more graphical visualisation of the delimitation of the region one for S1 (Figure D.1), S2 (Figure D.2), S3 (Figure D.3), S4 (Figure D.4) and S5 (Figure D.5).

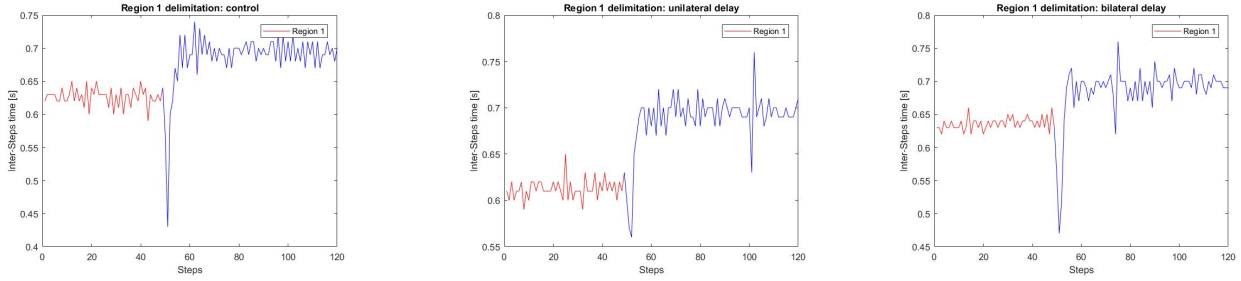

(a) S1: control (b) S1: unilateral delay (c) S1: bilateral delay

Figure D.1: Region delimitation for S1, according to the definition of n_{t1}

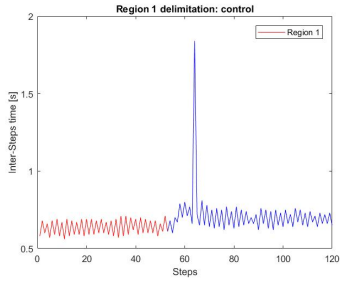

(a) S2: control

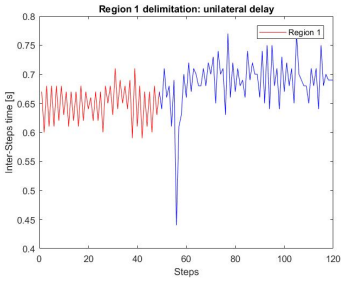

(b) S2: unilateral delay

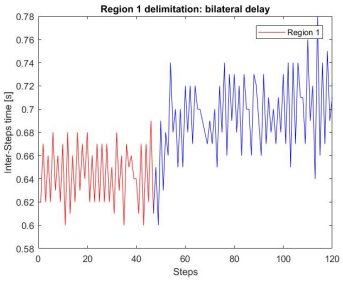

(c) S2: bilateral delay

Figure D.2: Region delimitation for S2, according to the definition of n_{t1}

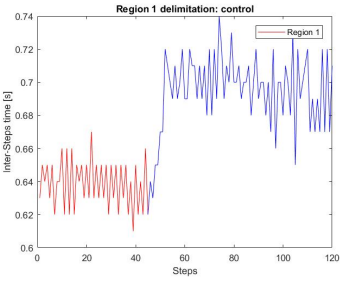

(a) S3: control

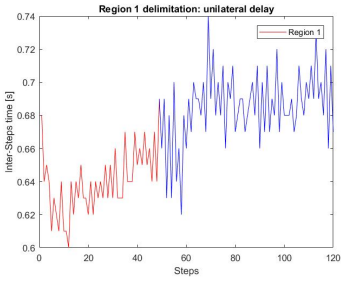

(b) S3: unilateral delay

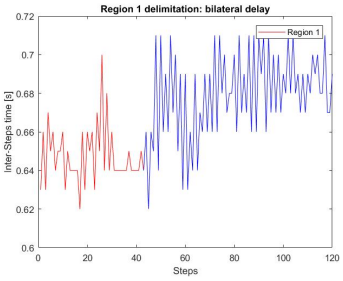

(c) S3: bilateral delay

Figure D.3: Region delimitation for S3, according to the definition of n_{t1}

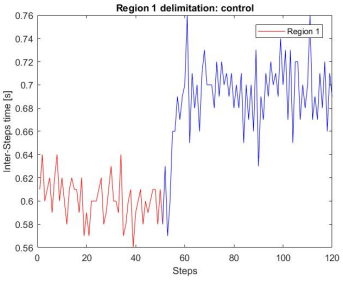

(a) S4: control

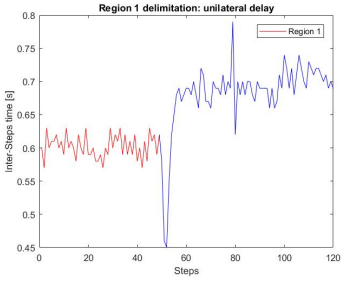

(b) S4: unilateral delay

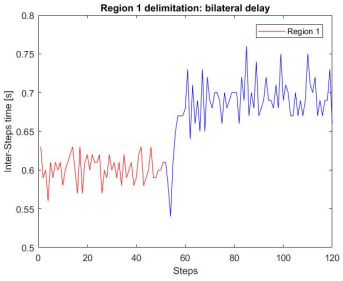

(c) S4: bilateral delay

Figure D.4: Region delimitation for S4, according to the definition of n_{t1}

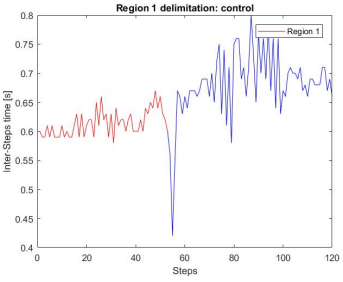

(a) S5: control

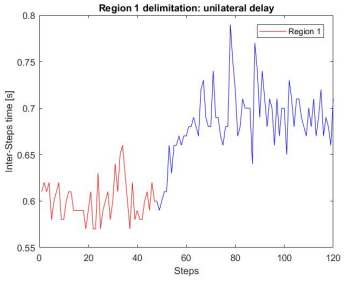

(b) S5: unilateral delay

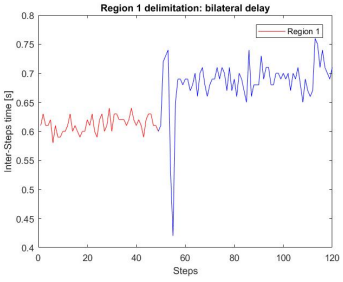

(c) S5: bilateral delay

Figure D.5: Region delimitation for S5, according to the definition of n_{t1}

D.2 S2 and S5 ISTs (not zoomed in)

The ISTs for S2 and S5 are represented without zoom on Figure D.6.

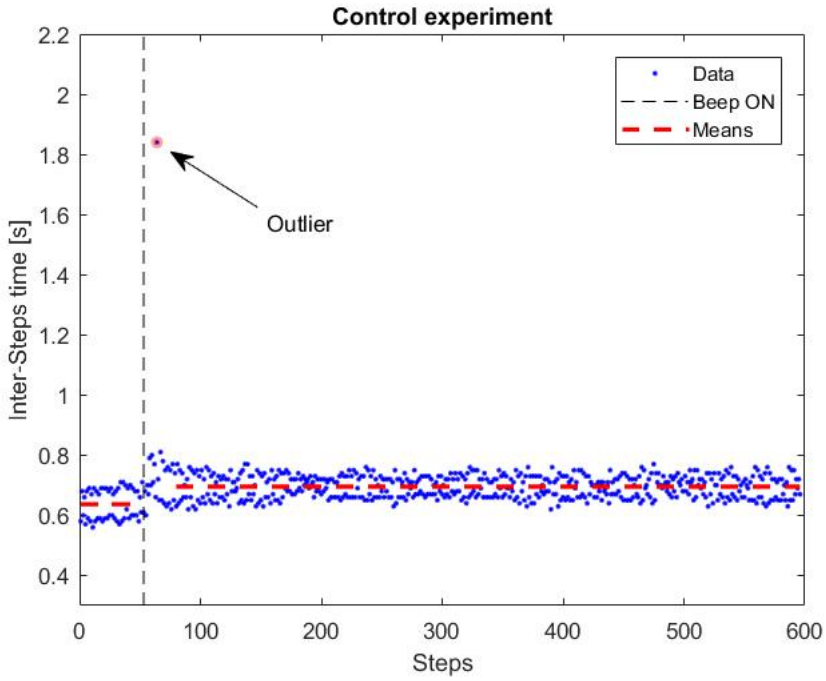

(a) S2

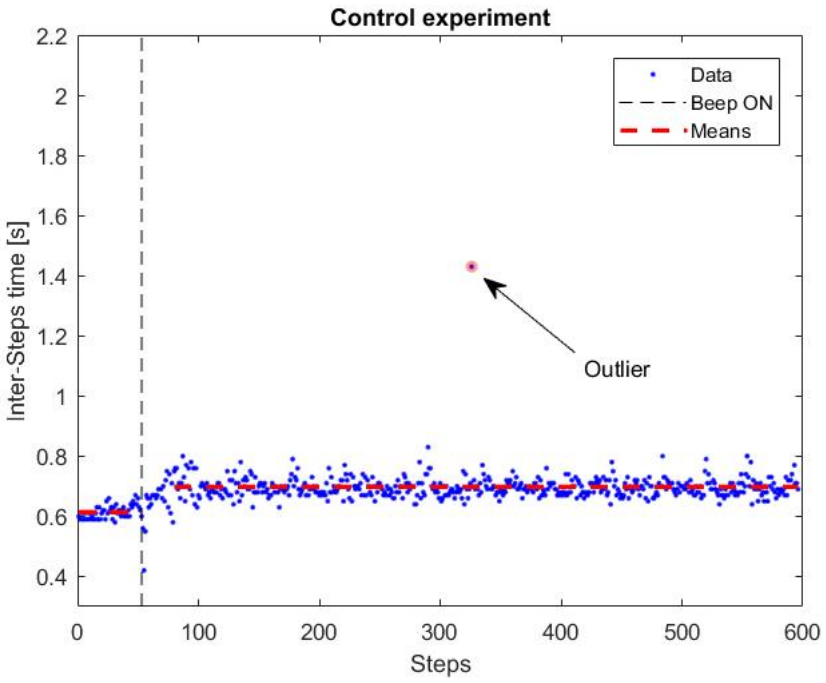

(b) S5

Figure D.6: S2 and S5 ISTs (not zoomed in)

D.3 Left-to-right and right-to-left step transition distributions

In this section, a graphical representation of each subject's left-to-right and right-to-left IST distributions in the control experiment will be presented. These representations can be found on Figure D.7 below.

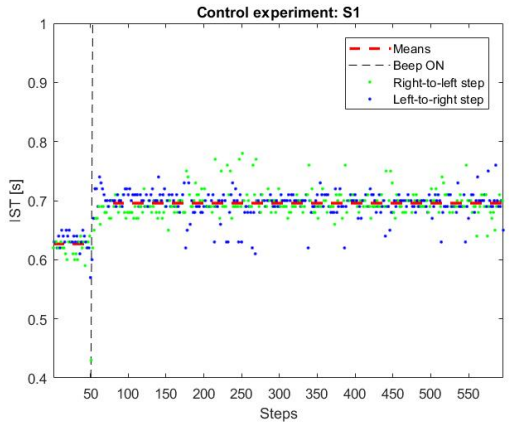

(a) S1 oscillating behavior: left-to-right step (blue dots) and right-to-left step transitions (green dots) highlighted

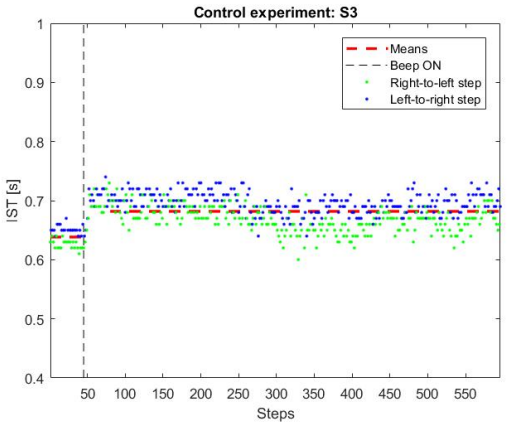

(b) S3 oscillating behavior: left-to-right step (blue dots) and right-to-left step transitions (green dots) highlighted

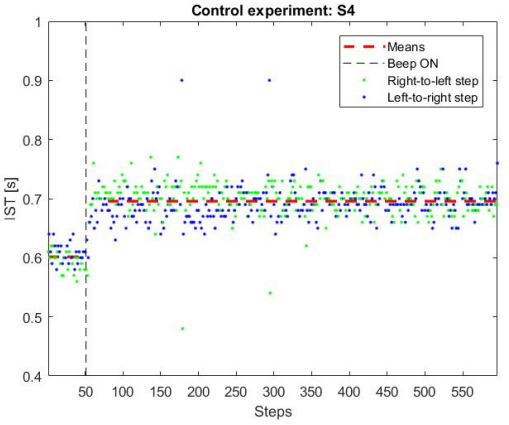

(c) S4 oscillating behavior: left-to-right step (blue dots) and right-to-left step transitions (green dots) highlighted

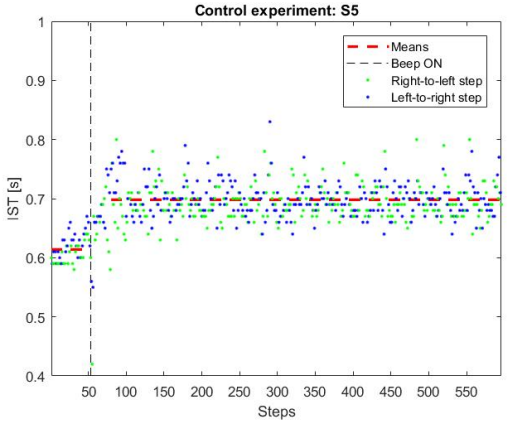

(d) S5 oscillating behavior: left-to-right step (blue dots) and right-to-left step transitions (green dots) highlighted

Figure D.7: S2 IST data model fitting for each experiment

D.4 Delay of *Matlab*

A representation of the iteration delay, which occurred in one execution of the *Matlab* code, can be found on Figure D.8.

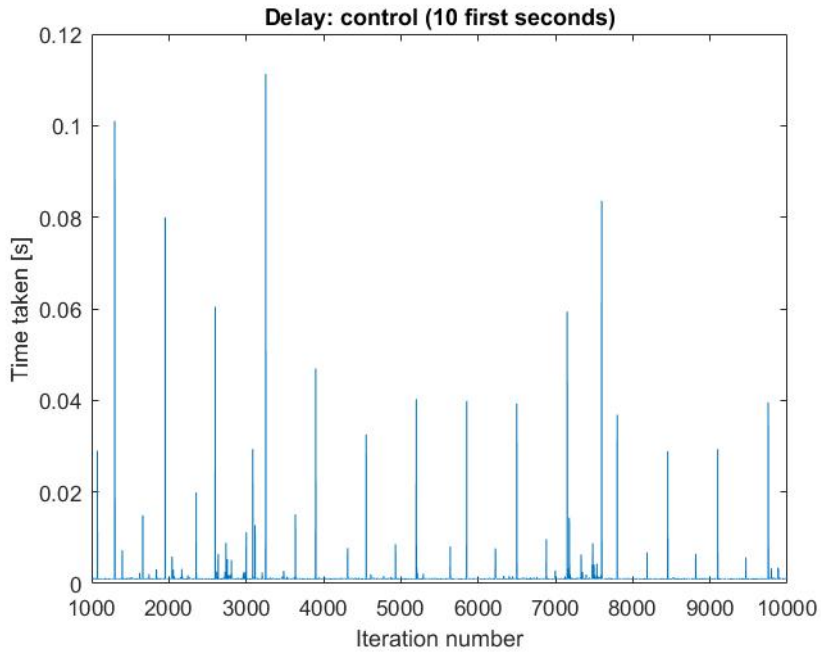

(a) Time taken per iteration for the 10 first seconds of execution. The theoretical iteration time is 1ms

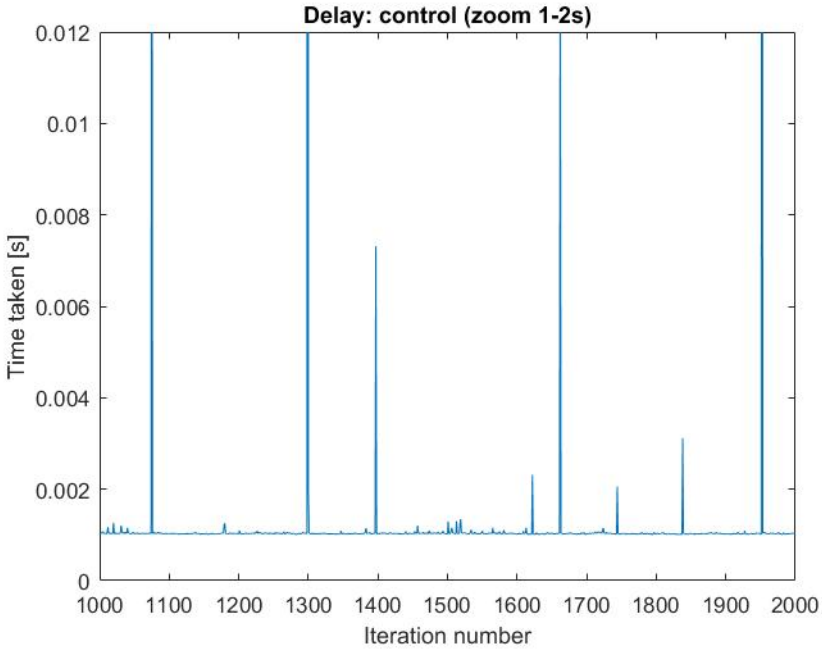

(b) Time taken per iteration zoomed around the two first second of execution

Figure D.8: *Matlab* execution delay

Appendix E

Rhythm memory

In this Appendix, one will find complementary information about the rhythm memory results, which have been presented in Section 4.2.

E.1 Model parameter fitting

In this section, appreciation of the model behaviour with respect to the IST data will be presented below, for S2 (Figure E.1), S3 (Figure E.2), S4 (Figure E.3) and S5 (Figure E.4).

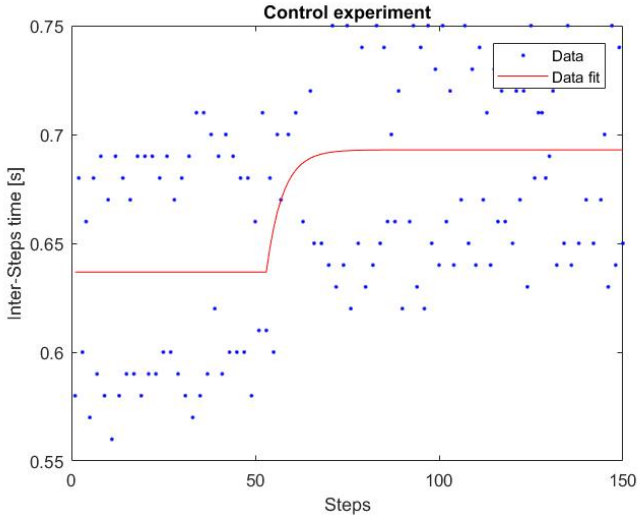

(a) S2: control

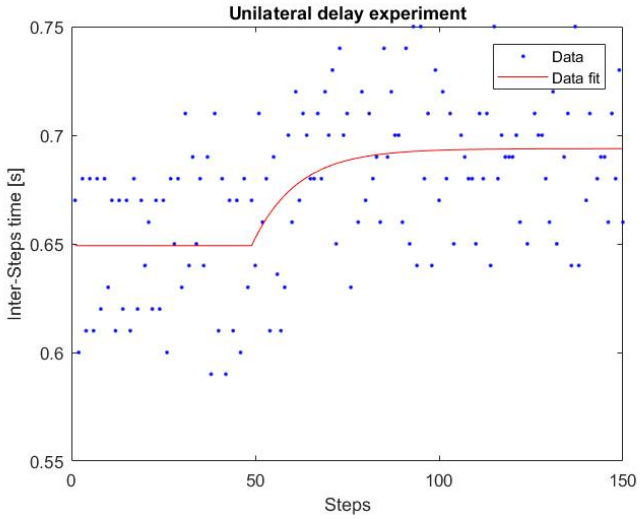

(b) S2: unilateral delay

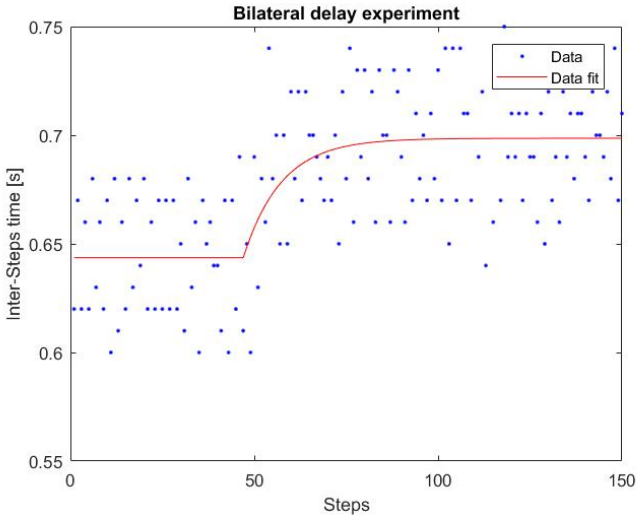

(c) S2: bilateral delay

Figure E.1: IST data model fitting throughout the experiments for S2

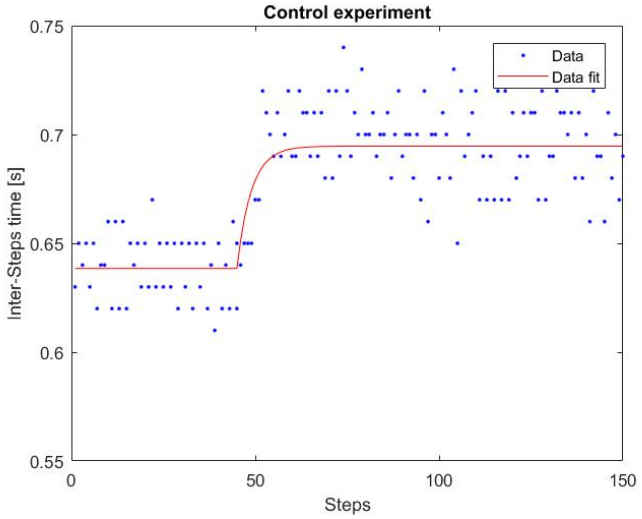

(a) S3: control

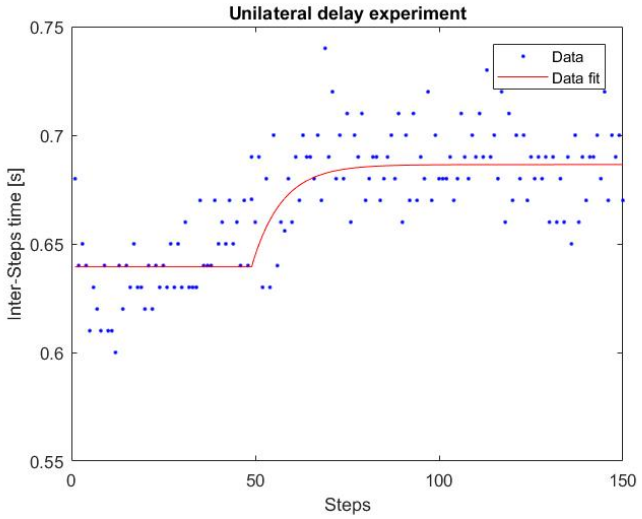

(b) S3: unilateral delay

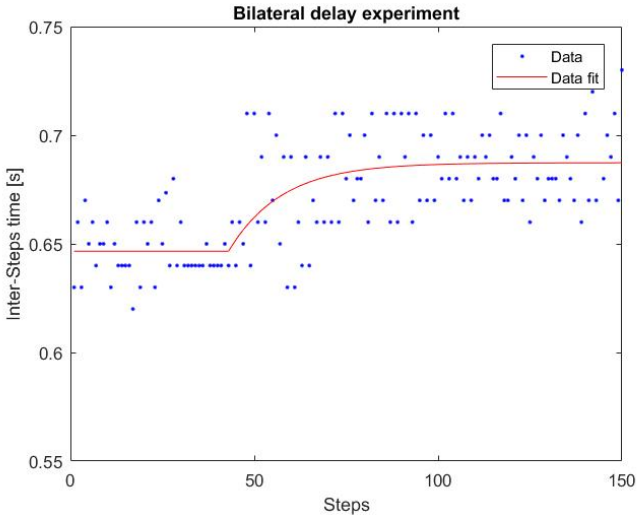

(c) S3: bilateral delay

Figure E.2: IST data model fitting throughout the experiments for S3

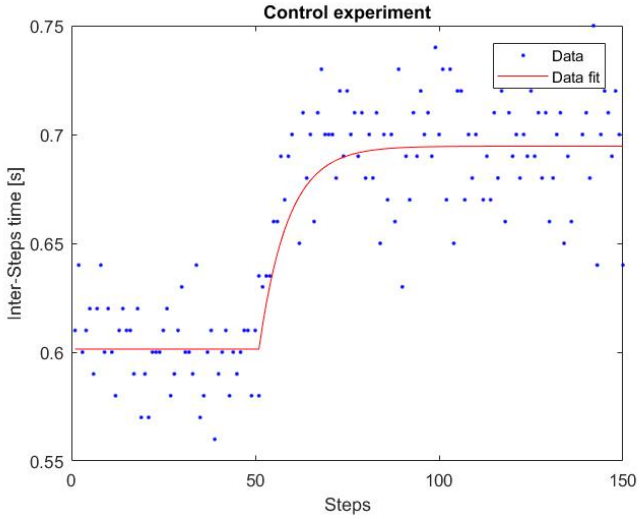

(a) S4: control

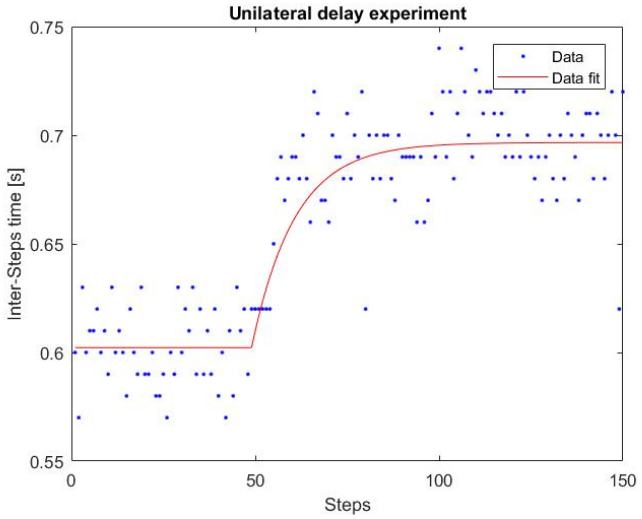

(b) S4: unilateral delay

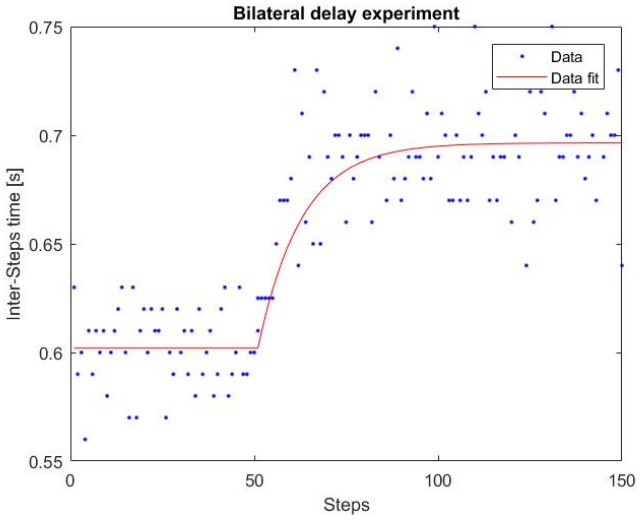

(c) S4: bilateral delay

Figure E.3: IST data model fitting throughout the experiments for S4

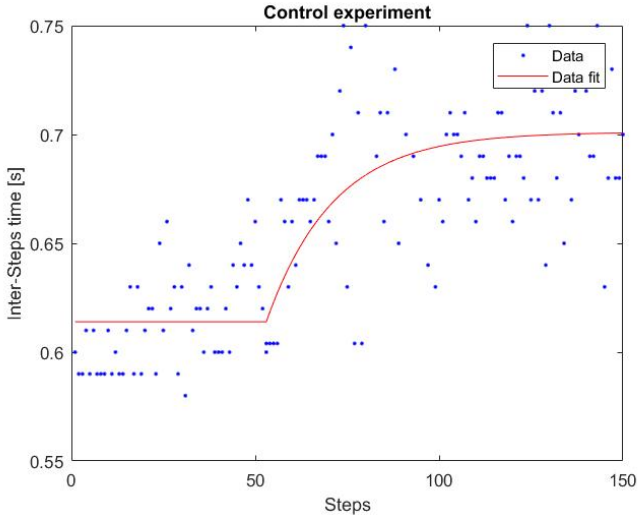

(a) S5: control

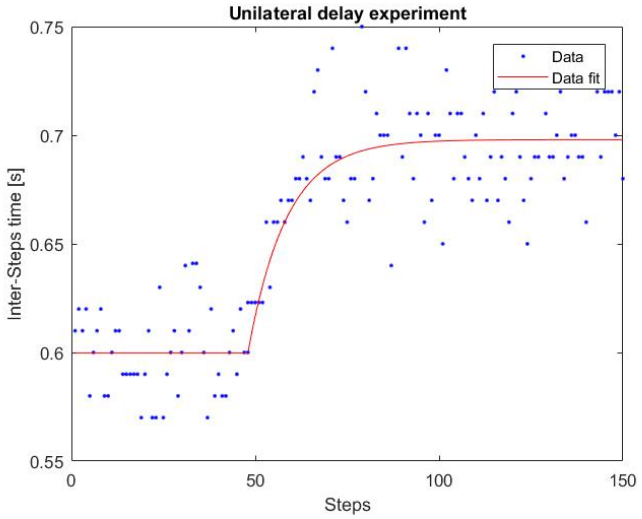

(b) S5: unilateral delay

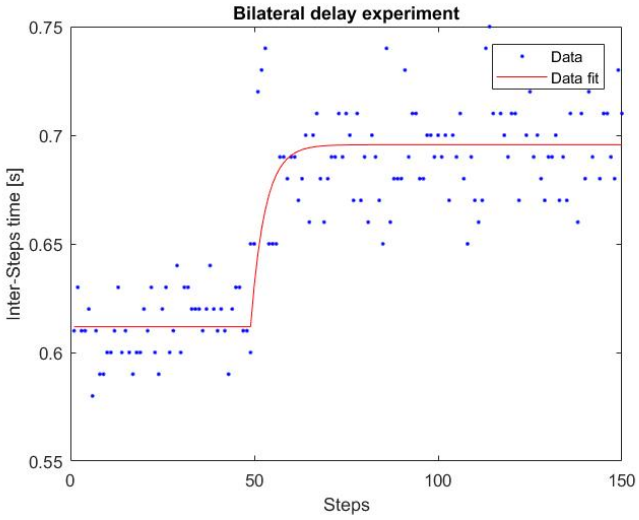

(c) S5: bilateral delay

Figure E.4: IST data model fitting throughout the experiments for S5

E.2 Evolution of the SR in region one

In this section will be presented the evolution of the SR in region one for S1 (Figure E.5), S2 (Figure E.6), S3 (Figure E.7) and S4 (Figure E.8).

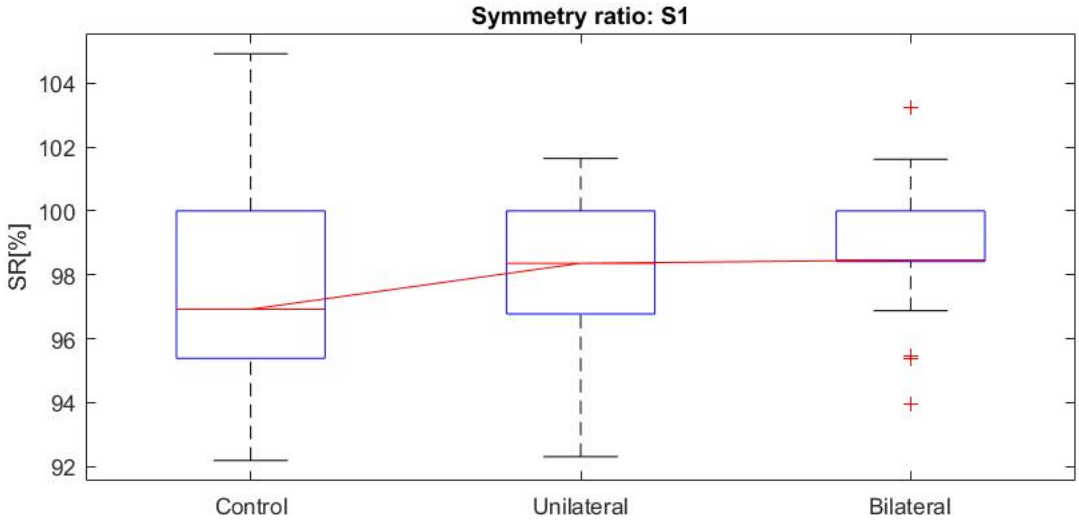

Figure E.5: Evolution of SR for S1 in region one, from the control experiment (Control), via the unilateral delay experiment (Unilateral) to the bilateral delay experiment (Bilateral)

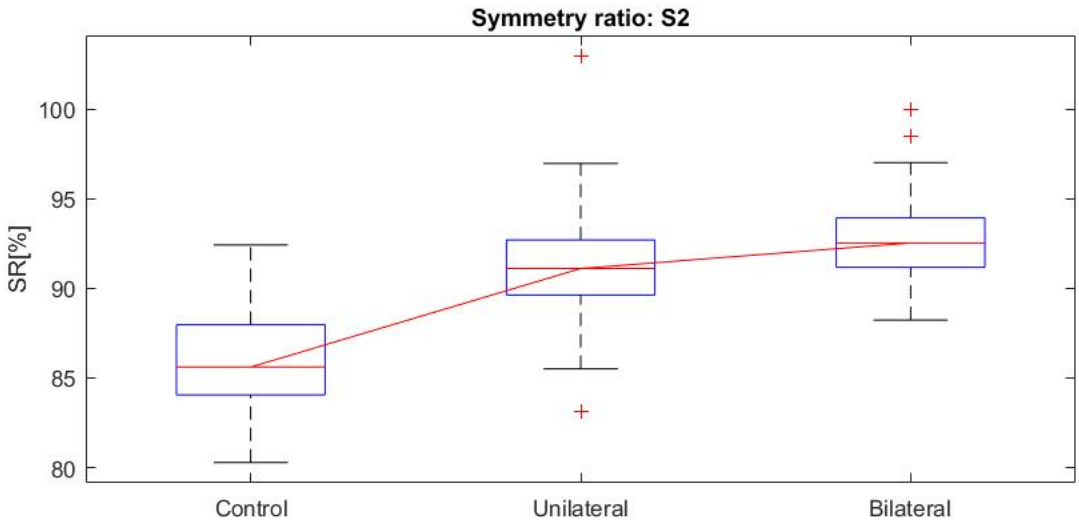

Figure E.6: Evolution of SR for S2 in region one, from the control experiment (Control), via the unilateral delay experiment (Unilateral) to the bilateral delay experiment (Bilateral)

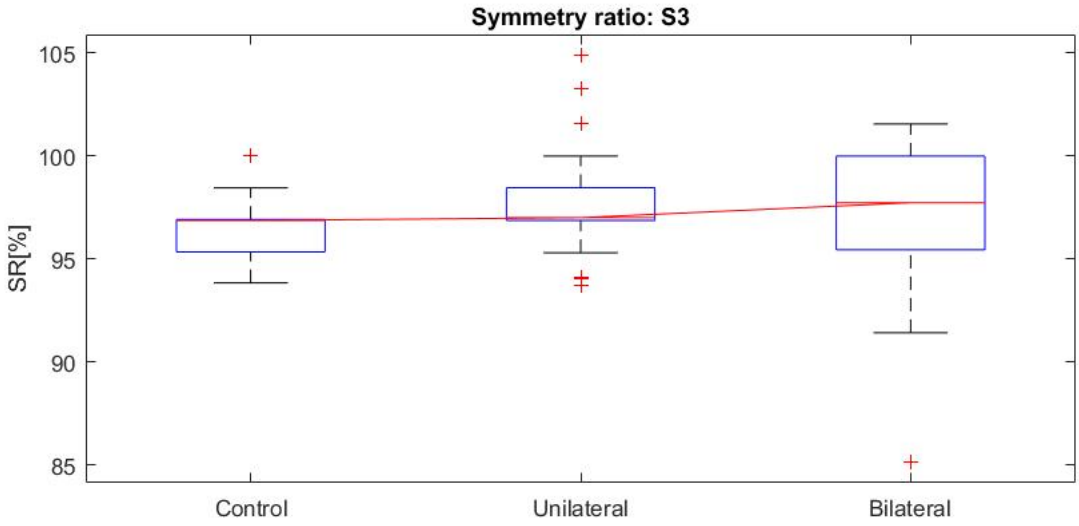

Figure E.7: Evolution of SR for S3 in region one, from the control experiment (Control), via the unilateral delay experiment (Unilateral) to the bilateral delay experiment (Bilateral)

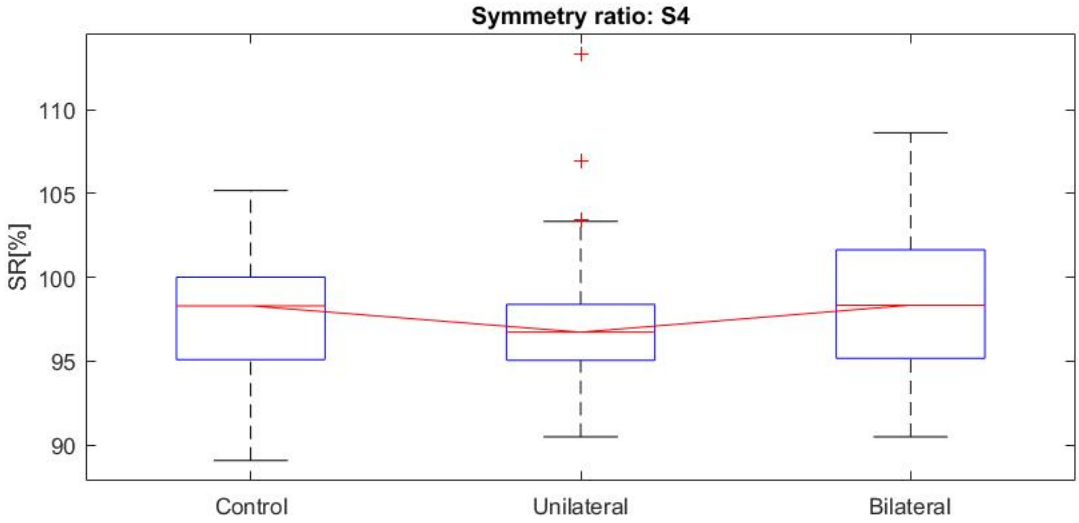

Figure E.8: Evolution of SR for S4 in region one, from the control experiment (Control), via the unilateral delay experiment (Unilateral) to the bilateral delay experiment (Bilateral)

Appendix F

Rhythm disturbance

Complementary information regarding the rhythm disturbance results (Section 4.3) will be presented. In particular, the evolution of the SR in region four will be presented for S2 (Figure F.1), S3 (Figure F.2), S4 (Figure F.3) and S5 (Figure F.4).

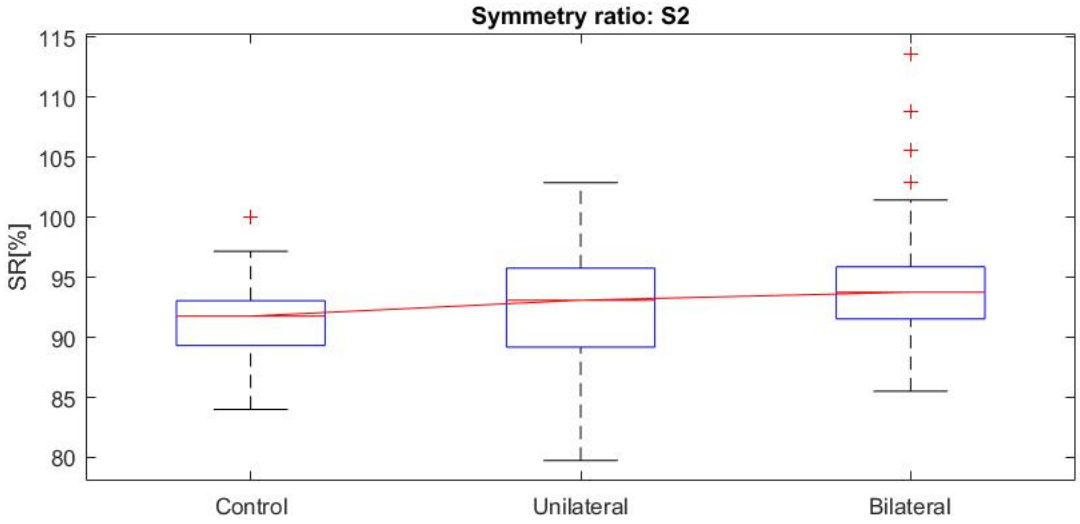

Figure F.1: Evolution of SR for S2 in region four, from the control experiment (Control), via the unilateral delay experiment (Unilateral) to the bilateral delay experiment (Bilateral)

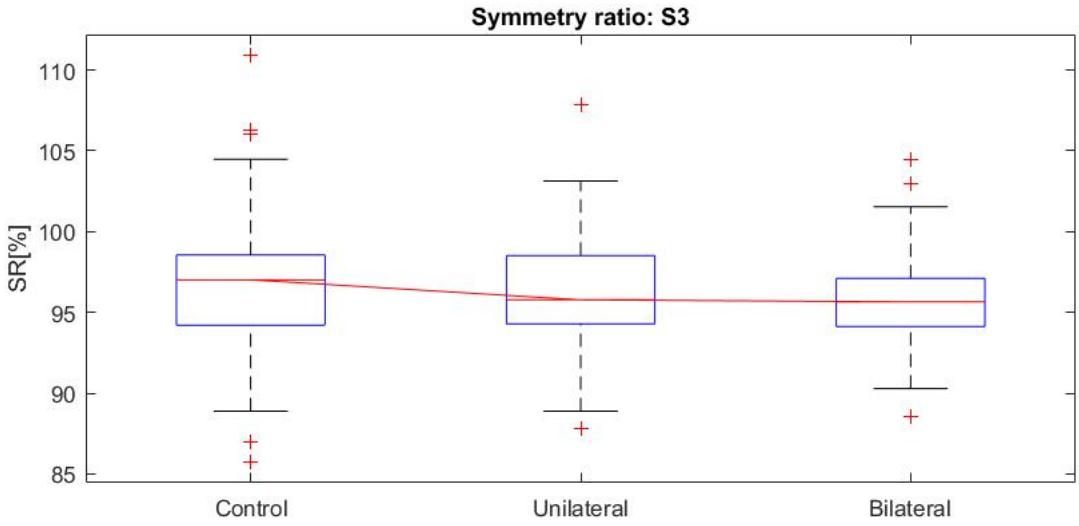

Figure F.2: Evolution of SR for S3 in region four, from the control experiment (Control), via the unilateral delay experiment (Unilateral) to the bilateral delay experiment (Bilateral)

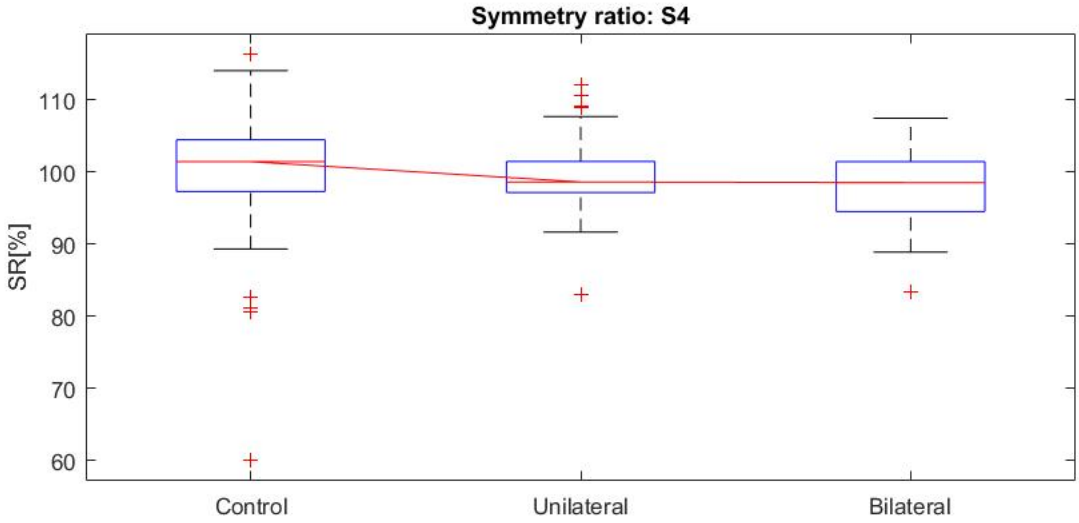

Figure F.3: Evolution of SR for S4 in region four, from the control experiment (Control), via the unilateral delay experiment (Unilateral) to the bilateral delay experiment (Bilateral)

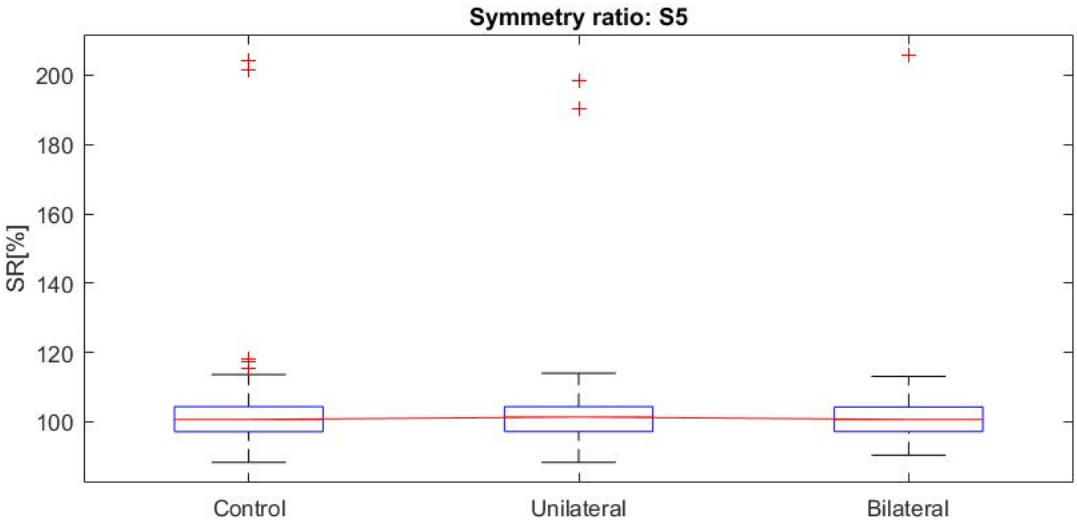

Figure F.4: Evolution of SR for S5 in region four, from the control experiment (Control), via the unilateral delay experiment (Unilateral) to the bilateral delay experiment (Bilateral)

Appendix G

Statistical tests: assumptions verification

In this Appendix, one will find the verifications of the different assumptions made by the statistical tests presented in Section 3.5.

1. **One-sample T-Test**: the test assumptions need to be verified on the ISTs from region three to six in the control experiment (see Figure 3.14). The start of region three was approximated as corresponding to the 150th step for each subject. As no delays were induced in this experiment, this approximation is not a problem. The assumptions are the following [66]:

   (a) **Continuity of the dependant variable**: a continuous dependant variable is a variable that can take an infinite amount of value. Here, the dependant variable is a time measure (i.e. the IST), which is continuous.

   (b) **Observation are independent of one another**: this one is not testable. However, it can be safely assumed if the data collection was random. Still, this was not the case in this pilot experiment.

   (c) **The dependant variable should not contain significant outliers**: this can be seen on the boxplots in Figure G.1. Only S5 had an outlier, which was removed according to the rule defined in Section 3.5.2.

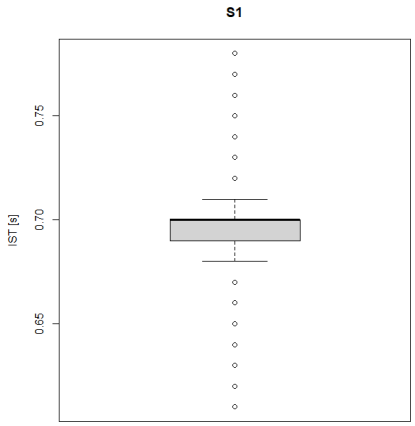

(a) S1

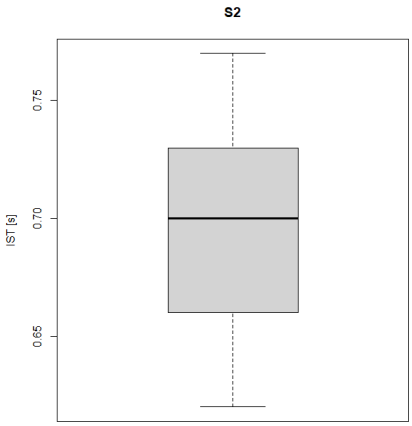

(b) S2

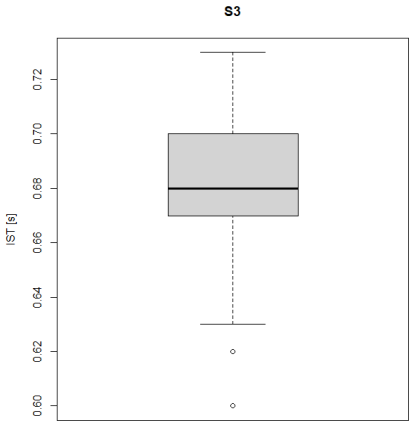

(c) S3

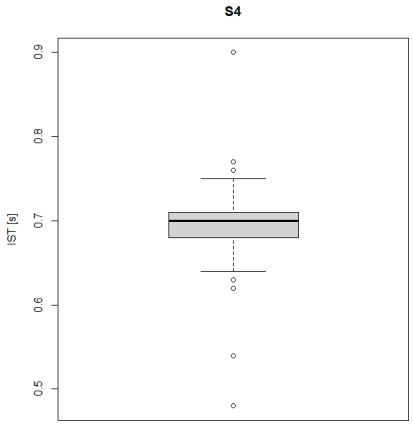

(d) S4

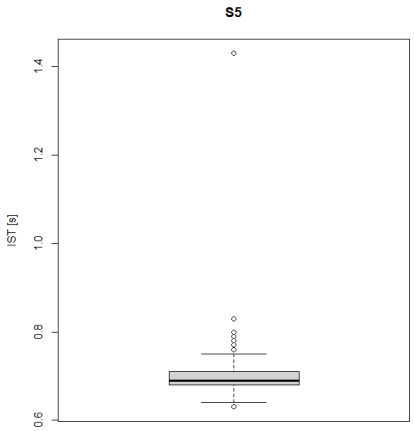

(e) S5

Figure G.1: ISTs boxplots from region three in the control experiment

(d) **The dependent variable is normal**: the distribution of the ISTs are represented in Figure G.2. For all subjects this looks close to normal, except for S2 whose distribution is bimodal. To assess normality, a Schapiro test and a measure of the distributions skewness was performed. The Schapiro test is a normality test, whose null hypothesis states that the distribution is normal. The skewness is an indicator for symmetry. The closer to zero, the more symmetric the distribution and thus, the closer to the normal distribution. Results can be found in Table G.1. The p-values are below the significance level, implying that the distribution are not normal. Still, the T-Test may be performed. According to [75, 76], the one-sample T-Test can handle skewness up to magnitude one. Moreover, if the sample size is above 30 observations, the test is considered robust. In other words, the T-Test is robust if the distribution is more or less symmetrical, as it is the case here (even for the bimodal distribution) [76].

Table G.1: Skewness and Schapiro test ($\alpha = 0.05$)

Subjects	**Skewness**	**Schapiro: p-value**
S1	-0.0953	<2.2e-16
S2	-0.0032	3.799e-13
S3	-0.2460	3.607e-07
S4	0.2894	<2.2e-16
S5*	0.3829	4.802e-10

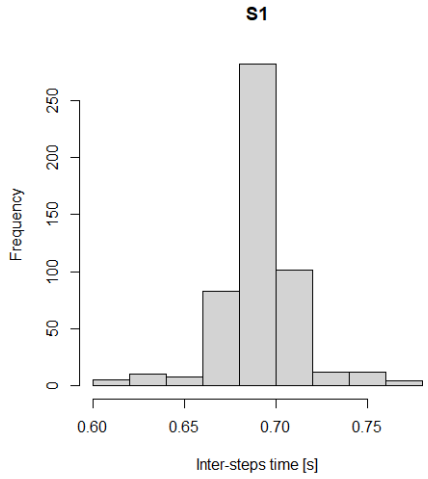

(a) S1

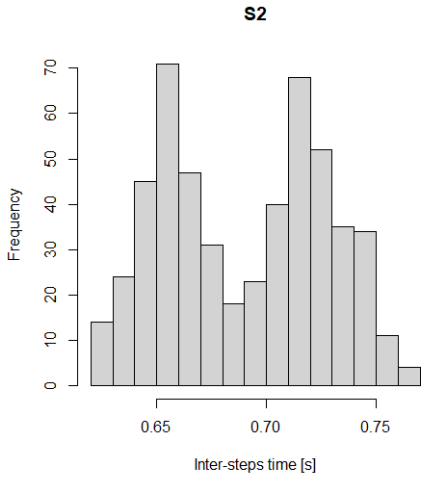

(b) S2

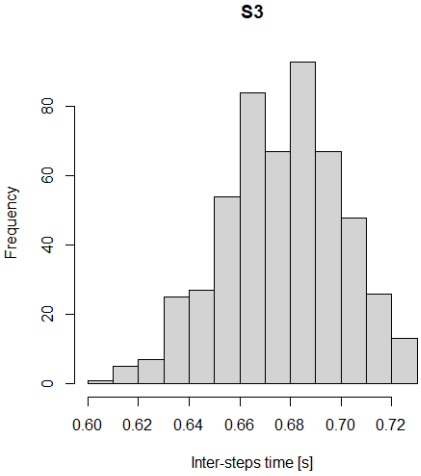

(c) S3

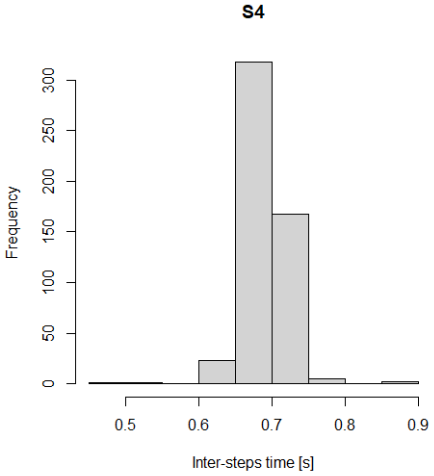

(d) S4

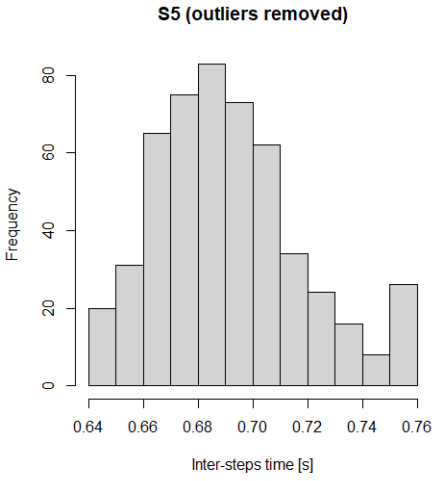

(e) S5 (outliers removed)

Figure G.2: ISTs distribution from region three in the control experiment

2. **One-way ANOVA with repeated measures**: the data of interest are the ISTs and SRs in region one. The conditions of utilisation are [77]:

   (a) **The normality of the dependent variable**: normality must be assessed for the data of each experimental condition. The results of the different Schapiro tests can be found in Table G.2. The normal distribution are those which have their p-value above the significance level (see in red in Table G.2 and G.3). As it can be seen, lots are considered non normal. However, according to the Central Limit Theorem, the sample mean will approach a normal distribution with increasing number of trials. Therefore, "if a sufficient number of trials is collected per subject and experimental condition" - i.e. the number of ISTs and SRs measured per subjects, for each experiments - "the dependent variable in the repeated measures ANOVA can always be considered normally distributed" [78].

Table G.2: Schapiro test: IST distribution ($\alpha = 0.05$)

Subjects	**p-value (Experiment one)**	**p-value (Experiment two)**	**p-value (Experiment three)**
S1	0.0059	0.0006	0.0003
S2	6.418e-06	0.0022	0.0011
S3	0.0037	0.1015	0.0002
S4	0.1168	0.0219	0.0546
S5	0.0027	0.0226	0.0428

Table G.3: Schapiro test: SR distributions ($\alpha = 0.05$)

Subjects	**p-value (Experiment one)**	**p-value (Experiment two)**	**p-value (Experiment three)**
S1	0.2247	0.0036	0.0234
S2	0.6779	0.0471	0.0011
S3	0.0003	0.0031	0.0002
S4	0.3873	4.446e-05	0.3147
S5	0.1355	0.1737	0.1505

   (b) **The variance are homogeneous (sphericity)**: the second hypothesis is tested through a Mauchly sphericity test. Fortunately, if this condition is not met, some procedures, such as the Greenhouse-Geisser Epsilon correction, can be used to adjust for the lack of sphericity. The Mauchly's test ($\alpha = 0.05$) gave a p-value of 0.3406 for the IST and 0.1339 for the SR distributions. Hence, Greenhouse-Geisser sphericity correction will be applied. The latter is included in the one-way repeated measures ANOVA *R* function.

   (c) **The independence of the data**: the experiments were not conducted randomly, hence independence can not be guaranteed.

3. **Levene's test**: the Levene's is robust to departure from normality. To the knowledge of the author, no specific assumptions are made by this test.

4. **Two-sample T-Test**: the assumptions of the two-sample T-Test need to be verified on the SR of S3 in region four. Its assumptions are the same as the one-sample T-Test, which were presented previously. The SR is continuous by definition and outliers were removed according to the rule defined in Section 3.5. However, independence can not be guaranteed as the experiments were not randomised. Verification of the normality of the data, after outliers removal ("*"), can be found in Table G.4. As it can be seen, only one distribution of the SR is normally distributed (red in Table G.4), while the others have skewness magnitudes below one, which are normality deviations to which the two-sample T-Test is robust [75].

Table G.4: Skewness and Schapiro test ($\alpha = 0.05$)

Experiment	**Skewness**	**Schapiro: p-value**
Control*	0.3143	0.0069
Unilateral*	-0.067	0.1959
Bilateral*	0.3340	0.0027

Bibliography

[1] K. Demet et al. Health related quality of life and related factors in 539 persons with amputation of upper and lower limb. *Disability and rehabilitation*, 25:480–486, 2003.

[2] R. Sinha et al. Factors affecting quality of life in lower limb amputees. *Prosthetics and Orthotics International*, 35:90–96, 2010.

[3] N. Ahmad et al. The prevalence of major lower limb amputation in the diabetic and non-diabetic population of england 2003–2013. *Diabetes and Vascular Disease Research*, 13:348–353, 2016.

[4] M. Spoden et al. Amputation rates of the lower limb by amputation level - observational study using german national hospital discharge data from 2005 to 2015. *BMC Health Services Research*, 9:8, 2019.

[5] S. Fosse et al. Incidence and characteristics of lower limb amputations in people with diabetes. *Diabetic Medicine*, 26:391–396, 2009.

[6] J.M. Vanmarsenille. Amputations: types d'appareillages. *Service d'orthopédie des Cliniques universitaires Saint-Luc (Bruxelles-Woluwe)*, 2013.

[7] M. Ezzati et al. Worldwide trends in diabetes since 1980: a pooled analysis of 751 population-based studies with 4.4 million participants. *Lancet*, 387:1513–1530, 2016.

[8] A. Plauché et al. A haptic feedback system for phase-based sensory restoration in above-knee prosthetic leg users. *IEE Transactions on haptics*, 9:421–426, 2016.

[9] E. Fan et al. A haptic feedback system for lower-limb prostheses. *IEE Transactions on neural systems and rehabilitation Engineering*, 16:270–277, 2008.

[10] R. Gailey et al. Review of secondary physical conditions associated with lower-limb amputation and long-term prosthesis use. *Journal of Rehabilitation Research Development*, 45:15–30, 2008.

[11] S.W. Hunter et al. Risk factors for falls in people with a lower limb amputation: a systematic review. *The journal of injury, function and rehabilitation*, 9:170–180, 2016.

[12] P.L. Ephraim et al. Phantom pain, residual limb pain, and back pain in amputees: Results of a national survey. *Archives of Physical Medicine and Rehabilitation*, 86:1910–1919, 2005.

[13] A.G. Cutti et al. Reference values for gait temporal and loading symmetry of lower-limb amputees can help in refocusing rehabilitation targets. *Journal of neuroengineering and rehabilitation*, 15(1):61, 2018.

[14] Orthotic Prosthetic Associates. Limb replacement (prosthetics), consulted the 30 of April 2020. `https://orthoticprostheticassociates.com/products-services-3/`.

[15] Physiopedia. Prosthetic feet, consulted the 19 of January 2020. `https://www.physiopedia.com/Prosthetic_Feet`.

[16] D-Rev. Remotion polycentric knee joint, consulted the 19 of January 2020. `http://d-rev.org/projects/mobility/`.

[17] P. Shull et al. Haptic wearables as sensory replacement, sensory augmentation and trainer – a review. *Journal of Neuroengineering and Rehabilitation*, 12:59, 2015.

[18] C. Dietrich et al. Sensory feedback prosthesis reduces phantom limb pain: Proof of a principle. *Neuroscience Letters*, 507:97–100, 2012.

[19] Smith PA Hassani S. Abu-Faraj ZO, Harris GF. Human gait and clinical movement analysis. In *Wiley Encyclopedia of Electrical and Electronics Engineering*, pages 1–34. Second edition, 2015.

[20] E. Lederman. *Neuromuscular Rehabilitation in Manual and Physical Therapy*. Elsevier, 2010.

[21] A. Bubic et al. Prediction, coginition and the brain. *Frontiers in Human Neuroscience*, 4:25, 2010.

[22] J.L. Taylor. Encyclopedia of neurosciences: Proprioception. *ScienceDirect*, 346:1143–1149, 2009.

[23] J.B. Nielsen et al. Afferent feedback in the control of human gait. *Journal of Electromyography and Kinesiology*, 12:213–217, 2002.

[24] Reece, Urry, Cain, Minorsky Wasserman, and Jackson. *Campbell Biologie*. Pearson, 2011.

[25] A. Zimmerman et al. The gentle touch receptors of mammalian skin. *Science*, 346:950–954, 2014.

[26] Wikipedia. Group a nerve fiber, consulted the 30 of April 2020. `https://en.wikipedia.org/wiki/Group_A_nerve_fiber`.

[27] Wikibooks. Skin proprioception, consulted the 5 of May 2020. `https://fr.m.wikibooks.org/wiki/Fichier:Skin_proprioception.svg`.

[28] Physiopedia. Muscles spindles, consulted the 7 of November 2019. `https://www.physiopedia.com/Muscle_spindles`.

[29] Neuroscience Online. Motor units and muscle receptors, consulted the 5 of May 2020. `https://nba.uth.tmc.edu/neuroscience/m/s3/chapter01.html`.

[30] Raising An Extraordinary Person. How does the proprioceptive system work?, consulted the 5 of May 2020. `https://hes-extraordinary.com/how-does-the-proprioceptive-system-work`.

[31] P. Svensson et al. A review of invasive and non-invasive sensory feedback in upper limb prostheses. *Expert Review of Medical Devices*, 14:439–447, 2017.

[32] M. Seps et al. Study on lower back electrotactile stimulation characteristics for prosthetic sensory feedback. *IEEE/RSJ International Conference on Intelligent Robots and Systems*, pages 3454–63459, 2011.

[33] G. Lundborg et al. Hearing as substitution for sensation: a new principle for artificial sensibility. *The Journal of Hand Surgery*, 24:219–224, 1999.

[34] M. D'Alonzo et al. Hyve—hybrid vibro-electrotactile stimulation—is an efficient approach to multi-channel sensory feedback. *IEEE transactions on haptics*, 7(2):181–190, 2013.

[35] D. Zambarbieri et al. *Sensory feedback for lower limb prostheses*, volume 1999, pages 129–151. 2001.

[36] P. Saal et al. Biomimetic approaches to bionic touch through a peripheral nerve interface. *Neuropsychologia*, 79:344–353, 2015.

[37] C. Antfolk et al. Sensory feedback from a prosthetic hand based on airmediate d pressure from the hand to the forearm skin. *Journal of rehabilitation medicine : official journal of the UEMS European Board of Physical and Rehabilitation Medicine*, 44:702–7, 06 2012.

[38] S. Verschueren et al. Effects of tendon vibration on the spatiotemporal characteristics of human locomotion. *Experimental brain research*, 143:231–239, April 2002.

[39] E.C. Wentink et al. Vibrotactile stimulation of the upper leg: Effects of location, stimulation method and habituation. In *33rd Annual International IEEE EMBS Conference*, pages 1668–1671. IEEE Engineering in Medicine and Biology Society, August 2011.

[40] A. Sharma et al. Toward an artificial sensory feedback system for prosthetic mobility rehabilitation: Examination of sensorimotor responses. *Journal of Rehabilitation Research Development*, 6:907–918, Nov 2014.

[41] S. Crea et al. Providing time-discrete gait information by wearable feedback apparatus for lower-limb amputees: Usability and functional validation. *IEEE Transactions On Neural Systems And Rehabilitation Engineering*, 23:250–257, March 2015.

[42] C. Lauretti et al. A vibrotactile stimulation system for improving postural control and knee joint proprioception in lower-limb amputees. In *2017 26th IEEE International Symposium on Robot and Human Interactive Communication (RO-MAN)*, pages 88–93, Aug 2017.

[43] G. Buma et al. Intermittent stimulation delays adaptation to electrocutaneous sensory feedback. *IEEE Transactions On Neural Systems And Rehabilitation Engineering*, 15:435–441, Sept 2007.

[44] S. Pfeifer et al. Displaying centre of pressure location by electrotactile stimulation using phantom sensation. *University of Zurich*, 2010.

[45] A.H. Arieta et al. Apparent moving sensation recognition in prosthetic applications. *Procedia Computer Science*, 7:133–135, 2011.

[46] G. Webb et al. Electro-tactile sensation thresholds for an amputee gait-retraining system. *3rd annual conference of the international functional electrical stimulation society*, 01 2012.

[47] M. D'Alonzo et al. Hyve: hybrid vibro-electrotactile stimulation for sensory feedback and substitution in rehabilitation. *IEEE Transactions on Neural Systems and Rehabilitation Engineering*, 22(2):290–301, 2013.

[48] G. Lundborg et al. Artificial sensibility of the hand based on cortical audiotactile interaction: A study using functional magnetic resonance imaging. *Scandinavian Journal of Plastic and Reconstructive Surgery and Hand Surgery*, 39:370–372, 2005.

[49] L. Yang et al. Utilization of a lower extremity ambulatory feedback system to reduce gait asymmetry in transtibial amputation gait. *Gait Posture*, 36(3):631 – 634, 2012.

[50] B.H. Repp et al. Sensorimotor synchronization: a review of recent research (2006–2012). *Psychonomic bulletin & review*, 20(3):403–452, 2013.

[51] J. Hausdorff et al. Rhythmic auditory stimulation modulates gait variability in parkinson's disease. *European Journal of Neuroscience*, 26(8):2369–2375, 2007.

[52] M. Roerdink et al. Gait coordination after stroke: benefits of acoustically paced treadmill walking. *Physical therapy*, 87(8):1009–1022, 2007.

[53] A. Forner-Cordero et al. Effects of supraspinal feedback on human gait: rhythmic auditory distortion. *Journal of NeuroEngineering and Rehabilitation*, 16:159–168, 2019.

[54] JB. Dingwell et al. Use of an instrumented treadmill for real-time gait symmetry evaluation and feedback in normal and trans-tibial amputee subjects. *Prosthetics and orthotics international*, 20(2):101–110, 1996.

[55] B.L. Davis et al. Realtime visual feedback diminishes energy consumption of amputee subjects during treadmill locomotion. *JPO: Journal of Prosthetics and Orthotics*, 16(2):49–54, 2004.

[56] K. Day et al. Individualized feedback to change multiple gait deficits in chronic stroke. *Journal of NeuroEngineering and Rehabilitation*, 16(1):158, 2019.

[57] Clipart Library. Body outline, consulted the 25 of April 2020. `http://clipart-library.com/body-outline.html`.

[58] Wikipedia. Rectus femoris muscle, consulted the 11 of April 2020. `https://en.wikipedia.org/wiki/Rectus_femoris_muscle`.

[59] Healthline. Patellar ligament, consulted the 11 of April 2020. `https://www.healthline.com/human-body-maps/patellar-ligament#1`.

[60] Get Body Smart. Rectus femoris muscle, consulted the 11 of April 2020. https://www.getbodysmart.com/anterior-thigh-muscles/rectus-femoris-muscle.

[61] Amazon. Powerpeak ftim8317p treadmill, consulted the 22 of April 2020. https://www.amazon.fr/Powerpeak-fTM8317P-Comfort-Line-Tapis/dp/B00A7DK90G.

[62] C. Ochoa-Diaz et al. An above-knee prosthesis with magnetorheological variable-damping. In *5th IEEE RAS/EMBS International Conference on Biomedical Robotics and Biomechatronics*, pages 108–113. IEEE, 2014.

[63] R. Takeda et al. Drift removal for improving the accuracy of gait parameters using wearable sensor systems. *Sensors*, 14(12):23230–23247, 2014.

[64] Y. Moon et al. Stride-time variability and fall risk in persons with multiple sclerosis. *Multiple sclerosis international*, 2015, 2015.

[65] B. Greene et al. An adaptive gyroscope-based algorithm for temporal gait analysis. *Medical & biological engineering & computing*, 48(12):1251–1260, 2010.

[66] Statistics Solutions. One sample t-test, consulted the 8 of May 2020. https://www.statisticssolutions.com/manova-analysis-one-sample-t-test/.

[67] Laerd Statistics. Repeated measures anova, consulted the 8 of May 2020. https://statistics.laerd.com/statistical-guides/repeated-measures-anova-statistical-guide.php.

[68] Engineering Statistics Handbook. Levene's test, consulted the 8 of May 2020. https://www.itl.nist.gov/div898/handbook/eda/section3/eda35a.htm.

[69] L. Paternò et al. Sockets for limb prostheses: A review of existing technologies and open challenges. *IEEE Transactions on Biomedical Engineering*, PP:1–1, Jan 2018.

[70] Ottobock. Electronic knee joint 3e80, consulted the 19 of January 2020. https://www.ottobock.com.hk/en/prosthetics/products-from-a-to-z/knee-joint-3e80/.

[71] D.F. Collins et al. Cutaneous receptors contribute to kinesthesia at the index finger, elbow, and knee. *Journal of Neurophysiology*, 94:1699–1706, May 2005.

[72] D. Rusaw et al. Can vibratory feedback be used to improve postural stability in persons with transtibial limb loss? *Journal of Rehabilitation Research Development*, 49:1239–1254, Nov 2012.

[73] E. Demircan et al. Perception accuracy of vibrotactile feedback during locomotion. In *2019 16th International Conference on Ubiquitous Robots (UR)*, pages 673–677, June 2019.

[74] A. Pagel et al. Effects of sensory augmentation on postural control and gait symmetry of transfemoral amputees: a case description. *Medical & biological engineering & computing*, 54(10):1579–1589, 2016.

[75] George C Canavos. The sensitivity of the one-sample and two-sample student t statistics. *Computational Statistics & Data Analysis*, 6(1):39–46, 1988.

[76] John H. McDonald. Student's t–test for one sample, consulted the 18 of May 2020. http://www.biostathandbook.com/onesamplettest.html.

[77] Dr. Maher Khelifa. One-way repeated-measures analysis of variance, consulted the 4 of May 2020. https://www.zu.ac.ae/main/files/contents/research/training/One-wayRepeatedMeasureANOVA.pdf.

[78] D. Oberfeld et al. Evaluating the robustness of repeated measures analyses: The case of small sample sizes and nonnormal data. *Behavior research methods*, 45(3):792–812, 2013.

UNIVERSITÉ CATHOLIQUE DE LOUVAIN
École polytechnique de Louvain
Rue Archimède, 1 bte L6.11.01, 1348 Louvain-la-Neuve, Belgique | **www.uclouvain.be/epl**